The Plasticity of Neutrophil Subsets in Inflammation

A thesis submitted to The University of Dublin,

Trinity College for the degree of Doctor of Philosophy

31st March 2022

Submitted by:

Aisling Uí Mhaonaigh
MSc Immunology, BSc Biochemistry
Student number: 15338441

Under the supervision of:

Professor Mark Little, Professor Derek Doherty

Declaration

I declare that this thesis has not been submitted as an exercise for a degree at this or any other university and it is entirely my own work.

I agree to deposit this thesis in the University's open access institutional repository or allow the Library to do so on my behalf, subject to Irish Copyright Legislation and Trinity College Library conditions of use and acknowledgment.

I consent / do not consent to the examiner retaining a copy of the thesis beyond the examining period, should they so wish (EU GDPR May 2018).

- For a thesis which the work has been carried out jointly; the declaration must have a statement that it includes the unpublished and/or published work of others, duly acknowledged in the text wherever included.

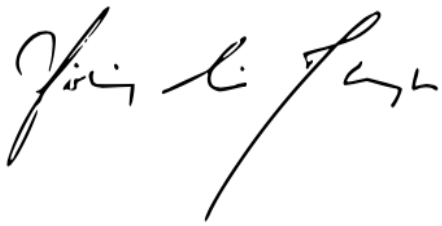

Acknowledgments

It is with immense gratitude that I acknowledge the support and guidance of Prof Mark Little, it has been an amazing few years, I have thoroughly enjoyed the journey and your clarity of vision and astute attention to detail in all aspects of this work have been inspiring. You have never been too busy although I expect you are always too busy. Thank you. Professor Derek Doherty thank you so much for your very knowledgeable support and help with this project and always so generous with your advice.

A special thank you has to go to Amrita, you radiate positivity and calm wherever you go, thank you for taking the time to discuss so many issues on this project it has been an absolute pleasure working with you.

A huge thanks to Emma, we started at the same time and there is a void that cannot be filled since you left, I have great memories of the Philadelphia conference and our nights in McSorleys in NYC.

Grainne, thank you so much for all your support and friendship over the years. Miss the chatty lunches and thanks for tech support and advice on lab and non-lab issues.

Thanks to the greater TTMI family, Izzy, Tom, Clara, Gareth, Derv, and Conor. A special thank you to Makala and Conor who have been so generous in helping with the assays. Thanks everyone, such a positive place to work.

A huge thank you to Niamh, Caoimhe and Oscar, if we could design our children, I would never have been so ambitious as to imagine you all, a joy each and every day, thanks for your love, support and patience over the past few months.

To Mom, always an inspiration so positive and loving, thank you. To Dad whose love of learning was instilled in me from an early age, always in my heart.

And the biggest heartfelt thanks have to go to Joe, for once words fail me, I am so indebted to you for your love and tireless support in everything and thanks for the past few months and especially this week. This would not be possible without you.

Table of Contents

1 Introduction 2

1.1 Steady State Neutrophil Life Cycle in Health 2

1.1.1 Granulopoiesis 3

1.1.2 Neutrophil granules 4

1.1.3 Neutrophil mobilisation and clearance 6

1.1.4 Tissue Neutrophils 7

1.2 Neutrophil subpopulations in inflammation 8

1.2.1 Low Density Neutrophils (LDN) or granulocytes (LDG) 8

1.2.2 Other Neutrophil Subsets 9

1.2.3 The origin of Neutrophil subsets 11

1.2.4 Neutrophils in the etiology of ANCA Vasculitis 14

1.2.5 Neutrophils in Covid -19 16

1.3 Phenotyping Neutrophils: Density, Nuclear Morphology and Maturity 18

1.3.1 Neutrophil Density and its association with neutrophil development 19

1.3.2 Nuclear Morphology 19

1.3.3 Neutrophil surface marker expression during granulopoiesis 19

1.3.4 Markers linked to activation 21

1.3.5 Chemokines 21

1.3.6 Arginase 22

1.3.7 Arginase enzymes 22

1.3.8 Arginase in COVID-19 26

1.4 The case for whole blood analysis of neutrophils 28

1.5 Hypothesis and aims 29

Chapter 2 30

2 Materials & Methods 31

2.1 Materials 31
2.1.1 Reagents 31
2.1.2 Buffers 32
2.1.3 Kits 32
2.1.4 Equipment 32
2.1.5 Software 33
2.2 Methods 34
2.2.1 Methodology Overview 34
2.3 Patients 34
2.4 Density Gradient Centrifugation 37
2.4.1 Cell counts and viability 38
2.5 Flow Cytometry 38
2.5.1 Intracellular Staining: Arginase 41
2.5.2 Whole blood staining 42
2.5.3 Imaging Flow Cytometry 42
2.6 T cell Supression 43
2.6.1 Isolation and culture of Neutrophils for T cell suppression assay 43
2.6.2 T cell suppression assay 43
2.6.3 Arginase Assay 44
2.6.4 Arginase 1 ELISA 45
2.7 Real-Time Quantitative Reverse Transcription PCR (rt-PCR) 47
2.7.1 RNA extraction 47
2.7.2 cDNA synthesis 48
2.7.3 rtPCR 48
2.8 Statistical Analysis 49
Chapter 3 51

3 Low density granulocytes (LDGs) are elevated and linked to disease severity in autoimmune AAV and in viral infection 52

3.1 Introduction 52

3.2 Design and rational 53

3.2.1 Hypothesis 53

3.2.2 Specific aims 53

3.2.3 Specific Methods 53

3.3 Results 55

3.3.1 Low Density Granulocytes (LDGs) are elevated in patients with Acute AAV and in patients with COVID-19 and are linked to severity in COVID-19 patients. 55

3.3.2 CD16 expression defines subpopulations of LDGs in both AAV and COVID-19. 56

3.3.3 Imaging flow cytometry confirms that AAV and COVID-19 LDGs are a mixed population of mature and immature cells as defined by CD16 expression and nuclear morphology. 58

3.3.4 CD10 and CD16 define maturity in neutrophil subsets with both markers identifying mature and immature LDGS by flow cytometry. 61

3.3.5 In AAV imaging Flow cytometry allows definitive phenotyping of PBMC populations. 63

3.3.6 Surface marker expression varies according to cell fraction and disease state. 64

3.3.7 Activation markers CD62l and myeloid marker CD33 expression on LDG and NDG fractions in AAV and COVID-19. 65

3.4 Discussion 66

Chapter 4 72

4 Immunomodulatory Arginase expression in Neutrophil Subsets 73

4.1 Introduction - the concept of Arginase 1-mediated immunosuppression 73

4.2 Design and Rationale 74

4.2.1 Hypothesis 74
4.2.2 Methods 74
4.3 Results 75
4.3.1 The percentage of LDGs in COVID-19 are elevated and linked to severity. Percentage arginase 1 positive LDGs are also linked to severity in COVID-19 77
4.3.2 LDGs are elevated in patients with Acute AAV compared to those in remission. BVAS scores do not correlate with percent LDGs or percent Arg positive LDGs 79
4.3.3 An expansion of immature LDGs as defined by maturation markers CD10 and CD16 are linked to outcome in COVID-19 81
4.3.4 NDG arginase 1 levels are inversely linked to severity in COVID-19 83
4.3.5 Arginase 1 is differentially expressed in cell fractions from AAV and COVID-19 displaying disease specific differences 85
4.3.6 Arginase 1 is differentially expressed in neutrophil populations from AAV and COVID-19 with both mature and immature neutrophils having significantly less arginase in COVID-19 than AAV 87
4.3.7 Imaging flow cytometry confirms disease specific intracellular arginase 1 expression in AAV and COVID-19 Neutrophils 89
4.3.8 Steroid use is linked to phenotypic alterations in the LDG populations 91
4.3.9 Severe COVID-19 neutrophil cell culture supernatant has a suppressive effect on T-cell proliferation but it is not reversed by arginase inhibitor nor-NOHA 92
4.4 Discussion 92
Chapter 5 99
5 Whole Blood Neutrophils 100
5.1 Introduction 100
5.2 Design and Rationale 101
5.2.1 Hypothesis 101
5.2.2 Specific Methods 101

5.3 Results 102

5.3.1 LDGs correlate with % PMN in whole blood In COVID-19 and Immature and activated neutrophils are significantly elevated in COVID-19 WB but not AAV .. 104

5.3.2 Levels of neutrophils correlate with WHO severity in COVID-19 whole blood, CD33 and CD62L are identified as key markers 107

5.3.3 LDGs correlate with WHO severity, immature activated and potentially suppressive neutrophils are identified in LDG fraction..... 109

5.3.4 NDGs do not correlate with WHO severity, suppressive markers CD33 and Arg 1 have a weak association and there is a clearly population of CD10int/- NDGs that correlate with severity the pattern is not repeated with CD16int/- NDGs..... 111

5.3.5 Phenotyping of neutrophil subsets using CD62l and CD16 does not identify a disease specific cell population in AAV. 113

5.3.6 Phenotyping of Neutrophil subsets using CD49d and CD101 does not identify subsets that correlate with disease activity 115

5.3.7 Altered composition of neutrophil populations is associated with disease severity in COVID-19 Whole Blood 117

5.3.8 UMAP analysis of LDGs reveals severity related populations and convalescent populations that differ from healthy controls 119

5.3.9 UMAP analysis of NDG identify neutrophil populations that are associated with disease severity in COVID-19 and in convalescence. 121

5.4 Discussion 122

Chapter 6 126

6 General Discussion 127

6.1 Unanswered questions 128

6.2 Future Work 130

6.3 Translational relevance 130

6.4 Final remarks 131

References 132

List of Figures

Figure 1.1.1 Granulopoiesis 4
Figure 1.1.2 Granule production and functionality during granulopoiesis 6
Figure 1.2.1 Neutrophils in the Etiology of ANCA Vasculitis..... 15
Figure 1.3.1 Surface Marker Expression during granulopoiesis 18
Figure 1.3.2 The immunosuppressive effects of Neutrophil derived Arginase 1..... 24
Figure 2.2.1 Thesis Workflow 34
Figure 2.4.1 Density gradient centrifugation of whole blood. 37
Figure 2.5.1 Gating strategy for identification of neutrophils in peripheral blood samples 41
Figure 2.6.1 Standard dilution protocol..... 46
Figure 3.3.1 Low Density granulocytes (LDGs) are elevated in patients with Acute AAV and in patients with COVID-19 and are linked to severity in COVID-19 patients. 56
Figure 3.3.2 CD16 expression defines subpopulations of LDGs in both AAV and COVID-19. 58
Figure 3.3.3 Imaging flow cytometry confirms that AAV and COVID-19 LDGs are a mixed population of mature and immature cells as defined by CD16 expression and nuclear morphology 60
Figure 3.3.4 CD10 and CD16 define maturity in neutrophil subsets with both markers identifying mature and immature LDGS by flow cytometry 62
Figure 3.3.5 AAV imaging Flow cytometry allows definitive phenotyping of PBMC populations. 63
Figure 3.3.6 Surface marker expression varies according to cell fraction and disease state. 65
Figure 3.3.7 Activation markers CD62l and myeloid marker CD33 expression on LDG and NDG fractions in AAV and COVID-19 66
Figure 4.1.1 Arginase in steady state neutrophils and in inflammation 74
Figure 4.3.1 The percentage of LDGs in COVID-19 are elevated and linked to severity. Percentage arginase 1 positive LDGs are also linked to severity in COVID-19 76
Figure 4.3.2 LDGs are elevated in patients with Acute AAV compared to those in remission. BVAS scores do not correlate with percent LDGs or percent Arg positive LDGs 78

Figure 4.3.3 An expansion of immature LDGs as defined by maturation markers CD10 and CD16 are linked to outcome in COVID-19 80
Figure 4.3.4 NDG arginase levels are inversely linked to severity in COVID-19 82
Figure 4.3.5 Arginase 1 is differentially expressed in cell fractions from AAV and COVID-19 displaying disease specific differences 84
Figure 4.3.6 Arginase 1 is differentially expressed in neutrophil populations from AAV and COVID-19 with both mature and immature neutrophils having significantly less arginase 1 in COVID-19 than AAV 86
Figure 4.3.7 Imaging flow cytometry confirms disease specific intracellular arginase 1 expression in AAV and COVID-19 Neutrophils 88
Figure 4.3.8 Steroid use is linked to phenotypic alterations in the LDG populations ... 90
Figure 4.3.9 Severe COVID-19 neutrophil cell culture supernatant has a suppressive effect on T-cell proliferation but it is not reversed by arginase inhibitor nor-NOHA 91
Figure 5.3.1 LDGs correlate with % PMN in whole blood In COVID-19 and Immature and activated neutrophils are significantly elevated in COVID-19 WB but not AAV 103
Figure 5.3.2 Levels of neutrophils correlate with WHO severity in COVID-19 whole blood, CD33 and CD62L are identified as key markers in whole blood 106
Figure 5.3.3 LDGs correlate with WHO severity, immature activated and potentially suppressive neutrophils are identified in LDG fraction 108
Figure 5.3.4 NDGs do not correlate with WHO severity, suppressive markers CD33 and Arg 1 have a weak association and there is a clearly population of CD10int/- NDGs that correlate with severity the pattern is not repeated with CD16int/- NDGs 110
Figure 5.3.5 Phenotyping of neutrophil subsets using CD62l and CD16 does not identify a disease specific cell population in AAV 112
Figure 5.3.6 Phenotyping of Neutrophil subsets using CD49d and CD101 does not identify subsets that correlate with disease activity 114
Figure 5.3.7 Altered composition of neutrophil populations is associated with disease severity in COVID-19 Whole Blood 116
Figure 5.3.8 UMAP analysis of LDGs reveals severity related populations and convalescent populations that differ from healthy controls 118

Figure 5.3.9 UMAP analysis of NDG identify neutrophil populations that are associated with disease severity in COVID-19 and in convalescence 120
Figure 6.1.1 Investigation of the aberrant expression of Arginase 1 in Severe COVID-19. 129

List of Tables

Table 1.1 LDG population characteristics in various disease conditions 13
Table 1.2 Differential roles for Arginase in viral-induced disease 27
Table 2.1 Baseline characteristics of the study subjects, by disease classification ..36
Table 2.2 Panel of antibodies used standard and Imaging flow cytometry experiments 40
Table 2.3 Arginase Staining Panel 42
Table 2.4 Antibody Panel for Imaging Flow cytometry.....43
Table 2.5 Antibodies for T cell suppression assay 44
Table 2.6 Lysis buffer volume recommended by number of cells. 47
Table 2.7 Parameters for the Thermocycler 48
Table 2.8 Primers for rtPCR.....49
Table 4.1 WHO Severity Score 77
Table 5.1 Whole Blood Phenotyping - Panel A 101
Table 5.2 Whole Blood Phenotyping Panel B 102

List of Abbreviations

AAV	ANCA associated vasculitis
AMLS	Acute myeloid Leukemia
ANCA	Antineutrophil cytoplasmic antibody
ARDS	acute respiratory distress syndrome
Arg 1	Arginase 1
BAL	bronchoalveolar lavage
BVAS	Birmingham vasculitis activity score
COVID-19	Coronavirus disease
cANCA	Cytoplasmic ANCA
CD	Cluster of Differentiation
cDNA	complimentary DNA
CFSE	Carboxyfluorescein succinimidyl ester
CHCC	Chapel Hill Consensus conference
CRP	c-reactive protein
CyTOF	Mass cytometry
DC	Disease controls
DEG	differentially expressed genes
EDTA	Ethylenediaminetetraacetic acid
EGPA	Eosinophilic granulomatosis with polyangiitis
ELISA	Enzyme-linked immunosorbent assay
FACS	fluorescence-activated cell sorting
FCS	Foetal Calf Serum
FSc	Forward scatter
fMLSF	formyl-methionyl-leucyl-phenylalanine
FMO	Fluorescence minus one

GBM	Glioblastoma
GCSF	granulocyte colony-stimulating factor
G-MDSC	Granulocyte -myeloid derived suppressor cell
GPA	Granulomatosis and polyangiitis
GPI	Glycosylphosphatidyl inositol
HC	Healthy Control
HIV	Human Immunodeficiency Virus
ICAM	intercellular adhesion molecule
IFN	Interferon
IL	Interleukin
LCMV	lymphocytic choriomeningitis
LDG	Low density granulocyte
LDIB	low-density inflammatory band
LDN	Low density neutrophil
LOX-1	Lectin-like oxidized low-density lipoprotein (LDL) receptor-1
MDSC	Myeloid derived suppressor cell
MFI	Mean Fluorescence Intensity
MPA	Microscopic polyangiitis
MPO	Myeloperoxidase
N1	anti-tumour neutrophils
N2	pro-tumour neutrophils
NDG	Normal density granulocyte
NE	Neutrophil Elastase
NETs	Neutrophil Extracellular Traps
NGAL	neutrophil gelatinase-associated protein lipocalin
NLR	Neutrophil to lymphocyte ratio
pANCA	Perinuclear ANCA

PBMCs	Peripheral blood mononuclear cells
PBS	phosphate buffered saline
PMN	polymorphonuclear cells
PR3	Proteinase 3
RA	Rheumatoid Arthritis
RBC	Red blood cells
RCC	Renal cell carcinoma
RNA	ribonucleic acid
rIM	reverse interstitial migration
RKD	Rare kidney disease
rM	reverse migration
ROS	Reactive Oxygen Species
rTEM	reverse transendothelial migration
SARS-CoV-2	Severe Acute Respiratory syndrome coronavirus 2
SJH	St James's Hospital
SLE	Systemic Lupus Erythematosus
SSc	Side scatter
TAN	Tumour associated Neutrophil
TCR	T cell receptor
TGF	transforming growth factor
TUH	Tallaght University Hospital
UCB	umbilical cord blood
UMAP	Uniform Manifold Approximation and projection for Dimension Reduction
VEGF	vascular endothelial growth factor
WB	Whole blood

Abstract

Neutrophils are a vital component of the innate immune system and the body's first line of defense against invading pathogens. The classic view of these cells is that they are a homogenous population of terminally differentiated cells with clearly outlined functions. Recently evidence has revealed that neutrophils are a functionally versatile cell type and are responsible for both inflammation and immune response. Indeed, the role played by neutrophils in various disease conditions ranging from autoimmunity to bacterial and viral infections and cancer has led to a renewed interest in their roles in pathological inflammation. In this thesis I set about investigating the plasticity of neutrophils in inflammation using ANCA vasculitis and COVID-19 (COVID-19) as disease models.

The presence of low-density neutrophils in a variety of diseases suggests a relationship between the underlying disease state and their production. ANCA vasculitis (AAV) is a systemic autoimmune disease in which neutrophils play a vital role. More recently there have been reports of LDGs in COVID-19 a systemic viral disease. I directly compared the frequency and phenotype of these cells in acute and remission AAV and in mild moderate and severe COVID-19. LDGs are elevated and linked to severity in both diseases. Immature neutrophils are elevated in both conditions, likely due to extreme left shift from emergency granulopoiesis. These results suggest that LDGs are a generic response to inflammation and not a result of disease specific triggers.

To establish an immunomodulatory role for neutrophils, I focused on arginase 1, an enzyme linked to T cell suppression. Interestingly, normal density granulocytes (NDGs) in severe COVID-19 had significantly lower arginase levels than their AAV counterparts and healthy controls (HC). Imaging flow cytometry confirmed dysfunctional arginase distribution within the cell. These differences may be severity related. I also investigated the levels of arginase 1 protein and enzyme activity in serum from COVID-19 patients, paradoxically these were lower than HCs suggested that arginase 1 may have been already exocytosed or that an aberrant release mechanism was at play. Neutrophils from COVID-19 patients failed to suppress T cell proliferation *in vitro*.

Having established that it was NDGs not LDGs that display disease-specific differences, and to reduce handling and user bias, I focused on the identification of neutrophil subsets in whole blood. Using traditional and imaging flow cytometry I identified higher levels of immature neutrophils and activated subsets in COVID-19 than AAV. I identified a population of $CD33^{+}$ cells in convalescent COVID-19 that was not present in HC. This population was confirmed by high-dimensional analysis using UMAP and clustering algorithms to identify novel subsets. This subset is of particular note because it is present in an otherwise healthy individual and not in response to inflammatory conditions.

Taken together, this data suggest that neutrophils respond to inflammation by both emergency granulopoiesis and degranulation leading to low density cells. The response is remarkably similar in both AAV and COVID-19, however the identification of a subset in convalescence not present in HC suggests that this neutrophil subset may be a bona fide subset and warrants further investigation.

Publications arising from this work

Front Immunol. 2019 Nov 7;10:2603. doi: 10.3389/fimmu.2019.02603.

Low Density Granulocytes in ANCA Vasculitis Are Heterogenous and Hypo-Responsive to Anti-Myeloperoxidase Antibodies.

Ui Mhaonaigh A, Coughlan AM, Dwivedi A, Hartnett J, Cabral J, Moran B, Brennan K, Doyle SL, Hughes K, Lucey R, Floudas A, Fearon U, McGrath S, Cormican S, De Bhailis A, Molloy EJ, Brady G, Little MA.

Rheumatology, Volume 58, Issue Supplement_2, March 2019, https://doi.org/10.1093/rheumatology/kez057.053

Low Density Granulocytes in Anca Vasculitis: Phenotype and **Function**

Aisling Ui Mhaonaigh, Alice Coughlan, Amrita Dwivedi, Aisling Morrin, Vincent O'Reilly, Fionnuala Hickey, Barry Moran, Joana Cabral, Mark Little

Front. Immunol., 15 April 2021 | https://doi.org/10.3389/fimmu.2021.602963

Neutrophils: Need for Standardized Nomenclature

Ellen McKenna, **Aisling Ui Mhaonaigh**, Richard Wubben, Amrita Dwivedi, Tim Hurley, Lynne A Kelly, Nigel J Stevenson, Mark A Little, Eleanor J Molloy

Manuscript under review

Nature Reviews Immunology

Are neutrophils key to immunopathology in COVID-19?

Ellen McKenna, Richard Wubben, Ashanty M Melo, **Aisling Ui Mhaonaigh**, Niall Conlon, James S O'Donnell, Cliona Ni Cheallaigh, Tim Hurley, Nigel Stevenson, Marl A Little, Eleanor J Molloy

Manuscript in preparation

Aberrant neutrophils are associated with poor outcome and display a disease specific response in COVID-19.

Aisling Ui Mhaonaigh, Amrita Dwivedi, Makala Carroll, Conor Finlay, Mark Little.

Poster Presentations and conferences

- International Vasculitis 2019, Philadelphia, USA. April 2019 **'Low Density Granulocytes in ANCA Vasculitis'** (Poster)
- Irish Nephrology Society Annual Conference INS, Dublin, April 2019 '**Low Density Granulocytes in ANCA Vasculitis'** (Poster)

- Irish Society for Immunology Annual meeting, RCSI Sept 19&20 2019 **'Phenotype and function of Granulocyte subsets in ANCA vasculitis'** (Poster)

- American Society Nephrology 2021, **Plasticity of Neutrophil Subsets in COVID-19** (Poster)

- European Congress Immunology 2021, **Neutrophil subsets in ANCA vasculitis and COVID-19: a disease specific response.** (Poster and oral presentation) Shortlisted for best poster

- Vasculitis and ANCA workshop 2022**, Neutrophil mediated T-cell suppression in ANCA vasculitis and COVID-19** (Poster and oral presentation)

Oral Presentations

- **IRF Immunology Research Forum**, TBSI November 28th 2018, 'Granulocyte Heterogeneity in Autoimmunity'

- **TTMI Seminar Series**, Durkan Lecture theatre, November 2018, 'Granulocyte Heterogeneity in Autoimmunity'

- **TTMI Post Graduate Research Symposium**, Durkan Lecture Theatre, March 2019, 'Neutrophils in Autoimmunity'

- **Imaging Flow Cytometry Open Day, Biomedical Sciences, NUI Galway** November 2019
  'Deciphering Granulocyte Subsets in Autoimmunity'

- **SFI Meeting** 'A preliminary view of Neutrophils in Covid -19' online via Zoom March 2021

- **International Vasculitis and ANCA workshop April 2022**
  'Neutrophil mediated T cell suppression in ANCA vasculitis and COVID-19'

Chapter 1

Introduction

1 Introduction

'There is a time for everything,
and a season for every activity under the heavens:
a time to be born and a time to die,
a time to plant and a time to uproot,
a time to kill and a time to heal,
a time to tear down and a time to build'

Ecclesiastes 3:4

Inflammation is a normal and natural part of the immune response. It is a process by which the immune system senses and removes harmful and foreign stimuli and begins the healing process. Once the insult is resolved the immune system returns to a homeostatic state. However, when this finely tuned balance becomes dysregulated, and the response can be excessive or too inadequate and the result can be damaging to the host. Excessive activation of the cellular immune response is manifested as immunopathology seen in autoimmunity and allergy; conversely, downregulation of the response may lead to increased susceptibility to infection and cancer

Neutrophils are the most abundant leukocytes in peripheral blood and are regarded as first line of defence of the innate immune system. They destroy and capture invading microorganisms through phagocytosis leading to intracellular degradation, the release of granules, and the formation of neutrophil extracellular traps (NETs). Neutrophils also act as mediators of inflammation. The classical view is that neutrophils constitute a homogenous population of terminally differentiated cells with a clearly defined function. However, more recently, evidence has revealed that neutrophils present a large phenotypic heterogeneity and functional versatility, which implicate neutrophils as important modulators of both inflammation and immunomodulatory responses. Indeed, the focus of a renewed interest in neutrophil biology is the roles played by neutrophils in homeostatic conditions as well as in pathological inflammation. In this thesis, I present the concept of neutrophil phenotypic and functional heterogeneity in inflammation and endeavour to establish whether these subsets are a generic response to inflammation or disease-specific immunomodulatory subsets that demonstrates neutrophil plasticity in inflammatory settings.

1.1 Steady State Neutrophil Life Cycle in Health

70% of all leukocytes are neutrophils and more than 10^{11} cells are produced daily by the bone marrow [1]. From the bone marrow, neutrophils enter peripheral blood where they circulate until they migrate into tissues. Neutrophils are short lived with an accepted half-life of less than one day,

however, recent research has challenged this dogma suggesting a lifespan of 5.4 days [2, 3]. Within tissues at the end of their lifespan, neutrophils are cleared by macrophages by phagocytosis[4]. A fine balance between elimination and production means that the numbers of neutrophils in circulation remains constant to maintain homeostasis[5].

1.1.1 Granulopoiesis

Neutrophils are produced from hematopoietic stem cells in vast numbers in the bone marrow[6]. Multipotent progenitor cells (MMPs) transform into lymphoid-primed multipotent progenitors (LMPPs) which in turn become granulocyte-monocyte progenitors (GMPs). GMPs commit to neutrophil generation under the control of granulocyte colony-stimulating factor (G-CSF) and differentiate into myeloblasts. These myeloblasts differentiate into promyelocytes, myelocytes, band cells and finally segmented neutrophils. The term band and segmented refers to the nuclear morphology of these cells (**Figure 1.1.1**)[7]. During development, the differentiating neutrophil changes its nucleus from a simple round morphology into a kidney shape, then banded and finally a multi-lobulated morphology. During granulopoiesis the neutrophil surface markers change to facilitate altered functions as the cell matures.

Inside the bone marrow there are three compartments where neutrophils reside: stem cell pool, mitotic pool and post-mitotic pool [8]. Undifferentiated progenitor cells such as HSCs, are found in the stem cell pool. The mitotic pool holds myeloblasts, promyelocytes and myelocytes and, finally, metamyelocytes, band cells and segmented neutrophils are localized within the post-mitotic pool [9]. At the metamyelocyte stage, the neutrophil can no longer proliferate, signalling the start of terminal differentiation [10]. In the absence of infection, there are more neutrophils stored in the bone marrow than in the circulation. In response to signals at the site of infection, only mature segmented neutrophils migrate out of the bone marrow in large numbers to the site of infection [11]. The lung is believed to be the main site of neutrophil margination, but this theory remains controversial [12].

The next stage involves the terminal differentiation of GMPs into neutrophils. This progression involves the acquisition of neutrophil specific granule components at various stages of neutrophil maturation.

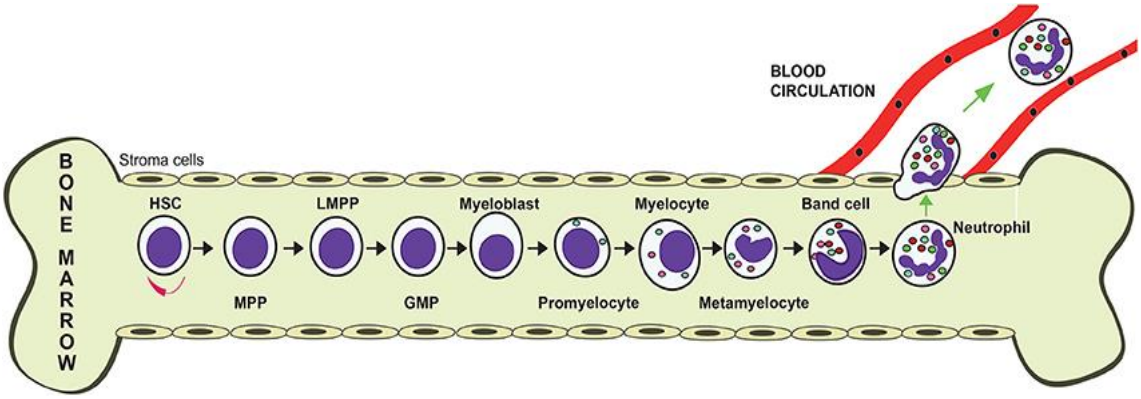

Figure 1.1.1 Granulopoiesis

Neutrophils are produced in the bone marrow. From a self-renewing hematopoietic stem cell (HSC), a multipotent progenitor (MPP) cell is formed. MPPs give rise to lymphoid-primed multipotent progenitors (LPMP), which differentiate into granulocyte-monocyte progenitors (GMP). These GMPs, under control of the granulocyte colony-stimulating factor (G-CSF) commit to neutrophil generation by turning into myeloblasts, which then follow a maturation process that includes the stages of promyelocyte, myelocyte, metamyelocyte, band cell, and finally a mature neutrophil. Rosales, C., *Neutrophil: A Cell with Many Roles in Inflammation or Several Cell Types?* Front Physiol, 2018

1.1.2 Neutrophil granules

Neutrophil granules contain critical antimicrobial proteins for fungal and bacterial killing, they are mobilised to the phagosome after ingestion by phagocytosis. The production of neutrophil granules begins as the immature neutrophil transitions from a myeloblast to a promyelocyte and continue to be produced up to the segmented neutrophil stage [13]. Mature neutrophils are considered largely transcriptionally silent, instead using extensive granules to store pre-synthesised peptides and enzymes. This accounts for the high side scatter observed in flow cytometry. There are four main groups of granules: azurophilic (primary) granules, specific (secondary) granules, gelatinase (tertiary) granules and (most recently discovered) ficolin-1 granules (Figure 1.1.2). Neutrophils also contain secretory vesicles, which are not defined as granules [14, 15]. A comprehensive review of granulopoiesis granule production and associated transcription factors is provided by Lawrence et al. [16].

Azurophilic granules contain MPO, neutrophil elastase (NE), proteinase 3 (PR3), lysozyme, azurocidin 1, cathepsin G and neutrophil serine protease 4 (NSP4) [13, 17, 18]. Prominent production of the heme enzyme myeloperoxidase (MPO) is the main characteristic feature of azurophilic granules. MPO makes up 5% of the weight of a neutrophil [16]. The main neutrophil antimicrobial peptides, α-defensins, are also stored in azurophilic granules [19]. The formation of azurophilic granules begins at the promyelocyte phase [17] (Figure 1.1.2). Cathepsin G and NE may contribute to downregulation of neutrophil adhesion by proteolysis of CD62L, preventing its binding to P-selectin on the endothelium [20]. Lysozyme mediates killing of bacteria by hydrolysing the

peptidoglycan cell wall [21]. NE, PR3, MPO, α-defensins and cathepsin G are all involved in NETosis [22-26]. Neutrophil extracellular traps are networks of DNA fibres from the neutrophil which binds pathogens (NETs). PR3, cathepsin G, NE and NSP4 contribute to extracellular matrix (ECM) degradation by mediating proteolysis of components such as laminin, elastin and type IV collagen [16].

Specific granules contain large amounts of lactoferrin, which plays a key role in NETosis [13, 17]. Other components are olfactomedin-4 (OLFM-4), which helps fight bacterial infections such as *Staphylococcus aureus*, resistin, a pro-inflammatory cytokine and T-cell chemoattractant, the receptor CD177 and antimicrobial neutrophil gelatinase-associated protein lipocalin (NGAL) [16, 27-30]. Specific granules are formed at the myelocyte stage [16] (**Figure 1.1.2**).

Gelatinase granules store arginase 1, matrix metallopeptidase (MMP-9), gelatinase and surface receptors including CD11b/CD18 (Mac-1), [13, 17]. The main function of gelatinase granules such as MMP-9 and gelatinase is to facilitate the breakdown of the ECM and basement membrane, aiding migration into tissue [31]. Metamyelocytes begin to form gelatinase granules [15] (**Figure 1.1.2**).

Segmented neutrophils form **ficolin-1 granules**, the contents of which play roles in migration and adhesion, for example, actin and vanin-2 [14, 16]. Segmented neutrophils also produce secretory vesicles, these contain actin, alkaline phosphatase and receptors including CD11b, CD10 and CD16 [14-16] (**Figure 1.1.2**).

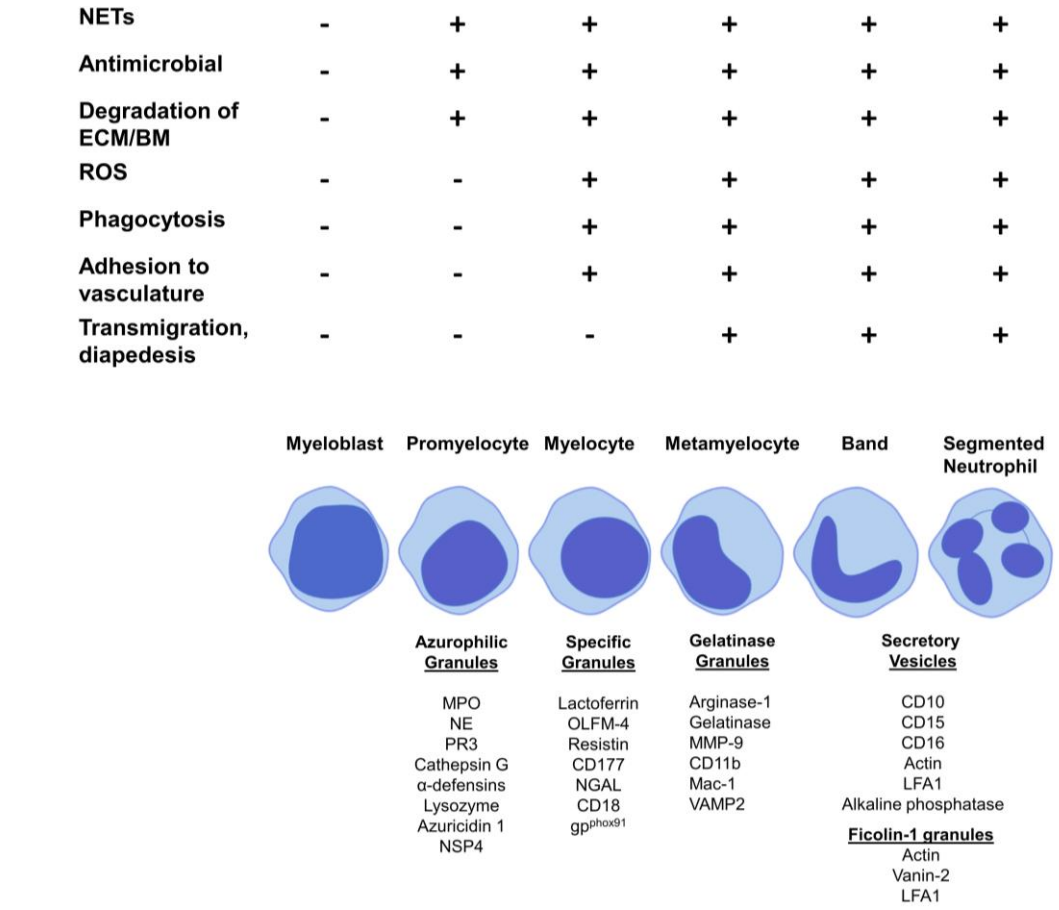

Figure 1.1.2 Granule production and functionality during granulopoiesis

Granule production during the stages of granulopoiesis. Granule formation begins with azurophilic granules at the promyelocyte stage, specific granules are first formed by myelocytes, gelatinase granules are formed at the metamyelocyte stage and only band cells and segmented neutrophils can form ficolin-1 granules and secretory vesicles. NET formation, antimicrobial functions and degradation of the extracellular membrane and basement membrane begin at the promyelocytes stage with azurophilic granule formation. ROS production, phagocytosis and adhesion to vasculature starts at the myelocytes stage with the formation of specific granules. Metamyelocytes are the first stage to perform transmigration and diapedesis through a vessel wall, which correlates with gelatinase granule formation.

1.1.3 Neutrophil mobilisation and clearance

Neutrophils from peripheral blood can be trafficked to sites of inflammation or infection through a process called the leukocyte adhesion cascade[32]. Blood vessel endothelial cells close to the site of infection get activated and upregulate expression of adhesion receptors such as P- and E-selectins. Glycoprotein ligands on neutrophils bind to these receptors and cause them to roll on the endothelium. The neutrophil is then activated by chemokines which induce a state of high affinity

beta 2 integrins, binding of these to their ligands intercellullar adhesion molecule-1 (ICAM-1) and ICAM-2 on the endothelium causes firm adhesion of the neutrophil. The neutrophil then migrates into peripheral tissues and once there, they follow chemotactic gradients of anaphylatoxin C5a and formyl-methionyl-leucyl-phenylalanine (fMLSF) to complete their function[3]. The numbers of neutrophils in the circulation are controlled by central signals that induce the expression of adhesion molecules on the endotheilium allowing neutrophils to bind and exit the circulation, this pattern of regulation has a circadian pattern [33]. The final step in the resolution of inflammation is the clearance of apoptotic neutrophils by resident dendritic cells and macrophages. Senescent neutrophils in blood upregulate CXCR4 which labels them for return to the bone marrow for clearance. This phagocytosis of apoptotic neutrophils is characterised by an anti-inflammatory response which leads to a reduction of IL-23 by macrophages this in turn leads to less IL-17 levels and reduced G-CSF production which leads to reduced granulopoiesis[34].

1.1.4 Tissue Neutrophils

In homeostasis neutrophils can be found in many tissues. Little is known about how these neutrophils are directed to different organs, but there is evidence to suggest that neutrophils exhibit different phenotypes in various organs. Lung neutrophils adhere to the interstitial space and vascular lumen and are maintained in the tissues by a CXCR4 dependent mechanism. It has been mooted that because aged neutrophils have higher expression of CXCR4 that it is likely that they then preferentially migrate to the lungs[35]. Marginal zone spleen neutrophils have a phenotype $CD11b^{hi}$, $ICAM\text{-}1^{hi}$ and $CD62L^{low}$ and a tendency to produce NETs which is similar to aged neutrophils in circulation[36]. Another neutrophil subpopulation is found in the lymph nodes where they carry antigens, interact with T cells and mediate T cell activation, these neutrophils express the CCR7 receptor the integrin LFA-1 and CXCR4[37]. Interestingly, another subset of neutrophils has been shown to induce angiogenesis by expressing a receptor for vascular endothelial growth factor (VEGF-A). These neutrophils display a $CXCR4^{hi}$, $CD49d^{hi}$ and VEGFR1 and are recruited under hypoxic conditions to non-vascularised tissues where they promote angiogenesis[38].

1.1.4.1 Neutrophil Reverse Migration (rM)

Neutrophils, having fulfilled their antimicrobial function are thought to be cleared efficiently in order to maintain homeostasis, apoptosis and phagocytosis by macrophages were considered the main ways to clear neutrophils. Some neutrophils have been shown to undergo reverse transendothelial migration (rTEM) or reverse interstitial migration (rIM), which is dictated by the starting location. With the advent of imaging technology, it has been demonstrated that neutriophils can migrate back into the bloodstream which is a relatively new concept of neutrophil

clearance at the site of injury or inflammation. These neutrophils are characterised by a high expression of ICAM-1 and a low expression of CXCR1. A phenotype of ICAM-1^{hi} and CXCR-1^{lo} are found on transmigrated neutrophils in the peripheral blood of patients with systemic inflammation[39, 40]. This neutrophil rM may be a protective response by resolving a potential tissue damaging event.

This description of the neutrophil life cycle suggests that neutrophils produced in the bone marrow egress to the circulation and when necessary, migrate to sites of inflammation or infection where they perform their antimicrobial functions and are quietly cleared by tissue resident macrophages. This oversimplified view of the neutrophil as mere pathogen killing cells is currently under question with neutrophils displaying far more complex behaviour. Neutrophils have been shown to be transcriptionally active with the potential to upregulate expression of surface molecules and to produce cytokines. Importantly, neutrophils are capable of executing different cellular functions depending on their location[41-43]. Thus, neutrophils and their plasticity in inflammation warrants further investigation.

1.2 Neutrophil subpopulations in inflammation

Elie Metchnikoff and Paul Ehrlich were awarded the Nobel prize in 1908 for their discovery of cells with polymorphous nuclei [44]. Since this discovery, these cells have be referred to by many names including phagocytes, granulocytes, neutrophils, polymorphonuclear cells (PMN), myeloid derived suppressor cells (MDSC), low density neutrophils (LDN) low density granulocytes (LDG), low-density inflammatory band (LDIB) and tumour-associated neutrophils (TANs) [45].

Recently however, using different models of infection, it is becoming progressively more evident that not all neutrophils have the same objective. Heterogeneity within the neutrophil population during infection has been demonstrated in multiple disease situations, and different subsets have roles in promoting and suppressing the inflammatory response[46-49]. This had led to the concept that biologically distinct populations of neutrophils exist, particularly in disease, when perhaps these are all one adaptable cell type. Neutrophils are an incredibly plastic cell type which allows them to respond and adapt to a variety of stimuli, which in fact may explain the apparent biological differences between these neutrophil “subpopulations” [50].

1.2.1 Low Density Neutrophils (LDN) or granulocytes (LDG)

In healthy individuals the average density of neutrophils is 1.080g/mls. Density gradient centrifugation exploits the density differences between neutrophils and peripheral blood mononuclear cells (PBMCs). In 1986, Hacbarth et al was first to report a form of low density neutrophil elevated in systemic lupus erythematosus (SLE)[51]. Low density granulocytes (LDGs)

are distinct from normal density granulocytes (NDGs) with a density below 1.07 g/mls and sediment in the PBMC layer after density gradient fractionation of whole blood[52-54]. LDGs are expanded in animal models of viral-infection[55] and arthritis[56] and in humans with cancer[47], sepsis[46], HIV[48, 53], COVID-19[57] and various autoimmune conditions, including SLE[52], AAV[58], rheumatoid arthritis (RA)[59] and psoriasis[60]. There is lack of clarity in the phenotypical and functional characteristics of LDGs and in the relationship of LDGs to myeloid-derived suppressor cells (MDSCs) (Table 1). Most studies in autoimmune diseases suggest that LDGs are pro-inflammatory, relatively long-lived and undergo NETosis more readily than NDGs[52, 61]. Therefore, it has been postulated that these cells are a key pathogenic force of autoimmunity[62].

1.2.1.1 LDGs in Autoimmunity

Since their discovery by Hacbarth and Balla in 1986, LDGs are particularly well characterised in SLE[51]. The autoimmune nature of SLE and their propensity to develop glomerulonephritis due to neutrophils makes the study of LDGs in SLE very valuable and may be translatable to the role of LDGs in AAV pathophysiology. In fact, depletion of neutrophils can protect against glomerulonephritis supporting a role for LDGs in the development of autoimmune responses and organ damage[63]. Several studies combine SLE and AAV in one cohort. LDGs have an increased capacity to synthesize type 1 interferons, decreased phagocytosis and an enhanced propensity to forms NETs in SLE [61, 64]. In SLE, the morphology of the nucleus reveals a mixed population of mature (segmented) and immature band or myelocyte like cells as our studies have found in AAV[49, 64]. These findings are supported by a recent study which has found that SLE LDGs have distinct epigenetic and translational heterogeneity and reveal two sub-populations of immature and intermediate mature neutrophils with differences in functionality between the subsets[65]. Furthermore, Rahman et al has examined the role of LDG subsets and found that LDGs are predominantly proinflammatory and do not have suppressive function whereas SLE NDGs were suppressive to T cells[66]

1.2.2 Other Neutrophil Subsets

There has been a burgeoning interest in immunomodulatory neutrophil subsets in the field of cancer in particular. These myeloid-derived suppressor cells (MDSCs) and tumour associated neutrophils (TANs) are associated with poor outcome. Although initially considered an immature neutrophil subset, there is evidence to suggest that these are mixed populations of mature and immature cells with differing immunomodulatory roles[67]. There is a lack of clarity in the phenotypical and functional characteristics of these neutrophil subsets and their relationship to LDGs, this is summarised in Table 1.1.

1.2.2.1 Myeloid derived suppressor cells (MDSC)

Initially MDSC were identified as immature myeloid cells that suppress immune responses and aid tumour progression in mouse models of cancer [68, 69]. The cells were named MDSC by Gabrilovich et al. [70]. There are two subpopulations of MDSC: monocytic (Mo-MDSC) and granulocytic (G-MDSC or polymorphonuclear (PMN)-MDSC) [71, 72]. Pillay et al. suggest that G-MDSC are a *bona fide* phenotype of neutrophils which are found in the low density fraction of peripheral blood and display morphology resembling myelocytes or bands [71, 73]. Mo-MDSC are also found in the low density layer and are morphologically similar to monocytes [74]. MDSC display similar surface marker expression patterns to neutrophils but it is their suppressive functions which define this population: $CD66b^{+}$, $CD16^{+}$, $CD15^{+}$ and $CD14^{-}$ [75]. As reviewed by Rosales in 2018, both Mo-MDSC and G-MDSC are low density, $CD11b^{+}$, $CD33^{+}$ and $CD66b^{+}$, [73]. Mo-MDSC differ from G-MDSC in being $CD14^{+}$ and $CD15^{-}$, whereas G-MDSC are $CD14^{-}$ and $CD15^{+}$ [73, 76]. More recently, mature neutrophils also have been proposed to have suppressive capacity, therefore G-MDSC are often further subdivided based on whether they are $CD16^{-}$ or $CD16^{+/INT}$ which is analogous to LDGs [75]. This highlights the similarities between these subsets. One of the key mechanisms of MDSC suppression involves the enzyme arginase-1 that is stored in the gelatinase granules[77]. When released arginase-1 converts L-arginine to L-ornithine and urea resulting in decreased availability of L-arginine. This inhibits T cell proliferation through several mechanisms, arginine depletion results in a downregulation of the T cell receptor (TCRζ) ζ-chain, which results in cell cycle arrest[78]. Arginine is necessary for the dephosphorylation of cofilin to modulate the actin cytoskeleton. This results in a lack of functional immunological synapses which in turn leads to impaired cell activation[79].

1.2.2.2 Tumour-associated neutrophils (TAN) / N2

Tumour-associated neutrophils (TAN) may be polarized towards two potential phenotypes similar to macrophages: N1, which are anti-tumour, and N2, which are pro-tumour. Each subpopulation has distinct functions, cytokines and gene expression profiles [80, 81]. N2 have circular nuclei while N1 show hypersegmented nuclei [82]. N2 are promoted by transforming growth factor-β (TGF-β) and N1 are recruited by interferon-β (IFN-β), N1 neutrophils are likely stimulated by the tumour microenvironment [80, 82, 83]. Tumour cells use chemokines to attract TANs to the tumour site, such as the potent neutrophil chemoattractant CXCL8, which entrains the CXCR1 and CXCR2 expression on neutrophils. CXCR1 has been shown to contribute to angiogenesis and tumour progression [80, 84]. TANs are believed to be distinct from normal density neutrophils (NDN) and

G-MDSC as TANS exhibit high chemokine production, few granules and low ROS production [85]. TANs may simply be evidence of the plasticity of neutrophils in response to factors in the tumour microenvironments of specific cancers, rather than a novel neutrophil subpopulation [74].

1.2.3 The origin of Neutrophil subsets

There are several theories about the origin of LDNs firstly, LDNs are immature neutrophils which may arise in chronic inflammation as a direct result of emergency granulopoiesis [64, 73]. Secondly, LDNs could be neutrophils after undergoing degranulation and hence display a lower density [73]. Our findings in AAV suggest that these cells are a mixed population of both immature and mature cells with the immature cells likely a result of emergency granulopoiesis [49]. Interestingly, after TGF-β stimulation in a mouse model, LDNs can be derived from mature neutrophils [86]. Deng et al demonstrated in an elegant study that LDGs could be induced from NDGs by in situ exposure to M tuberculosis (Mtb) [87]. As shown in Table 1, G-MDSC, TANs and LDN show very similar surface marker profiles. TANs and LDN also display similar pro-tumour properties, making it biologically difficult to distinguish between these subpopulations. It is possible that the plasticity of the neutrophil and the influence of the tumour microenvironment may explain how all these neutrophil "subpopulations" are in fact a normal neutrophil under the influence of a distinct local environment. There is not enough scientific evidence to confirm that G-MDSC, TAN and LDN are unique cell populations. Cassetta et al. suggest that information in the literature regarding neutrophil subsets, such as G-MDSC, LDN, TAN, is varied and contradictory due to the use of different models and isolation techniques. Surface markers on neutrophils isolated from murine models and non-human primates correlate poorly with corresponding human markers. Not only are cell surface markers different between mice and humans but some neutrophil subtypes, such as MDSC, are isolated from blood in humans but are studied at tissue level in mice [88]. Therefore, standardised protocols are essential to gain further insight into the biological significance of neutrophil subtypes [88].

Disease Area	Specific Condition	Population	Surface Marker Expression	Arginase	Nuclear Morphology	ROS	Reference
Infection	HIV	LDGs	$CD15^+$, $CD11b^+$, $CD13^+$, $CD33^+$,$CD16^{int/lo}$, $CD66b^+CD63^+$	Decreased	Mature		[53]
	COVID-19	G-MDSC	$CD11b^+CD66b^+CD14^-$	Increased	ND	Increased	[57]
	TB	LDGs	$CD15^+$,$CD14^{low}$ $CD16^+$, $CD33^+$, $CD66b^+$ and $CD62L^{low}$,		Mature	Increased in LDGs	[87]
	Sepsis	Interphase neutrophils	$CD16^{int}$, $CD11b^+$, $CD15^+$, $CD33^{-/low}$, $CD54^{-/low}$, $CD62L^{-/low}$, $CD66b^+$ and $CD14^{-/low}$ HLA-DR $^{-/low}$	Increased	Heterogeneous mixed banded and segmented	ND	[46]
Malignancy	Cancer	LDGs	$CD66b^+$, $CD33^+$, $CD16^{var}$, $CD11b^{Var}$, $CD125^-$ HLA-DR^-		Immature		[89]
	Cancer	G-MDSC	$CD11b^+$, $CD14^-$,$CD15^+$, $CD66b^+$, LOX-1^{var}	Increased expression in Lox-1^+	Lox-1^+ mature, Lox-1^- immature	LOX-1^+ increased	[90]
	Hepatocellular carcinoma	G-MDSC	$CD11b^+$,$CD14^-$,HLA-$DR^{-/low}$,$CD15^+$, LOX-1 $^+$	Increased on CD15+ Lox-1+	ND	Increased	[91]
	Renal cell carcinoma	MDSC	$CD66b^+$,$CD11b^+$,VEGFR1$^+$,CD62l ^{low},$CD16^{low}$	Decreased	Heterogeneous 90% segmented	ND	[92]
Autoimmunity	Rheumatoid arthritis	LDGs	$CD10^+$,$CD14^+$,$CD15^+$ $CD16^{int/low}$	ND	ND	Lower than NDGs	[59]
	AAV	LDGs	$CD15^+$ $CD14^-CD16^+$, $CD15^+CD14^-CD16^{int/low}$	Decreased	Heterogeneous mixed banded and segmented	Lower than NDGs	[49]
	Psoriasis	LDGs	$CD10^+CD14^{low}$	ND	ND		[60]
	SLE	LDGs	$CD10^+$,$CD11c^{lo}$,$CD14^{lo}$, $CD15^{hi}$,$CD16^{hi}$, $CD31^+$, $CD114^+$, $CD116^-$	ND*	Heterogeneous Mature, less segmented	ND	[52, 61]
Other	G-CSF treated donors	LDNs	CD66b+, $CD11b^{var}$, $CD10^{var}$, $CD16^{var}$	Increased mRNA, decreased activity	Heterogeneous mixed banded and segmented	Not involved in T Cell suppression	[93]
	Pregnancy	LDGs	$CD15^+$, $CD66b^+$,$CD63^+$,$CD33^+$, $CD16^{int/low}$	Increased on cord vs maternal	ND	ND	[54]

Table 1.1 LDG population characteristics in various disease conditions

Table 1.1 LDG population characteristics in various disease conditions

*HIV= Human Immunodeficiency Virus, TB= Tuberculosis, LDG= Low Density Granulocytes, G-MDSC=Granulocytic Myeloid Derived Suppressor Cells, LDN=Low Density Neutrophils, AAV=ANCA associated vasculitis, SLE=Systemic Lupus Erythematosus, NDG= Normal Density Granulocytes, ND= Not determined, LOX-1= Lectin-type Oxidized LDL receptor-1, var= variable, G-CSF= Granulocyte Colony Stimulating factor

Further work is necessary to determine the origin and relevance of neutrophil subsets in different pathological settings. This will be facilitated by further extensive phenotyping and functional analysis to fully characterise the plasticity of neutrophil subsets. For this work, I propose to compare the phenotype of LDGs in AAV as a model of autoimmune disease and LDGs in COVID-19 representing viral infection.

1.2.4 Neutrophils in the etiology of ANCA Vasculitis

Anti-neutrophil cytoplasm autoantibody (ANCA) vasculitis (AAV) is a systemic autoimmune disease in which neutrophils play a key role [94]. It is characterised by autoantibodies directed against neutrophil proteins myeloperoxidase (MPO) and proteinase-3 (PR3). It is associated clinically with rapidly progressive glomerulonephritis and inflammatory necrosis of small blood vessels in lungs, skin and other organs [95-97]. Binding of ANCA to these antigens leads to inappropriate neutrophil activation, and subsequent damage to endothelial cells, with consequent chronic, unresolving vascular inflammation. The contribution of neutrophils to ANCA induced activation is a complex and multifaceted one. In healthy individuals, mature circulating neutrophils have silenced MPO and PR3 transcription. Neutrophils isolated from patients with active AAV have been shown to aberrantly transcribe the autoantigens MPO and PR3, a feature that directly correlates with subsequent clinical outcome [98, 99]. Primed neutrophils are activated by autoantibodies binding to membrane expressed MPO and PR3. These neutrophils generate NETs, degranulate serine proteases and generate ROS which contributes to vascular tissue injury and AAV pathophysiology [100].

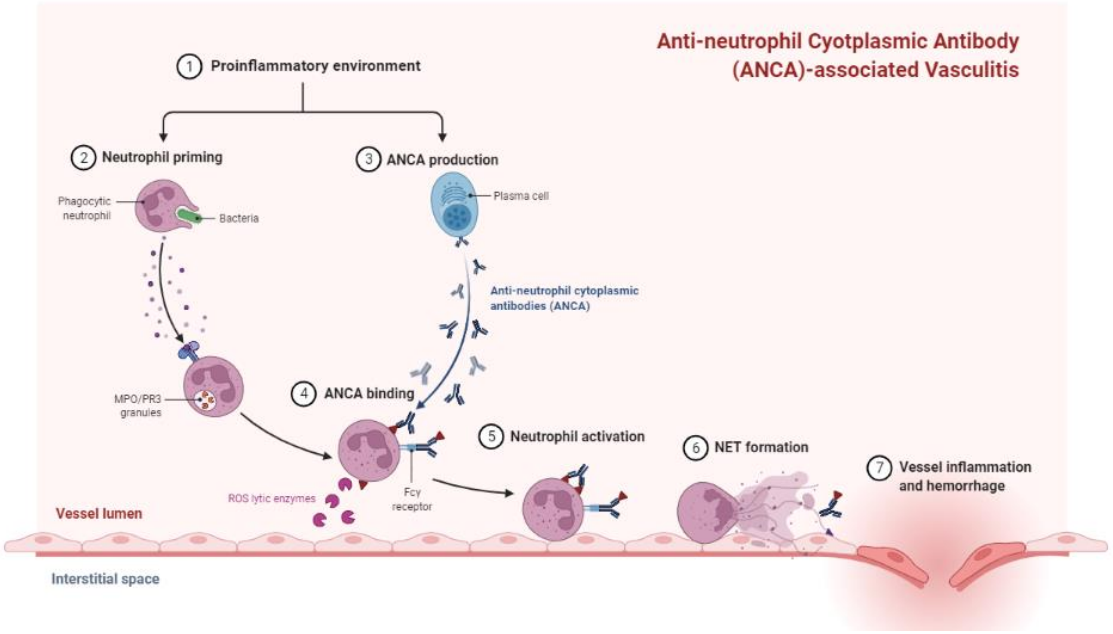

Figure 1.2.1 Neutrophils in the Etiology of ANCA Vasculitis

Schematic overview of neutrophil involvement in AAV. Briefly neutrophil priming leads to the surface translocation of MPO and PR3 that then engage with circulating ANCAs that activate the neutrophil with consequent release of lytic enzymes, ROS and formation of NETs, which cause endothelial cell inflammation and vascular damage.

1.2.4.1 LDGs in AAV

Two studies examined whole-genome gene expression in sorted NDGs versus PBMCs. Lyons et al reported that granulocyte-related gene expression was detected in the PBMC fraction of blood from patients with lupus and AAV compared to healthy controls and correlated directly with the quantity of granulocytes identified in PBMCs by flow cytometry [101]. Cheadle et al, in a recent study, showed that the transcription of granulocytic genes in the PBMC layer, including PR3 and MPO, differentiated AAV patients from healthy controls [102]. These data suggest that LDGs, which by definition are neutrophils that co-localize in the PBMC fraction, are the source of granulocyte gene expression signatures in AAV. More recently Grayson et al concluded that granulocyte-related gene expression in whole blood was associated with disease activity and relatively poor response to treatment in AAV and that LDGs are the likely source of this expression[103]. This data suggests that LDGs, are the source of granulocyte gene expression signatures in AAV. LDGs may play an important role in disease pathogenesis in AAV by promoting direct toxicity to endothelial cells and potentially, by direct involvement in the causal pathway for the generation of ANCAs through

autoantigen externalization due to enhanced NET formation. Endo et al recently reported that LDGs in peripheral blood of AAV patients were higher than healthy controls and were a mixed population of mature and immature cells as defined by CD10 expression with LDGs having a higher propensity to forms NETs than NDGs [104].

1.2.5 Neutrophils in Covid -19

Severe Acute Respiratory syndrome coronavirus 2 (SARS-CoV-2) is a novel beta coronavirus which emerged in the Wuhan region of China in December 2019 and rapidly spread to the rest of the world becoming a pandemic [105]. Neutrophilia and an increased Neutrophil to lymphocyte ratio (NLR) is a feature of this disease and it predicts severe illness in the early stages of disease and is linked to poor outcome [106]. The increase of neutrophils is not limited to peripheral blood but also in the lungs and neutrophil infiltration into the alveolar space was observed in lung biopsies [107]. Respiratory burst from activated neutrophils releases ROS such as superoxide radicals and H_2O_2 which causes oxidative stress that leads to the cytokine storm and thrombosis in severe disease [108]. Neutrophil elastase has been linked to severe COVID-19, this enzyme stored in the azurophilic granules is released to degrade antigens. However, an over-exuberant release can cause tissue damage in alveolar tissue [109]. Many studies have shown that where NETs are elevated in COVID-19 patients, the vascular occlusion NETs cause is not limited to the lungs as there are reports of NETs in the liver and kidney [110, 111]. This highlights the role of the neutrophil in the severity of COVID-19 disease. Clinically it can manifest towards acute respiratory distress syndrome (ARDS) with multiorgan dysfunction including glomerulonephritis and multi-organ failure. These features demonstrate a systemic aspect of this infection in common with the pathophysiology of AAV [112].

1.2.5.1 Neutrophil subsets in COVID-19

One of the most notable immune disturbances in severe COVID-19 is neutrophilia and an increased neutrophil to lymphocyte ratio (NLR). It is not surprising then, that neutrophil subsets varying in their density, maturity and expression of surface markers have been reported in COVID-19 [113-115]. Morrisey et al recently reported on the emergence of a population of low density subset of neutrophil that correlates with disease severity and hypercoagulable state in COVID-19 patients[114]. The authors note that low density neutrophils significantly contribute to COVID-19 related inflammation and coagulopathy. The study discovered a population of $CD45^{+}$, $CD66b^{+}$, $CD16^{int}$, $CD44l^{ow}$, $CD11b^{lnt}$, low-density inflammatory band cells (LDIB) in patients with severe disease. Band in the title refers to the immature nuclear morphology, and this is corroborated by the $CD16^{int}$ expression (a marker of immature neutrophils). The authors used Wright-Giemsa stain to determine the developmental stage of the neutrophils, $CD16^{neg}$ were myelocytes with an ovoid

nucleus, $CD16^{int}$ were band cells with distinctive band shaped nucleus and $CD16^{high}$ populations were segmented mature neutrophils. These cells displayed enhanced phagocytic capacity, spontaneous neutrophil extra-cellular trap formation and elevated cytokine production. These cells associate clinically with systemic TNFα and IL-6 levels and correlated with COVID-19 associated coagulopathy (CAC) and could be used as a marker clinically to monitor the progression of disease. Morrissey suggests that patients with increased $CD16^{int}$ low-density inflammatory band (LDIB) could be identified and appropriate treatment could be implemented early to improve all-cause mortality for severe COVID-19 patients[114].

In another approach, Daamen et al assessed available COVID-19 gene expression datasets from lung and blood using a number of bioinformatic tools to provide a view of the COVID-19 inflammatory response and potential points of therapeutic intervention[115]. To characterize the response to COVID-19 infection, they analysed transcriptomic data from peripheral blood mononuclear cells (PBMCs) and post-mortem lung tissue of COVID-19 patients and healthy controls as well as bronchoalveolar lavage (BAL) fluid of COVID-19 patients. Overall, they found 4,245 differentially expressed genes (DEGs) in the blood (2,166 up and 2,079 down) 2,220 DEGs in the lung (684 up and 1,536 down) and 8,952 DEGs in the airway (BAL) (4,052 up and 4,900 down). In blood, classical and lectin-induced complement pathways as well as the NLRP3 inflammasome, plasma cells (PCs) and monocytes (Mo) were significantly increased in COVID-19 patients, whereas cytotoxic cells and neutrophils were reduced. In lung, the NLRP3 inflammasome, Mo and low-density granulocytes (LDGs) were increased in COVID-19 patients, whereas in BAL, classical and alternative complement pathways were enriched whereas T cells and cytotoxic cells were reduced. LDGs have been shown to produce Type 1 interferons and form NETs and may therefore contribute to disease progression as the formation of NETs is associated with poor disease outcome in COVID-19 patients[107, 109, 116]. This is in contrast to Blanco Mello's findings of a reduced IFN 1 & 111 response in COVID-19[117].

The expansion of the MDSCs is linked to G-CSF and G-CSF is one of the cytokines increased in the lungs of COVID-19 patients[118]. Agrati et al longitudinally analysed four severe and four mild cases of COVID-19 from hospital admission to early convalescence[119]. Shortly after admission all patients showed marked lymphopenia and neutrophilia. A vast expansion of MDSCs was noted. The authors followed this longitudinally for 20 days after admission, the frequency of MDSCs decreased on recovery. MDSCs were shown to suppress T cell function which dampened an excessive immune response. Additionally, a study by Parackova et al describe a shift toward immature neutrophils as the driver of hyperinflammation associated with severe COVID-19 disease[120]. COVID-19 induced ARDs is associated with MDSC expansion, reduced lymphocyte

function and arginine shortage through increased arginase activity. Reizine et al suggest the possibility of arginase supplementation as a therapy for ICU patients aiming to decrease immunosuppression by MDSC and aid viral clearance[108]. Cabrera et al have reported LDGs in COVID-19 that were immature and immunosuppressive that may play a role in COVID-19 pathogenesis[121].

1.3 Phenotyping Neutrophils: Density, Nuclear Morphology and Maturity

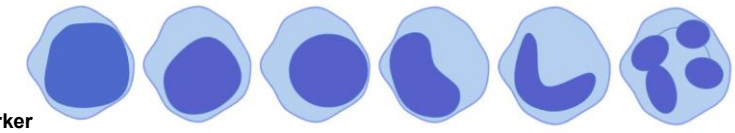

Surface Marker	Myeloblast	Promyelocyte	Myelocyte	Metamyelocyte	Band	Segmented Neutrophil
CD66b	-	+++	+++	++	++	++
CD15	+	+++	+++	+++	+++	++
CD33	+++	+++	++	+	+	+
CD62L	++	++	++	++	++	++
CXCR2	+	+	+	+	++	++
CXCR4	++	++	++	++	+	+
CD18	++	+	+++	++	++	++
CD24	-	-	++	++	++	++
CD11b	-	-	+/++	++	++	++
CD11c	-	-	++	++	++	++
CD177	-	-	+	+	+	+
CD16	-	-	-	+	++	+++
CD87	-	-	-	-	++	++
CD10	-	-	-	-	-	++
CD35	-	-	-	-	++	++
HLA-DR	+	-	-	-	-	-
CD34	+	-	-	-	-	-
CD117	+	+	-	-	-	-
CD49d	+	+	+	+	-	-
CD101	-	-	-	+	++	+++

Figure 1.3.1 Surface Marker Expression during granulopoiesis

1.3.1 Neutrophil Density and its association with neutrophil development

The increased granularity and cell size that occurs with neutrophil maturity is directly proportional to a change in density [122]. Therefore, neutrophil lineages can be separated using density gradient centrifugation [122]. Mature neutrophils localize in normal to high density fractions, while immature neutrophils reside in low density fractions, although this is probably preparation dependent and the low-density fraction is likely a mixed population of neutrophil maturity [86, 122].

1.3.2 Nuclear Morphology

Neutrophil subtypes differ in their nuclear morphology. The most immature neutrophils, the myeloblasts have large, sphere-shaped nuclei containing few nucleoli [123]. Promyelocytes and myelocytes lack nucleoli and exhibit elevated chromatin condensation compared to myeloblasts [123]. An indented nucleus is characteristic of a metamyelocyte. The band cell nucleus is shaped like a horseshoe and it constricts to form nuclear lobes, while segmented neutrophils are distinguishable by their segmented nucleus with three to five lobes [123]. The thin filaments which connect the lobes contribute to the migratory capability of mature neutrophils [124].

1.3.3 Neutrophil surface marker expression during granulopoiesis

Neutrophil surface markers change to facilitate altered functions as the neutrophil matures (Table 2). During this process, immature surface markers are no longer expressed (e.g. CD49d) and markers of maturity appear (e.g. CD10) [125]. Although there is no consensus on human neutrophil phenotypic markers on flow cytometry, the following are commonly used: $CD11b^{+}CD66b^{+}CD15^{+}CD14^{-}$ [74]. CD16 is a marker of phagocytic capacity and may be used to exclude $CD16^{-}$ eosinophils. $CD14^{+}$ cells are considered to be mostly macrophages and monocytes, although some studies indicate that neutrophils express CD14 at low levels [126, 127]. CD16 is exclusively expressed at the metamyelocyte stage and is highly expressed by banded and segmented neutrophils, while activation marker CD11b is only found at the myelocyte stage onwards [128-132]. CD11b and CD18 form the Mac-1 complex which plays a role in phagocytosis and migration with CD18 expression commencing at the myeloblast stage of granulopoiesis [125]. Differentiation marker CD15 and activation marker CD66b are found on all neutrophil subpopulations; these are also core markers of neutrophil lineage [125, 133, 134]. Surface markers may be expressed at low, medium or high intensities (**Figure 1.3.1**) [125, 133].

1.3.3.1 Markers of maturity and immaturity

As neutrophils differentiate, their nucleus progresses from an immature banded morphology to a segmented one allowing for the identification of distinct staged of maturity. Neutrophils express receptors for IgG antibodies, which allow phagocytosis of IgG opsonized microbes and can trigger activation of cell by the crosslinking of many receptors [135]. CD16 is a type 111 Fcγ receptor (FcγR). FcγRs through IgG antibodies allow neutrophils to adopt a key feature of adaptive immunity: an antigen-specific response There are two isoforms in humans, CD16a and CD16b. They have a sequence similarity of 96% in their extracellular immunoglobulin binding regions[136]. CD16a is predominantly expressed on mast cells, macrophages and natural killer cells as a transmembrane receptor. CD16b is present exclusively on neutrophils and is anchored by a glycosyl-phosphatidylinositol linker (GPI) to the plasma membrane. CD10 is a known marker of neutrophil maturity[137]. There is evidence to support that CD16 is shed on apoptosis, so is there evidence to suggest that LDGs are apoptotic cells [138]? In rheumatoid arthritis, Wright et al show that RA LDGs have a constitutively lower rate of apoptosis than normal density neutrophils [59]. They cocultured LDGs and NDGs for 18 hours and then measured levels of Annexin V by flow cytometry. Despite having low levels of CD16, these cells were not apoptotic and furthermore there was significantly lower expression of apoptotic genes in LDGs than NDGs.

CD10, a marker of differentiation and maturity is found only on mature segmented neutrophils, and absent on immature neutrophils. Immature $CD10^-$ neutrophils may be important drivers of inflammatory disease and neutropenia [128, 133, 134]. Reduced surface expression of CD10 and CD16 on granulocytes predicts poor outcome in sepsis patients [139]. $CD10^{dim}$ immature neutrophils have been implicated in the immunosuppression observed in sepsis [140].

HLA-DR, which is involved in antigen presentation to $CD4^+$ T cells, and CD34, an adhesion marker, are two markers exclusively expressed on the most immature neutrophil, the myeloblast [131, 141]. CD33 is a differentiation marker found on myeloid blast cells in acute myeloid leukemia (AMLS) [142]. CD33 surface expression is gradually downregulated from the myeloblast stage to segmented neutrophil, with a low level expressed on the latter [143, 144]. CD33 is strongly expressed on monocytic MDSC and maybe used to identify very immature MDSC that are both CD14 and CD16 negative. These are called early stage MDSC (eMDSC)[145].

Evrard et al recently reported using CD101 as a marker for mature neutrophils. This marker is not an established maturation marker and requires validation. They screened for differentially expressed genes (DEGs) that could distinguish mature neutrophils and identified CD101 which

encodes a surface marker and was upregulated significantly in bone marrow mature and peripheral blood neutrophils[146].

The integrin very late antigen complex 4 (VLA-4) is involved in the adhesion of hematopoietic progenitor cells and leukemic blast cells in AMLS [147]. VLA-4 is composed of CD49d and CD29, CD49d being a commonly used marker of neutrophil immaturity [147, 148]. Promyelocytes, myelocytes and metamyelocytes are $CD49d^+$ while more mature bands and segmented neutrophils are $CD49d^-$ [130]. Given the role of CD49d in the recruitment of progenitor cells leukemic blast cells and their migration from the bone marrow, it is likely that CD49d must be expressed on neutrophil blast cells [149, 150]. Interestingly, CD49d expression reappears on the surface of aged neutrophils [151].

Surface expression of CD177, a receptor involved in extravasation and surface expression of proteinase-3, begins at the myelocyte stage [152]. Interestingly, there is an increase in $CD177^+$ circulating neutrophils in diseases such as sepsis, ANCA vasculitis and SLE [153, 154].

1.3.4 Markers linked to activation

The expression of lectin-like oxidized low density lipoprotein receptor-1 (LOX-1) is reported as one of the most upregulated genes in PMN-MDSC. It is a receptor for oxidised lipoprotein linked to oxidative stress and has not been associated with steady state neutrophils, it has been suggested to differentiate between MDSCs and NDGs[90]

CD62L L-selectin is constitutively expressed on neutrophils and is linked to the rolling and tethering of these cells. It is enzymatically cleaved and shed from cell surface by members of a desintegrin and metalloprotease domain (ADAM) family of surface metalloproteinase on neutrophil activation[155].

CD63 is a tetraspanin expressed on the membrane of azurophilic granules on neutrophil degranulation. CD63 is expressed on the neutrophil cell surface and is therefore a valuable marker of neutrophil degranulation and activation[156]. It is known as an activation antigen as its surface expression is upregulated on stimulation[157]

1.3.5 Chemokines

Immature neutrophil retention in the bone marrow is achieved by the crosstalk between CXCR4 expressed on neutrophils and CXCL12 by bone marrow stromal cells [146, 158]. CXCR4 is involved in neutrophil retention in the bone marrow and return of aged neutrophils to the bone marrow [146, 158]. Upregulated expression of CXCR4 on segmented neutrophils ready to undergo senescence or apoptosis triggers their return to the bone marrow where they are engulfed by

macrophages [43, 159]. While both immature and mature neutrophils express CXCR4, immature neutrophils may express a higher level of CXCR4 than mature cells [133, 146]. The chemokine receptor CXCR2 plays a role in neutrophil mobilisation and exit from the bone marrow [125, 160]. Immature neutrophils before the band stage exhibit reduced CXCR2 surface expression compared to bands and segmented neutrophils [133, 146]. However, CXCR4 and CXCR2 may not be useful in differentiating between neutrophil subtypes due to similar expression levels in each population.

Thus, surface markers on neutrophils demonstrates that flow cytometry and imaging techniques could be employed to separate neutrophil lineages based on surface marker expression and nuclear morphology. This information highlights that banded neutrophils and segmented neutrophils are the most similar in their surface expression of markers and may be the most difficult to differentiate due to a lack of unique markers on either cell type [161, 162]. Some surface markers undergo changes following migration, e.g. CD62L and activation, e.g. CD11b/CD18, which makes it difficult to identify highly specific markers of maturity [122].

1.3.6 Arginase

Neutrophils have long been considered to function mainly as very efficient innate killers of micro-organisms at infected sites, their immunomodulatory role has only recently been recognized and has gained considerable attention [163]. Amino acid metabolism has been shown to be a crucial regulator of the immune response by restricting concentrations of essential amino acids, T-cell proliferation and activation can be modulated[164]. One of the key modulators of T cell suppression has been the enzyme arginase that degrades arginine. L-arginine is a semi-essential amino acid that may be sourced from the diet or produced by certain cells through a partial or complete urea cycle. L-Arginine has a vital role in the composition of essential proteins and l-arginine is a substrate for the enzyme nitric oxide synthase (NOS) which catalyses' the conversion of arginine into nitric oxide (N0) and citrulline [165].

1.3.7 Arginase enzymes

Arginases are manganese-containing enzymes that hydrolyse l-Arginine to L-ornithine and urea in the liver urea cycle [166]. Arginases have another primary physiological function, to produce ornithine necessary for the production of polyamines and proline. Polyamines have an essential role in wound healing and tissue repair and proline is needed for collagen formation [167]. Originally, it was thought that arginase was only expressed in the liver, however, further studies have shown that arginase is expressed in many cell types [165]. There are two different isoforms of arginase - cytoplasmic arginase 1 and mitochondrially-located arginase II. These are encoded by different genes. Arginase 1 consists of 322 amino acids, is cytoplasmic and is expressed by liver cells

where it catalyses highly toxic ammonia to excretable urea. It is also found in myeloid cells of granulocytic origin [168]. Arginase 2 has 354 amino acids and has a 58% sequence homology to arginase 1 and both enzymes have an almost identical catalytic region[169].

1.3.7.1 Arginase in the immune system

The concept of arginase-related immunosuppression was mooted nearly 40 years ago where the complete depletion of arginine suppressed cultures [170]. Arginine metabolism was shown to be vital for immune response. Murine macrophages have an inducible form of iNOS when stimulated with microbial products or cytokines and this is the main mechanism of cytotoxic activity of macrophages against bacteria viruses helminths and tumour cells [171]. The concept that arginase expression in macrophages is inducible by the activation of the cells by T cell cytokines in particular Th 2 cytokines led to a renewed interest in the balance of arginine metabolism as controlling the immune response. The synergy of Th1 and Th2 cytokines and their induction of the enzymes iNOS and arginase respectively clearly illustrate the role of arginine metabolism in the adaptive immune response [172, 173].

1.3.7.2 Mechanism of the immunomodulatory function of Arginase

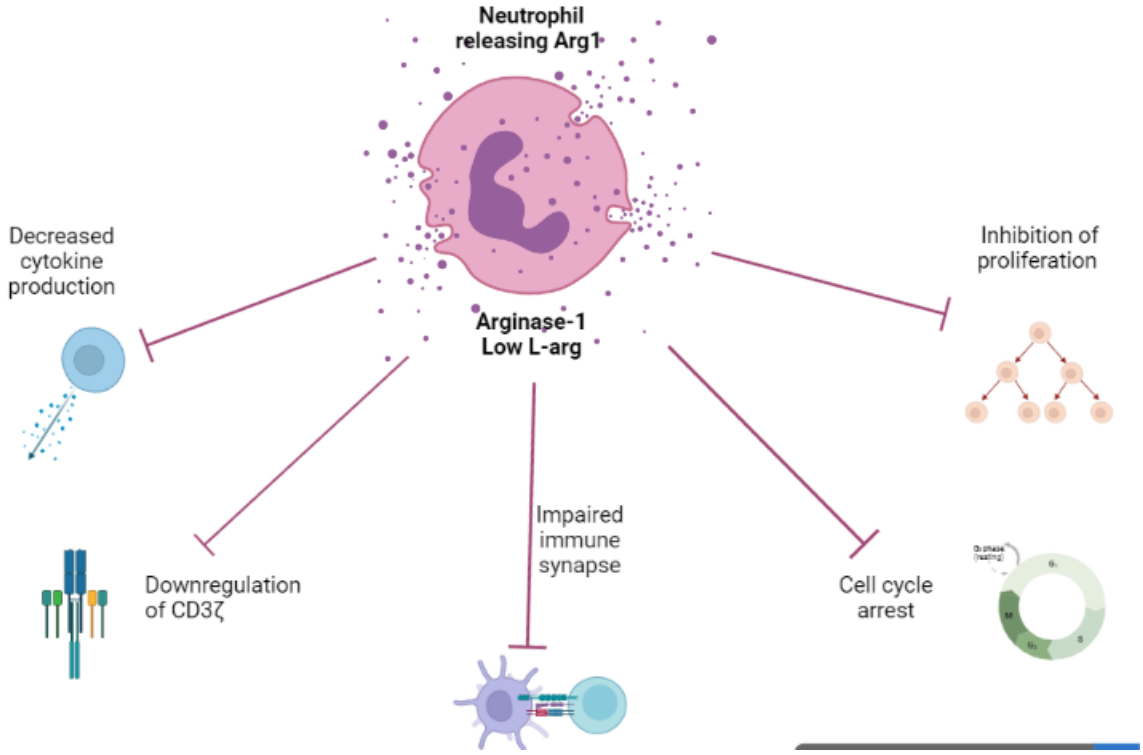

Figure 1.3.2 The immunosuppressive effects of Neutrophil derived Arginase 1

L-arginine depletion by Arginase 1 inhibits the immune response by T cells. Low L-arginine levels result in the inhibition of Tcells by inhibiting proliferation and causes decreased cytokine production. This is a result of the downregulation of the CD3ζ part of the T cell receptor, impaired immune synapse formation between Tcells and APCs and cell cycle arrest. Schematic created with Biorender.

One of the key hallmarks of arginase in the immune response is the impaired proliferation of T cells **(Figure 1.3.2).** The proliferation of human T cells is completely inhibited in l-arginine-free medium following stimulation with anti-CD3/CD28 coupled beads. This effect can be restored by l-arginine supplementation[174]. The exact mechanism of T cell suppression is unknown but it has been shown that deprivation of l-arginine can affect the expression of the T cell receptor, CD3ζ chain[175]. CD3ζ is a critical component of the T cell receptor complex that couples intracellular signalling to antigen recognition. Another mechanism by which depletion of l-arginine restricts T cell proliferation and activation is cell cycle arrest. Low levels of l-arginine arrests T cells in the G_O-G_1 phase of the cell cycle thereby preventing T cell development and proliferation[78]. Another mechanism is impaired immune synapse formation, In the absence of arginine, formation of the immune synapse is impaired due to lack of dephosphorylation of cofilin. Cofilin is an actin-

remodelling protein that couples the activation of T cells via co-stimulatory receptors and the TCR in the immune synapse, this was reversed by the use of an arginase inhibitor[79]. These results give a mechanism whereby l-arginine depletion by high arginase activity can contribute to T cell dysfunction in diseased states.

1.3.7.3 Arginase expression in Neutrophil subsets in disease

There has been a growing interest in immunomodulatory neutrophil subsets in the field of cancer in particular. These myeloid derived suppressor cells (MDSCs) and tumour associated neutrophils (TANs) are associated with poor outcome. One of the key features of these cells is their immunosuppression by Arginase 1, this is summarised in **Table 1.1**

Arginase 1 is constitutively produced by the gelatinase granules of polymorphonuclear cells[176]. Normal resting neutrophils do not release arginase. It is stored in the gelatinase granules and released intracellularly to combat microbial attack. A study showed that in contrast to healthy patients, patients with colorectal cancer (CRC) had increased levels of arginase activity in peripheral blood released by cells during inflammation [177]. If arginase I is released from MDSC, one would expect a decrease in intracellular arginase I in MDSC. Rodriguez et al reported that MDSC purified from RCC patients had a far lower arginase activity and expression compared with healthy control neutrophils and autologous normal neutrophils. They reported that arginase I mRNA expression was increased in MDSC compared with PMN from normal controls and autologous neutrophils suggesting an increase in arginase I transcription to compensate for the increased release of enzyme[92].

1.3.7.4 Mechanism of Arginase release from Neutrophils

Concomitant release of azurophilic and tertiary granules is required to ensure active enzyme activity. Arginase enzymatic activity is dependent on pH, in fact the optimal pH is a strong alkaline environment (pH 9.5-10.5) with negligible activity at physiological pH. Can exocytosed Arginase 1 effectively catabolize arginine and under normal physiological conditions cause immune suppression? An elegant study by Rotondo et al addressed these key issues[178]. The authors reported that Arginase released from the gelatinase granules of neutrophils is in fact inactive at physiological pH. Concomitant release of factors stored in azurophilic granules is required for activity of the enzyme. By using protease inhibitors, the authors demonstrated that serine proteases are involved in arginase activation and processing. The requirement for arginase to be cleaved to function at physiological pH could underlie a control mechanism whereby accidental activation of the enzyme could result in immune suppression. It is reported that gelatinase granules are easily mobilised and azurophilic granule release is tightly controlled, this results in the release

of extracellular arginase 1 as a stringently controlled phenomenon [13]. IL-8 is a key cytokine involved in the exocytosis of arginase 1 by neutrophils [179].

1.3.7.5 Arginase activity in peripheral blood is reflective of cellular immunomodulation

In human solid tumours, neutrophils infiltrating lung tumours were found to have reduced intracellular Arginase 1 suggesting arginase release into the tumour microenvironment. This was also demonstrated in renal cell carcinoma (RCC) [92, 180]. In a seminal study by Sippel, they demonstrated an expanded population of degranulated neutrophils and elevated serum levels of Arginase 1 in the serum of patients with glioblastoma (GBM), they also found that T cell CD3ζ expression was decreased and a population of neutrophils were shown to suppress T cell function *in vitro*[181]. This is corroborated by a study in RCC whereby MDSC-type neutrophils released arginase into the circulation[182]. Subsequently, increased serum levels of Arginase 1 have been correlated to disease activity in many conditions including viral infection, sepsis and cancer (**Table 2**). Inhibiting arginase activity using an arginase inhibitor can restore T cell function and the immunosuppressive action of arginase can be ameliorated by supplementation with arginine providing a potential therapeutic target in many disease states[181, 183]

1.3.8 Arginase in COVID-19

A recent study by Derakhshani et al reported that Arginase 1 was an upregulated gene in Covid -19 and has the potential to be a useful marker for the pathogenesis of this disease [184]. Using a cohort of 21 healthy and 21 COVID-19 patients gene expression of Arg 1 was measured by real time PCR. The results indicated that Arg 1 expression was significantly upregulated in COVID-19 patients compared to their healthy counterparts and there was 2.3-fold increase in Arg 1 expression in whole blood. Interestingly, the receiver operating characteristic (ROC) analysis showed that Arg 1 expression could have significant prognostic potential for the pathogenesis of COVID-19. A bioinformatics study identified Arg 1 as one of the most important genes involved in this disease. This study also demonstrated that neutrophil degranulation and neutrophil activation are the most activated biological processes in COVID-19 and suggest that arginase inhibitors could be beneficial in treating COVID-19 [185]. Work on a murine model of Asthma showed sex differences in response to Arg 1 deletion, emphasizing that ablation of Arg 1 improved lung function in male mice only, the authors suggest that the modulation of Arg 1 activity would benefit only male mice [186].

1.3.8.1 Arginase role in viral-induced disease

As a result of coevolution with their hosts, viruses have developed strategies to ensure their own replication and survival and evade the host immune system. Arginase 1 activity has important wound healing functions but also can diminish the antiviral immune response during viral infection [187]. In an interesting murine study of acute and chronic strains of LCMV (lymphocytic choriomeningitis) infection, the acute strain was cleared by a robust CD8 T cell response. However, the persistent chronic strain had T cells with impaired functionality which allowed the virus to persist. This study found that Arginase 1-releasing cells were responsible for the suppression [188, 189]. In human viral infection, a study by Cai et al has shown that that patients with chronic HCV had high levels of MDSCs in their PBMCs that suppressed T cells in an Arg 1 dependent manner [190]. In HIV and Leishmania parasitic infection, both conditions have reported high levels of arginase in patient plasma. However, coinfection patients had increased arginase activity with the authors suggesting that increased arginase activity in coinfection may lead to poor outcome and impaired immune responses in these patients [191, 192]

Detrimental to Host	Immunopathologic		
		SARS-CoV-2	[184]
		Murine herpesvirus-69 (MHV-68)	[193]
	Promotes Viral resistance	LCMV clone 13	[194]
		Hepatitis C (HCV)	[195]
		Human Immunodeficiency virus(HIV)	[191]
		Hepatitis B (HBV)	[196]
		Human papillomavirus	
Beneficial to host	Tissue repair/regeneration	Influenza	[197]
		Respiratory syncytial virus	[198]
		Coxsackievirus B3(CVB3)	[199]

Table 1.2 Differential roles for Arginase in viral-induced disease

1.4 The case for whole blood analysis of neutrophils

The discovery of low density and immature neutrophils in the PBMC layer had led to a resurgence of interest into the role of neutrophils in disease settings. However, most studies have focused on this population erroneously perhaps, excluding most of the neutrophil population. To elucidate all neutrophil subsets that could trigger severe pathology it is imperative that all putative subsets are identified by performing whole blood immunophenotyping. To identify these cells in whole blood, surface markers would have to define the immature low-density fraction and the mature low-density fraction whereas the normal density neutrophils are predominantly CD16 positive, additional markers are required to define the mature low-density cells. Preliminary work had led to CD62l being a definitive marker of LDGs. The literature highlighted two groups who claim that CD10 or LOX-1 definitively define the LDG subsets [90, 200]. A 2012 study by Pillay et al identified an immunosuppressive population of $CD16^{+}CD62l^{low}$ neutrophils induced in humans (volunteers) following injection of a low dose of bacterial liposaccharide LPS, these cells inhibited T cell function, and these potentially allow identification of a subtype of neutrophils that may reflect the mature LDG phenotype ($CD16^{+}$)[162]. To categorically define the LDG immature subset, markers of immature neutrophils are necessary. Evrard's mass cytometry (CyTOF) study of the developmental analysis of bone marrow neutrophils, provided additional markers to identify the subpopulations in whole blood. In particular, Evrard used CD49d and CD101 to identify pre-neutrophils in human bone marrow and further gated on CD10 and CD16[146]. Finally, Ng et al's definitive review collated known markers of neutrophils and suggested a panel for identification of neutrophil subsets [2]. Despite recent efforts to phenotype and characterise neutrophil subsets there is not a definitive panel of surface markers that will allow identification of these cells in whole blood. The current phenotyping of LDGs is reliant solely on density gradient centrifugation. Density gradient centrifugation itself may enrich for activated neutrophils and surface markers may be altered by shedding during the centrifugation step. Our aim is to develop a panel of markers that will allow identification of these cells in peripheral blood and ideally in tissues which would allow further insight into the role of these cells in autoimmune disease. Neutrophils are short lived and circadian rhythms are particularly relevant. Marked diurnal changes can occur in a phenomenon known as neutrophil ageing. It has been shown that neutrophils lose CD62l and gain CD11b and CXCR4 expression over 6 hours and nuclei may become hypersegmented [35, 201]. The development of a definitive phenotyping panel would eliminate the need for time consuming and potentially activating centrifugation and allow for a more accurate characterisation of LDGs in AAV. It is also unclear at present whether LDG subsets originate by granulopoiesis from dedicated progenitors in bone marrow or whether they are a functional subset whose phenotype is acquired in response to

specific signals in peripheral blood. Our study suggests that emergency granulopoiesis is the source of the immature subsets but further work needs to be carried out to determine the origin and function of these cells and of the mature LDG subsets[49].

1.5 Hypothesis and aims

The hypothesis of this study is that neutrophil subsets are implicated in the pathogenesis of many inflammatory conditions and display a plasticity in their phenotype and function in different disease states. Using AAV as an example of autoimmunity and COVID-19 as a model for viral infection, the main aims of this study are:

- to phenotype neutrophil subsets in AAV and COVID-19
- to Investigate the immunomodulatory potential of neutrophils subsets using arginase expression and activity
- to identify neutrophil subsets in whole blood removing the requirement for density gradient centrifugation

Chapter 2

Materials & Methods

2 Materials & Methods

2.1 Materials

2.1.1 Reagents

Reagents	Company
4% paraformaldehyde (PFA)	Santa Cruz, Texas, USA
4% PFA	Santa Cruz USA
BD FACS lysing solution	BD Biosciences, Oxford, UK
Bovine serum Albumen (BSA)	Fisher Scientific
DAPI	Sigma-Aldrich , Missouri, USA
Dextran	Sigma-Aldrich, Missouri, USA
DMSO	Fisher Scientific
EDTA	Sigma Aldrich
Ethanol	Sigma Aldrich, Wicklow, Ireland
Ethanol	Sigma Aldrich
FACS tubes	BD Biosciences, Oxford, UK
Fc Block (Human)	BD Biosciences, Oxford, UK
FCS	Sigma Aldrich, Wicklow, Ireland
Foetal Calf Serum(FCS)	Greiner Bio-One, Kremsmunster, Austria
Glasstic slides	KOVA International , California, USA
Hoechst dye	Thermo Fisher Scientific, Loughborough,UK
Lithium heparin vacuettes	Greiner Bio-One, Kremsmunster, Austria
Live/Dead Aqua stain	Invitrogen, Loughborough, UK
NaOH	Sigma Aldrich, Wicklow, Ireland
NH_4Cl	Sigma Aldrich, Wicklow, Ireland
OneComp beads	eBioscience, California, USA
PBS	Thermo Fisher Scientific, Loughborough, UK
Penicillin/Streptomycin	Gibco
Percoll	GE healthcare, Uppsala, Sweden
Phosphate buffered Saline (PBS)	Thermo Fisher Scientific, Loughborough,UK
PowerUp SYBR Green Master Mix	Thermo
RNase	Roche
Roswell Parks Memorial Institute Medium (RPMI)	Thermo Fisher Scientific, Loughborough,UK
Saponin	Sigma Aldrich, Wicklow, Ireland
Sodium Azide	Sigma Aldrich, Wicklow, Ireland
Sodium Bicarbonate	Sigma Aldrich, Wicklow, Ireland
Tris-HCL	Sigma Aldrich, Wicklow, Ireland
Trypan Blue	Thermo Fisher Scientific, Loughborough,UK
Trypan Blue	Sigma Aldrich, Wicklow, Ireland
Tween 20	Fisher Scientific
Virkon	Thermo Fisher Scientific, Loughborough,UK

2.1.2 Buffers

Buffers	
2% Dextran	2% in PBS
2% PFA	4% PFA in FACs buffer
20% Blocking Buffer	20% FCS in PBS
Cell Culture Medium	RPMI-1640+10%FCS+100IU/mls penicillin/streptomycin
FACS buffer	2% fetal calf serum in PBS
Permeabilisation Buffer	0.2% Saponin in FACs buffer
RBC lysis buffer	155mM NH_4Cl, 0.1mM EDTA, 12mM $NaHCO_3$ pH 7.4

2.1.3 Kits

Kits	
Arginase assay kit	Sigma -Aldrich
Cell proliferation Cell trace violet kit	Invitrogen
High-Capacity cDNA Reverse Transcription Kit	Applied Biosystems.
Human Arginase 1 HK386	Hycult Biotech
Pure link RNA extraction kit	Ambion

2.1.4 Equipment

Equipment	
0.2µm minisart plus	Sartorius
6 well plate	Sarstedt
96 well plate	Sarstedt
Amnis CellStream	Amnis Corporation, Seattle, WA
Centrifuge	Eppendorf Hamburg, Germany
Eppendorf tubes	Sarstedt
FACS Canto II flow cytometer	BD, San Jose, USA
FACs tubes	Fisher Scientific
ImageStream X MkII imaging flow cytometer	Amnis Corporation, Seattle, WA
Laminar air flow class II safety cabinet	Thermo Electron Gmbh Germany
Light Microscope	Olympus Corporation ,Japan
Multichannel pipette	Thermofisher
NanoDrop™ 2000/2000c Spectrophotometer.	Labtech International UK
Ph Meter	Hanna Instruments
Pipette tips p200/p100/p1000	Sarstedt
Pipettes 5/10/25 mls	Corning
Plate Reader	Molecular Devices
Syringes 10/50mls	Terumo N.V
Tissue culture plates 6/24	Sarstedt

Tubes .2/2/5/10mls	Sarstedt
Vortex	Scientific Industries NY, USA
Water Bath	Fisher Scientific USA

2.1.5 Software

Software	
FACSDiva software	BD Oxford
FlowJo 10.8.1	Treestar INC, NJ,USA
GraphPad Prism 9.1.0 software	GraphPad Software, San Diego, CA, USA
IDEAS 5.0 software (Amnis).	Amnis Corporation, Seattle, WA
INSPIRE data acquisition software	Amnis Corporation, Seattle, WA
Kaluza software Version 2.1	Beckman Coulter, USA
QuantStudio™ Real-Time PCR Software 1.3	Applied Biosystems

2.2 Methods

2.2.1 Methodology Overview

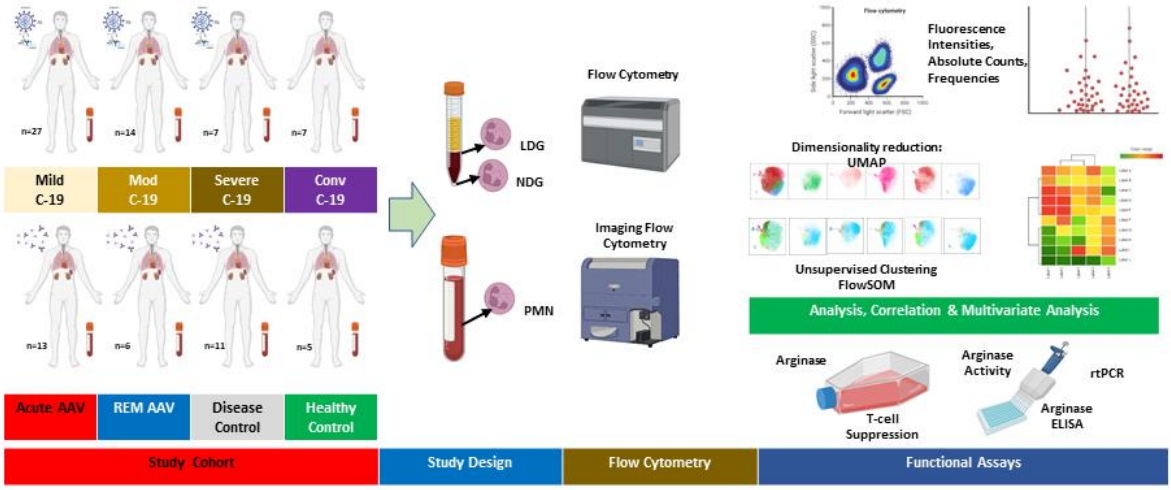

Figure 2.2.1 Thesis Workflow

2.3 Patients

We recruited AAV patients with acute disease (n=13), those in remission (n=6), age matched healthy controls (HC, n=5) and disease controls (DC, a mix of renal impairment and non-AAV systemic inflammation, n=11, Chronic kidney disease n=3, Coronary artery disease n=1, Stroke n=1, Colorectal carcinoma n=1, IgA vasculitis n=1, rheumatoid arthritis n=4). All patients with AAV fulfilled the revised Chapel Hill Consensus Conference classification (Jennette, Falk et al. 2013). Active AAV was defined by a Birmingham vasculitis activity score (BVAS) ≥2 and remission by BVAS=0. All treated acute patients had steroid administered on the day of blood draw. The median duration of steroid use was 1 day (range 1-25 days). Disease/healthy controls and patients with AAV were recruited from the Rare Kidney Disease Registry and Biobank (www.tcd.ie/medicine/thkc/research/RKD-Registry-Biobank.php). Umbilical cord blood (UCB) was obtained from mothers undergoing vaginal deliveries with healthy term pregnancy; the babies had normal Apgar scores. The

study was approved by institutional ethics committees of Tallaght, St Vincent's, St James and Beaumont Hospitals, and all recruits provided written informed consent. COVID-19 blood samples were obtained with full consent from individuals with a positive SARS-CoV-2 nasopharyngeal swab PCR at St James's Hospital (SJH). See Table 2. This study was carried out in accordance with the Code of Ethics of the World Medical Association. Ethical approval was granted by the Tallaght University Hospital (TUH) / St. James's Hospital (SJH) Joint Research Ethics Committee (reference REC 2020-03). Informed consent was obtained from all participants. We recruited patients with a positive real-time PCR test for SARS-CoV-2 on nasopharyngeal aspirates at SJH and TUH over a six-month period. Demographic, clinical and immunological measures were recorded for participants enrolled in this study (**Table 2.1**).

Characteristics			**HC**	**DC**	**AAV-Active**	**AAV-Remission**	**COVID-19**
n			5	11	13	6	55
Age, median (range), years			70 (66-72)	53 (43-87)	73 (40-85)	57 (41-70)	64(28-96)
Male/Female			3/2	5/6	6/7	4/2	33/22
ANCA status, *n* (%)	**Anti-MPO**		NA	NA	9 (69)	3 (50)	NA
	Anti-PR3		NA	NA	4 (31)	3 (50)	NA
WHO severity, n (%) 0 Conv| 1-3 Mild| 4 moderate| 5-8 Severe			NA	NA	NA	NA	7(13) | 27(49) |14(25) | 7(13)
Diagnosis, *n* (median disease duration at sampling, mth)	**GPA**		NA	NA	4 (0)	3 (143)	
	MPA		NA	NA	9 (0)	3 (35.2)	
Disease duration at sampling, Median(range) days	**COVID-19**						7(0-23)
BVAS, median (range)			N/A	N/A	16 (3-25)	0	N/A
CRP (mg/dL), median (IQR)			N/A	9 (3-26)	24 (4-60)	6 (1.8-14)	27 (6.8-48.8)
Creatinine (µmol/L), mean (SEM)			N/A	187 (63)	253 (69)	153 (52)	
eGFR (ml/min), mean (SEM)			N/A	57.1 (8.3)	17.0 (7.9)	36.0 (6.9)	
Immunosuppression treatment, *n* (%)	**Treatment naïve**		5 (100)	5 (45)	5 (38)	0	34(62)
	CYC	**0-6 mths**	0	1 (9)	1 (8)	4 (67)	
		6-12 mths	0	0	0	0	
		>12 mths	0	1 (9)	0	2 (33)	
	Aza	**Current**	0	0	1 (8)	2 (33)	
	MMF	**Current**	0	0	0	2 (33)	
	MTX	**Current**	0	0	0	1 (17)	
	Anti-TNF	**Current**	0	4 (36)	0	0	1(0.55)
	Corticosteroids	**Current**	0	2 (18)	8 (62)	6 (100)	18(38)

Table 2.1 Baseline characteristics of the study subjects, by disease classification

*AAV= Anti-neutrophil cytoplasmic antibody (ANCA)-associated vasculitis; BVAS= Birmingham Vasculitis Activity Score; CRP= C-reactive protein; eGFR=Estimated glomerular filtration rate, GPA=Granulomatosis with polyangiitis, MPA=Microscopic polyangiitis, CYC=duration since cyclophosphamide exposure, Aza=Azathioprine, MMF=mycophenolate mofetil, MTX=Methotrexate WHO= World Health Organisation

2.4 Density Gradient Centrifugation

Venous blood samples were collected in lithium-heparin vacutainers (Becton Dickinson, New Jersey, USA). PBMC/LDGs and NDGs were isolated by a modified Percoll (GE healthcare, Uppsala, Sweden) gradient centrifugation procedure [53, 64] and stained immediately for surface markers as listed **(Table 2.2).** Time from blood draw was <4 hours in all cases. Briefly, an equal volume of 2% Dextran (Sigma-Aldrich, Missouri, USA) was added to 6-12mls blood and inverted 20 times. Erythrocytes were left to sediment by gravity for 30 min; the supernatant was then spun at 200g with no brake. The pellet was re-suspended in 3mls 55% Percoll, slowly layered over 4.5mls 65% Percoll and spun without brakes for 30 min at 1500g **(Figure 2.4.1).** The PBMC/LDG and NDG layers were carefully removed to fresh tubes, cells were washed with PBS and the resulting cell pellets incubated with 10mls of RBC lysis buffer (155mM NH_4Cl, 0.1mM EDTA, 12mM $NaHCO_3$ pH 7.4) for 5 min. After washing, the cells were re-suspended in 1mls of FACS buffer (2% fetal calf serum in PBS). Viability was determined using Trypan blue (Gibco) and in all cases was >90%.

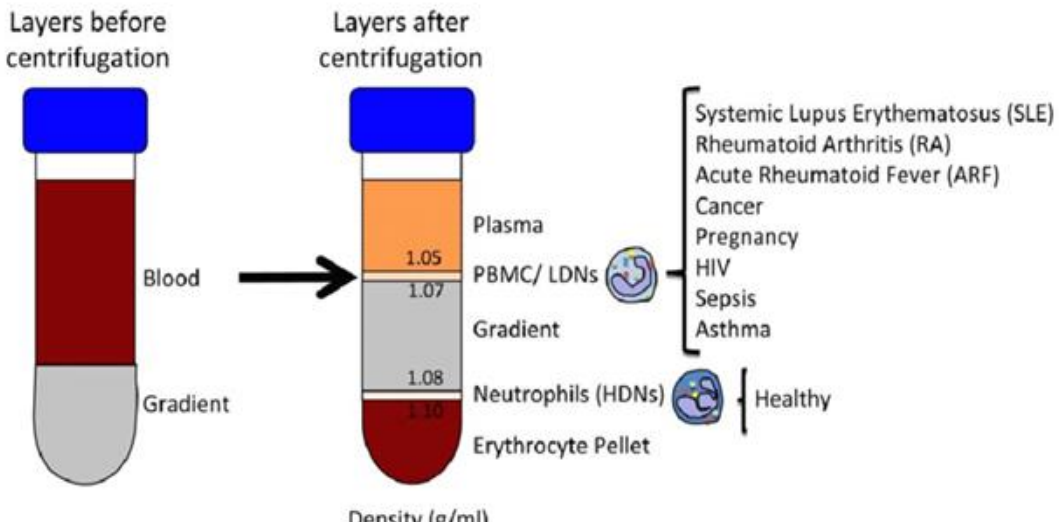

Figure 2.4.1 Density gradient centrifugation of whole blood.

Diagram adapted from Farzeen et al [202]

2.4.1 Cell counts and viability

To count cells and establish initial viability Trypan blue dye was used. Cells were diluted in Trypan blue between 1:2 and 1:50 as appropriate for the initial volume of blood. 10µl of cells/Trypan blue solution was transferred to a chamber of a Glasstic slide (KOVA international, California, USA). Slides were visualised using a light microscope. Glasstic chambers consist of a 3 X 3 layout of large squares each containing a 3 X 3 layout of smaller squares. The number of cells in 3 large squares was counted and the average number was found. Cells touching the bottom and right border of each large square were not counted to avoid duplication. The average number of cells in one large square by the dilution factor times $1X10^4$ to calculate the number of cells per ml. Trypan blue is excluded from live cells and therefore dead cells could be excluded from the counted.

2.5 Flow Cytometry

The appropriate antibodies **(Table 2.2)** were added and incubated in the dark at room temperature for 20 min. Cells were washed with PBS before being resuspended in 500µl FACS buffer (if run immediately) or 2% paraformaldehyde (PFA) (Santa Cruz, Texas, USA) if being stored overnight at 4°C. Fluorescence minus one (FMO) controls were prepared for each fluorophore and used to define positive staining. The most widely used staining control, the isotype control, is of limited use in determining the level of background fluorescence threshold of positivity due to unspecific binding. The rationale behind using isotype controls is the assumption that unspecific staining is due to the isotype of the antibody. Isotype controls are by nature different reagents than the staining antibody, with a different amino acid composition in the variable region, different numbers of fluorochromes bound to the antibody and different concentrations, and, therefore, have different "unspecific" binding properties. Therefore, a negative staining with the isotype control does not necessarily infer that the staining observed with the experimental antibody is specific. In fact, positive staining with isotype controls may indicate that antibodies bind via Fc receptors to the cell[203]. In that case, Fc receptor blocking reagents should be used to prevent such an interaction, CD16 acts as an Fc block and was included in all panels. Compensation was performed with OneComp beads (eBioscience, California, USA) stained with appropriate antibodies. A minimum of 10,000 events were collected for each sample. Cells were acquired on a FACS Canto II flow cytometer (BD, San Jose, USA) and the data were analysed using Kaluza software (Beckman Coulter, USA). To assess the fraction and absolute cell count of LDGs in the different patient and control groups, LDGs were defined as SSC^{hi} and $CD15^+$ $CD14^-$ after gating on singlets **(Figure 2.5.1).** Mature and immature neutrophils were gated as $CD16^+$ or $CD16^{int/-}$ respectively.

Antibody	Fluorophore	Clone	Company
CD14	PE-Vio770	TÜK4	Miltenyi Biotech
CD15	PerCP/Cy5.5	W6D3	Biolegend
CD16	AlexaFluor-488	368	Biolegend
CD10	BV 421	HI 10a	Biolegend
Lox-1	APC	15C4	Biolegend
Siglec-8	PE-Dazzle	7C9	Biolegend
PR3	FITC	W6M2	Abcam
CD177	PE	MEM-166	Molecular Probes
HLA-DR	APC	L243	Biolegend
CD88	APC	S5/1	Biolegend
CD66b	FITC	G10F5	Biolegend
CD62l	FITC	Dreg-56	BD Biosciences
CD33	APC	WM53	BD Biosciences
CD101	BV421	V7.1	BD Biosciences
CD49d	PE	9F10	BD Biosciences
Arg-1	PE	14D2C43	Biolegend
MPO	PE	2C7	Bio-Rad

Table 2.2 Panel of antibodies used standard and Imaging flow cytometry experiments

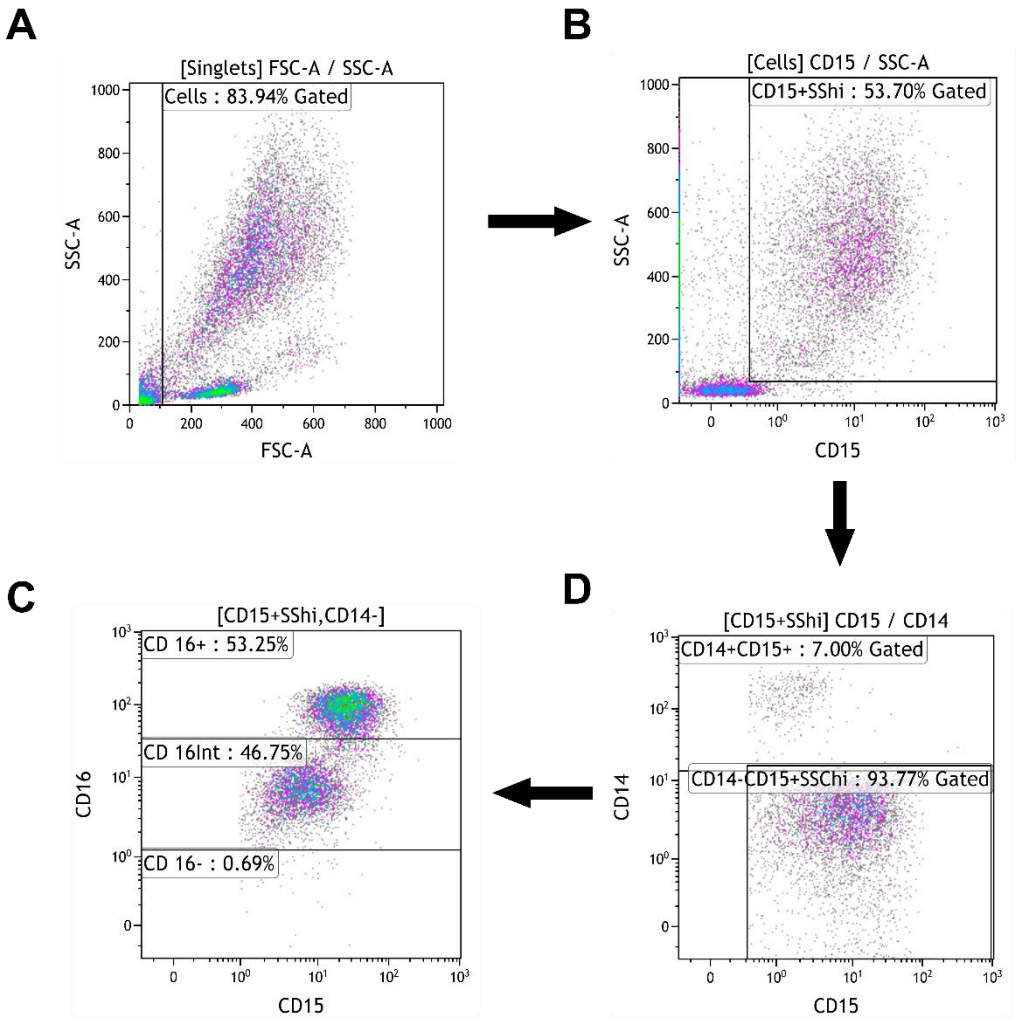

Figure 2.5.1 Gating strategy for identification of neutrophils in peripheral blood samples

Peripheral blood from patients was stained with CD14, CD15 and CD16, and analysed by flow cytometry. Flow cytometry dot plot showing forward scatter (FSC) and side scatter (SSC) gated singlets (**A**). Dot plot showing gating of $CD15^+$ cells (**B**). Monocytes are excluded by the selection of $CD15^+$ $CD14^-$ cells (**C**). Mature and immature neutrophils were gated as $CD16^+$ or $CD16^{int/-}$ respectively (**D**).

2.5.1 Intracellular Staining: Arginase

After surface staining (all except Arg 1as indicated) BD FACS lyse was diluted 1:10 with RO water and 2mls added to each FACs tube and incubated at room temp for 10mins then 2mls PBS added then cells were spun @400g 5mins. The cells were then permeabilised with 1mls 0.2% saponin in FACs buffer for 10 min then 2mls 20% blocking buffer for 10 mins, then spun @ 400g, 50ul left in the tube add 50ul 0.2% saponin, 3ul Arginase 1 added as indicated for 15min in the dark at room temperature, the tube was then washed with PBS centrifuged at 400g and resuspended in 200µl 2% PFA and stored cells were acquired on the BD FACS Canto II flow cytometer (BD, San Jose, USA).

If cells were to be stored for longer than overnight the cells were spun after 10 min in 2% PFA and resuspended in FACs buffer to ensure integrity of fluorophores.

Marker	Fluorophore	Volume/test	Concentration/test	Supplier	Cat no.
CD14	PE-Vio770	2µl	0.40µg	Invitrogen	25014942
CD15	PercpCy5.5	2µl	0.40µg	Biolegend	323020
CD62l	FITC	8µl	0.002µg	BD Biosciences	555543
CD16	APC Cy7	2µl	0.40µg	Biolegend	302018
Arg 1	PE	3µl	0.15µg	Biolegend	369704
CD10	BV421	2µl	0.05µg	Biolegend	312218
CD33	APC	8µl	0.20µg	BD Biosciences	551378

Table 2.3 Arginase Staining Panel

2.5.2 Whole blood staining

75µl Whole blood was mixed with an equal volume of FACs buffer. BD FACS lyse was diluted 1:10 with diH_2O and 2mls was added to each FACs tube. The tubes were incubated for 10 min at room temp then 2mls PBS was added and the cells were centrifuged at 400g for 5 min. The cells were then stained for surface antibodies and intracellular arginase as described.

2.5.3 Imaging Flow Cytometry

After isolation from whole blood, LDGs and NDGs were immediately stained with combinations of monoclonal antibodies as detailed in table 1. DAPI 0.2 µg/mls (Sigma-Aldrich, Missouri, USA) was used for nuclear staining. One million cells were stained and re-suspended in 50µl FACS buffer (2% fetal calf serum in PBS) in Eppendorf tubes before analysis. Images were acquired on an ImageStream X MkII imaging flow cytometer (Amnis Corporation, Seattle, WA) using INSPIRE data acquisition software (Amnis). Compensation and data analysis were performed using IDEAS 5.0 software (Amnis).

Marker	Fluorophore	Channel	Volume	Conc	Supplier
CD15	PC7	6	2µl	0.4µg	Biolegend
CD16	FITC	2	2µl	0.4µg	Biolegend
CXCR2	PECy 5.5	5	5µl	0.125µg	BD Biosciences
CD63	BV-711	11	2µl	0.4µg	BD Biosciences
Lox 1	PE-Vio 615	4	1µl	0.4µg	Miltenyi
Arg 1	PE	3	3µl	0.15µg	Biolegend
Nucleus	DAPI	7	5µl	0.2µg/ml	Sigma

Table 2.4 Antibody Panel for Imaging Flow cytometry

2.6 T cell Supression

2.6.1 Isolation and culture of Neutrophils for T cell suppression assay

NDGs were separated by density gradient centrifugation using modified percoll prep as previously described. RBCs were lysed, 10mlsRBC lysis/5mins then top up with PBS and spin 400g 5mins. Cells were resuspended in RPMI Media and counted. Percent dead cells were determined using Trypan blue. After isolation, cells were cultured (1x10^6cells/ml) for 20 hours in growth medium RPMI-1640 supplemented with 10% inactivated FCS, 100 IU/ml Penicillin, 100 µg/ml Streptomycin, at 37°C. Cells were plated at 1mls in triplicate in a 6 well plate. Three control wells of media were plated.20 hours later cells were removed at 400 x g for 5 min at 22°C and their supernatants were pooled and stored at – 70°C.

2.6.2 T cell suppression assay

Day 1. A 96 well flat bottomed was coated with 50µl of anti-CD3 at 10µg/mls in PBS and incubated overnight at 4˚C.

Day 2. PBMC isolation from HC blood

PBMC were isolated using the modified percoll method in Section 2.3, and counted. Cell trace violet; 2.5mM (2 µL) cell trace violet (CTV) was prepared. 50µl of 8 x 10^6 cells in RPMI were added. A control tube without CTV was set up. Both tubes were incubated at 37˚C for 15 min, then washed in RPMI. Anti-CD3 was removed from the

plate with PBS. 200µl COVID-19 neutrophil culture supernatants were added and 200µl of media was added to blank wells. 25µl of CTV+ and CTV- was added to the wells. 5ul of anti-CD-28 was added to selected wells. 2ul of working stock nor-NOHA was added to selected well. The plates were incubated at 37 ˚C and T cell proliferation was monitored each day.

Day 3 Flow cytometry

The plate was spun at 400g for 3 min and the plate was washed with 200µl PBS and then resuspended. Cells were stained with Live/dead aqua, a surface at 1:2000, a surface stain master mix was prepared according to table and incubated at room temperature in the dark. Cells were washed with FACs buffer and centrifuged at 400g for 5 min. Cells were fixed with 4% PFA and incubated for 10min, cells were washed with FACS buffer and resuspended at 100µl FACs buffer for flow cytometry.

Cell were aquired on Amnis CellStream and analysed using Flowjo software

Antibody	**Dilution**	**Volume in 2500µL FB**	**Concentration**
CD3 APCy7	1/400	6.25 µL	0.25µg
CD4 BV605	1/400	6.25 µL	0.25µg
CD8 BV711	1/400	6.25 µL	0.25µg

Table 2.5 Antibodies for T cell suppression assay

2.6.3 Arginase Assay

Arginase concentrations were determined using an Arginase assay kit (Sigma-Aldrich). 200µl of passive lysis buffer was added to $1x10^6$ cells to prepare lysates. The lysates were then centrifuged at 14,000 rpm the resulting supernatants were then decanted and used for analysis. The lysates were diluted 1in 10 in ddH_2O. A 1.0mM UREA working standard solution was prepared using 12µl of the provided urea standard and 88µl H_2O. 25µl of working standard solution was added to a 96 well microtitre plate. 25µl of neat high standard were added. The controls were 25µl H_2O and 20µl of sample to which the substrate is not added until the end of the assay (sample blank).

Assay reaction; 5x substate buffer was prepared by adding 50µl Mn solution to 200 µl arginine buffer. 5µl of the substrate buffer was added to each well except the sample blank well. The plate was mixed well by pipetting. The plates were covered with cling film and incubated at 37^0C for 2 hours. The arginase reaction is stopped by adding 80µl of prepared urea reagent to the wells. Using the kit reagents A and B in equal volumes. Then 5µl of the 5X substrate buffer was added to the

sample blank. The absorbance was measured at 430nm (A_{430})using using a Versamax microplate reader (Molecular Devices) and analysed using SoftMax Pro software.

Arginase activity was determined by the following equation:

$$\text{Arginase Activity (units/l)} = \frac{(A_{430})\text{sample} - (A_{430})\text{blank}}{(A_{430})\text{standard} - (A_{430})\ H_2O} \times \frac{(1\text{mM} \times 25 \times 10^3)}{20 \times 120\ \text{min}}$$

2.6.4 Arginase 1 ELISA

REAGENT PREPARATION; The reagents to equilibrated to room temperature (20 – 25°C) prior to use.

Wash buffer

Wash buffer was prepared by mixing 60 mls of 20x wash buffer with 1140 mls of distilled or de-ionized water.

Dilution buffer

Dilution buffer was prepared by mixing 15 mls of the 10x dilution buffer with 135 mls of distilled or de-ionized water

Standard solution

The standard was reconstituted by pipetting the amount of dilution buffer mentioned on the CoA in the standard vial. Using the standard vial as Tube 1 in **Figure 2.6.1** each human Arginase-I standard in polypropylene tubes was prepared by serial dilution of the reconstituted standard with dilution buffer as shown in **Figure 2.6.1**.

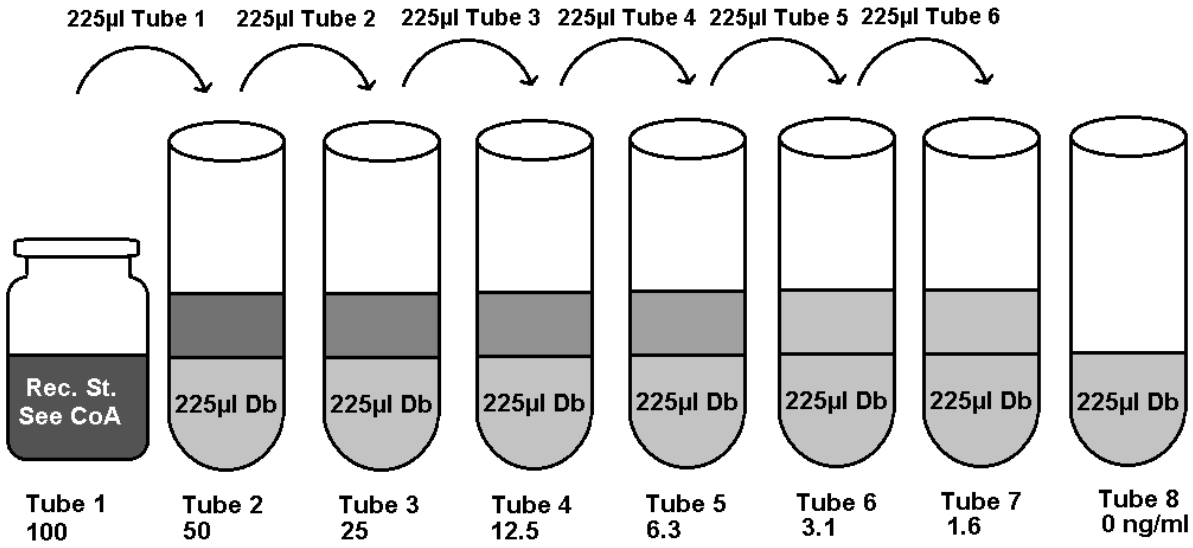

Figure 2.6.1 Standard dilution protocol

Tracer solution

The tracer was reconstituted by pipetting 1 mls distilled or de-ionized water. The reconstituted 1 mls tracer with diluted with 11 mls dilution buffer

Streptavidin-peroxidase solution

The streptavidin-peroxidase solution was prepared by mixing 0.25 mls of the 100x streptavidin-peroxidase solution with 24.75 mls dilution buffer.

ELISA PROTOCOL

The number of test wells required was determined, the necessary microwell strips was put into the supplied frame. Samples were diluted 1:2 in dilution buffer in eppendorf tubes. 100 µl in duplicate of standard, samples, or controls was transferred into appropriate wells. The side or bottom of the wells was not touched. The tray was covered and tapped to eliminate any air bubbles. The plate was incubated for 1 hour at room temperature. The plates were washed 4 times with wash buffer. 100 µl of diluted tracer was added to each well using the same pipetting order as applied in step 2. The plate was incubated for 1 hour at room temperature. The plate was washed 4 times. 100 µl of diluted streptavidin-peroxidase was added to each well, using the same pipetting order as applied in step 2. The plate was incubated for 1 hour at room temperature. The plate was washed 4 times. 100 µl of TMB substrate was added to each well, using the same pipetting order as applied in step 2. The plate was incubated for 30 min at room temperature. The reaction was stopped by adding 100µl of stop solution with the same sequence and timing as used in step 12. The solutions were mixed in the wells thoroughly by gently swirling the plate. Gently tap the tray to eliminate any air

bubbles trapped in the wells. The plate was read within 30 min after addition of stop solution at 450 nm using a plate reader. ODs were exported and analysed in Graphpad Prism.

2.7 Real-Time Quantitative Reverse Transcription PCR (rt-PCR)

The pellet was either stored with 600 µl to 1 mls of prepared lysis buffer from the Pure link RNA extraction kit or without it. Note, samples taken from the previous year were stored in 1 mls of FACs buffer (DPBS and foetal calf serum).

2.7.1 RNA extraction

RNA extraction was carried out using Pure link RNA extraction kit from Ambion. Kit Instructions were followed. In summary, freshly prepared lysis buffer with 2-mercaptoethanol (10 µl/1 ml of lysis buffer) was added to the sample according to the number of cells isolated through density centrifugation with Percoll.

Cell Count	**Lysis buffer**
< 1 x 10^6	300 µl
1x10^6 - 5x 10^6	600 µl
5x10^6 - 5x10^7	1.2-6 mls

Table 2.6 Lysis buffer volume recommended by number of cells.

The cells were then homogenized by using a 1 ml syringe with a 24 G needle, syringing 10 times. 70% ethanol prepared by diluting with distilled water and added in a 1:1 ratio. The samples were vortexed for 20 seconds, then filtered by adding 700 µl of the mixture into the filtering tubes from the kit until all the sample was filtered, spinning at 1200 g for 20 seconds at room temperature. The flow through was discarded. The filters were washed with 700 µl of wash buffer 1 by spinning at 1200g for 20 seconds at room temperature. The collection tubes were changed. The filters were then again washed twice with 500 µl of wash buffer II, spinning at 1200g for 20 seconds at room temperature. The filters were allowed to dry by spinning at 1200 x g for 1 minute at room

temperature. The RNA was eluted from the filter by adding 30-50 µl of RNase free water and spinning at 8000g for 1 minute. This was repeated three times, using the same volume to remove all RNA from the filter. The RNA was afterwards quantified using NanoDrop™ 2000/2000c Spectrophotometer. Only RNA with a concentration of more than 50 ng/µl was used. The samples were stored at -80ºC until use.

2.7.2 cDNA synthesis

Prior to cDNA synthesis, RNA was purified by treating it with DNase I (Thermo). 500 ng of RNA was used, diluting it to a volume of 8.5 µl. 1 µl of the kit's buffer plus 0.5 ul of the DNase was added to each sample. The samples were incubated at room temperature for 15 min. The treatment was stopped by adding 1 µl of EDTA and heating for 10 min at 65°C.

The cDNA synthesis was made by using the 500 ng of RNA in 8.5 µl suspension from each sample, using High-Capacity cDNA Reverse Transcription Kit from Applied Biosystems. Instructions were followed as recommended by the kit. A control without the reverse transcriptase (RT) enzyme was also prepared per sample. A master mix made with 2.5 µl of assay buffer, 0.8 µl of dNTPs, 2 µl of RT primers, 0.5 µl of RT and 9.2 µl of RNase free water (in the case of the control, 9.7 µl of RNase free water). 15 µl of this preparation was added to each sample. They were placed in the thermocycler with the following protocol:

	Step 1	**Step 2**	**Step 3**	**Step 4**
Temperature	25ºC	37ºC	85ºC	20ºC
Time (min)	10	120	5	Infinity

Table 2.7 Parameters for the Thermocycler

The samples were stored at -20 °C until use.

2.7.3 rtPCR

To quantify the genes, 2 µl of diluted cDNA (at 1:10 ratio with RNase free water) was mixed with 8 µl of a master mix consisting of 5 µl of SYBR G (PowerUp SYBR Green Master Mix,Thermo), 2.6 µl of

RNase free water and 0.4 µl of a mix of the primers (consisting of 10 µl of the Forward primer and 10 µl of the Reverse primer diluted with 80 µl RNase free water) was added to a PCR plate. They were quantified using QuantStudio Standard curve protocol.

The analysis of the gene amplification was normalized by using a housekeeping gene (ACTB) and then the delta-delta Ct (DDCt) value was calculated.

Protein	Gene	Transcripts (RefSeq)		Sequence (5'->3')	Length	Tm	GC%	Self- 5' complementarity	Self-3' complementarity
Arginase 1	ARG1	NM_001244438.1 NM_000045.3	Forward primer	CTTGTTTCGGACTTGCTCGC	20	60	55	3	2
			Reverse primer	CACTCTATGTATGGGGGCTTA	21	56	48	2	2
Proteinase 3	PRTN3	NM_002777.3	Forward primer	CTGAGCAGCCCAGCCAACCT	20	65	65	7	0
			Reverse primer	GAAGCAGATGCCGGCCTTGC	20	65	65	8	8
Myeloperoxidase	MPO	NM_000250.1	Forward primer	ATCGCCAACGTCTTCACCAA	20	60	50	4	0
			Reverse primer	CATGGGCTGGTACCGATTGT	20	60	55	6	0
S100 calcium binding protein A8	S100A8	NM_002964.5 NM_001319201.1 NM_001319198.1 NM_001319197.1 NM_001319196.1	Forward primer	GCTAGAGACCGAGTGTCCTCAG	22	62	59	4	3
			Reverse primer	GCCCATCTTTATCACCAGATTG	22	57	45	4	2

Table 2.8 Primers for rtPCR

2.8 Statistical Analysis

All statistical analysis was performed using GraphPad Prism 9.1.0 software (GraphPad Software, San Diego, CA, USA). p values between groups were obtained using the Kruskal Wallis test, with comparison between individual groups using Dunn's multiple comparison test. The fraction cells between LDGs and NDGs was assessed with a Wilcoxon ranked sum test, with sub-group analysis performed using ANOVA with correction for multiple comparisons using Tukey's test. The change in CD16 expression on granulocytes in humanised mice was assessed with 2-way ANOVA and Sidak's multiple comparison tests. Differences between subsets, were tested using Friedman's paired test, with *post hoc*

comparison of groups using Dunn's test. The number of neutrophil lobes in $CD16^{+}$ and $CD16^{int/-}$ cells was compared using the Chi square test. Correlations were calculated using Spearman r and linear regression to estimate best fit lines. Data are presented as median with interquartile range. * = $p<0.05$; ** = $p<0.01$; *** = $p<0.001$; **** = $p<0.0001$; ns = non-significant

Chapter 3

Low density granulocytes (LDGs) are elevated and linked to disease severity in autoimmune AAV and in viral infection

3 Low density granulocytes (LDGs) are elevated and linked to disease severity in autoimmune AAV and in viral infection

3.1 Introduction

Low density granulocytes (LDGs), are a subset of granulocytes that copurify with PBMCs in a Percoll density gradient. LDGs are reported in an extensive variety of conditions from sepsis to cancer and autoimmune conditions like ANCA -associated vasculitis (AAV) and rheumatoid arthritis [47, 59, 64, 204]. LDGs are a mixed population of mature and immature neutrophils, one hypothesis is that LDGs are elevated in response to emergency granulopoeisis which may account for the immature subsets of LDGs but falls short of explaining the presence of mature granulocytes in the PBMC layer [205]. In order to investigate the origin of these cells, I set about phenotyping these subsets in AAV using a panel of markers to define their maturity and activation status. In COVID-19 patients, early reports suggested that LDGs are also elevated [206]. Studying LDGs from two diverse conditions one autoimmune the other a viral infection and compare them phenotypically provides an opportunity to determine if LDGs are similar in both pathologies or if they represent a disease specific response. Despite their very different triggers both AAV and COVID-19 have surprisingly similar pathologies.

AAV is a systemic autoimmune disease in which neutrophils play a key role [94]. It is characterized by antibodies directed against neutrophil proteins, proteinase 3 (PR3) and myeloperoxidase (MPO) and is associated clinically with rapidly progressive glomerulonephritis (GN) and inflammatory necrosis of small blood vessels in lungs, skin and other organs [95, 97, 207, 208].

Severe Acute Respiratory syndrome coronavirus-2 (SARS-CoV-2) is a novel beta coronavirus which emerged in the Wuhan region of China in December 2019 and rapidly spread to the rest of the world becoming a pandemic. Clinically it can manifest towards acute respiratory distress syndrome (ARDS) with multiorgan dysfunction including glomerulonephritis and multi organ failure. These features demonstrate a systemic aspect of this infection in common with the pathophysiology of AAV.

Pulmonary-renal syndromes are clinical syndromes that are a combination of diffuse alveolar hemorrhage (DAH) and glomerulonephritis, these can be caused by a wide variety of diseases, the majority of pulmonary-renal syndrome are associated with antibodies to MPO or PR3, ANCAs [209]. More recently however COVID-19 patients present with pulmonary-renal syndrome in severe disease, in one reported case a patient with rapid proliferative GN and lung symptoms was presumed COVID-19 but was actually severe AAV[210]. Determining the phenotype of LDGs in both

diseases should allow us to establish if they are a bona fide disease specific subset or if they are merely an uncontrolled release of granulocytes in inflammatory settings due to emergency granulopoiesis. Although the clinical manifestations of COVID-19 are similar to AAV their pathogenesis is very different and poorly understood, perhaps neutrophils can be the key to unlocking the clinical relevance of LDGs and indeed neutrophils in the development of disease be it in autoimmunity or viral infection.

3.2 Design and rational

3.2.1 Hypothesis

Low density granulocytes (LDGs) are elevated in a variety of inflammatory conditions, phenotyping LDGs from AAV and COVID-19 provides the perfect opportunity to study these cells and determine if they are bona fide disease specific subsets or a generic response to inflammation. I therefore hypothesized that:

1. LDGs are present and correlate with severity in AAV and COVID-19
2. LDGs subsets display disease specific phenotypes
3. LDGs from both diseases are a mixed population of mature and immature cells

3.2.2 Specific aims

1. Characterise LDG subsets by traditional and imaging Flow cytometry
2. Correlate LDGs with disease severity using Birmingham score in AAV and WHO severity scale in COVID-19 and clinical data

3.2.3 Specific Methods

Patients were recruited according to the guidelines in Chapter 2.3. Density gradient Centrifugation as outlined in Chapter 2.4. Flow cytometry and Imaging Flow cytometry as outlined in Chapter 2.5

G-CSF Treatment of Humanized Mice; To assess the impact of granulocyte colony stimulating factor (G-CSF) on human CD16 granulocyte expression, humanized mice were generated as described previously [211]. Briefly, NOD.Cg-*Prkdc*^{scid}Il2rg^{tm1Wjlt}Tg(hu-mSCF) mice were obtained from Jax (Bar Harbor, Maine, USA) and engrafted by injecting 1×10^5 purified human cord blood derived CD34$^+$ stem cells (Lonza, Slough, Berkshire, UK) into the lateral tail veins of 10–14 week-old mice ∼24 h post irradiation (2.4 Gy). Following confirmation of engraftment, mice were injected subcutaneously with 50 µg pegylated filgrastim (Neulasta R , Amgen, Cambridge, UK), with repeat peripheral cell granulocyte phenotype assessed by flow cytometry 4 days later. Cells were stained with CD45, CD66b and CD16 antihuman antibodies after blocking with 2.5µg/ml human BD Fc Block (clone: Fc1.3070) and 1µg/ml mouse BD Fc Block (clone: 2.4G2). Flow cytometric analysis was

performed on a CyAn ADP Analyzer (Beckman Coulter, California, USA) using Summit software (Beckman Coulter). Data were analyzed using Kaluza software. Human granulocytes were identified as CD45+CD66b+. This work was undertaken by Dr Alice Coughlan previously of our lab.

3.3 Results

3.3.1 Low Density Granulocytes (LDGs) are elevated in patients with Acute AAV and in patients with COVID-19 and are linked to severity in COVID-19 patients.

To determine whether LDGs were elevated in acute and remission AAV and Covid -19 peripheral blood, PBMC were isolated from peripheral blood of patients with AAV and patients with COVID-19 by density gradient centrifugation within 90 min of blood draw. Representative flow cytometry plots clearly show an expansion of high side scatter cells in both disease states compared to healthy controls (**Figure 3.3.1 A, B, C**). To further phenotype this population LDGs were classified as live $SSC^{hi}CD15^{+}$singlets (data shown from a representative patient with acute AAV) **(Figure 3.3.1 D)**. LDGs were quantified as the percentage of PBMC in the peripheral blood of 23 acute AAV patients (12.4%, IQR 6.8-26.7), 14 remission AAV (6.8%, IQR 3.9-10.9), 11 disease controls (DC) (4.5%, IQR 2.9-5.6) and 8 age matched healthy controls (HC)(2.17%, IQR 0.6-4.5), the values from 6 samples of umbilical cord blood(UCB) (17.0%, IQR 11.8-25.33) are shown for comparison **(Figure 3.3.1 E)**. The absolute numbers per ml of blood were also quantified **(Figure 3.3.1 F)**. I found that both the LDG fraction (12.4%, IQR 6.8-26.7) and the absolute number of LDGs per ml of blood ($1.2x10^5$, IQR 0.3-3.3 $x10^5$) were significantly increased in acute AAV. For comparison blood containing a high level of immature neutrophils umbilical cord blood contained a median fraction of 17.0% (IQR 11.8-25.33). I noted a significant increase in both the LDG fraction and the absolute number of LDGs when compared to the fraction of LDGs in disease controls (4.5%, IQR 2.9-5.6) and absolute number ($2.4x10^4$, IQR 1.2-2.9 $x10^4$) which were a mix of patients with renal impairment and non-AAV systemic inflammation. LDGs as a percent of PBMCs from 31 mild, 14 moderate and 9 severe COVID-19 patients based on WHO severity scale were quantified and compared to 7 healthy controls and 10 convalescent COVID-19 patients **(Figure 3.3.1 G)** and the absolute numbers per ml of blood **(Figure 3.3.1 H)**. LDGs were also elevated and linked to severity in COVID-19 patient peripheral blood, mild moderate and severe disease status were defined by WHO criteria. Severe patients had significantly increased LDG fraction, 28.48% (IQR, 18.19-31.48) of the PBMC layer were low density neutrophils. This is in contrast to convalescent patients that had 2.46% (IQR, 1.02-7.7) LDGs. Interestingly there was no significant difference between HC (2.96%, IQR 1.11-4.5) mild (7.91%, IQR 3.8-16.31) and convalescent (2.46%, IQR 1.02-7.7) percentage LDGs. Both moderate (21.1%, IQR 13.6-35.1) and severe patients were significantly increased compared to both HC and convalescent cases. When the absolute number of neutrophils per ml of blood was determined both the moderate ($3.9x10^6$, IQR 1.8-6.6 $x10^6$) and severe cases ($8.8\ x10^6$, IQR 1.1-12.2 $x10^6$) were increased compared to the convalescent patients ($7.9\ x10^5$, IQR 1.6-14.6 $x10^5$) but not the healthy controls ($1.4\ x10^6$, IQR 0.5-1.9 $x10^6$). There is a notable spread of data in Covid 19 patients particularly in the

severe and moderate patients (**Figure 3.3.1 G, H**), this is also seen in Acute AAV (**Figure 3.3.1 E, F**) reflecting the emergence of these cells in severe disease.

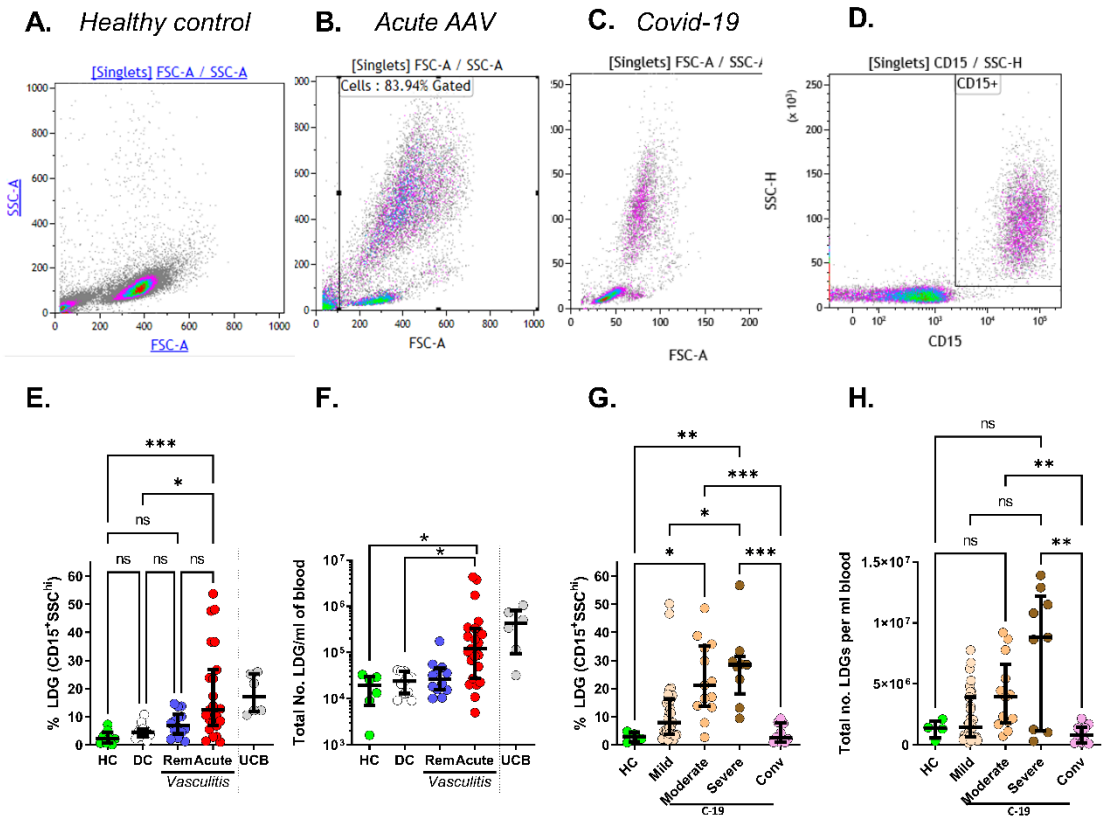

Figure 3.3.1 Low Density granulocytes (LDGs) are elevated in patients with Acute AAV and in patients with COVID-19 and are linked to severity in COVID-19 patients.

PBMC were isolated from peripheral blood of patients with AAV and patients with COVID-19 by density gradient centrifugation. Representative flow cytometry plots are shown from healthy control PBMC **(A)**, a patient with acute AAV **(B)** and a patient with COVID-19 **(C)**. LDGs were classified as live $SSC^{hi}CD15^{+}$singlets (data shown from a representative patient with acute AAV) **(D)**. LDGs were quantified as the percentage of PBMC in the peripheral blood of 23 acute AAV patients,14 remission(rem), 11 disease controls (DC) and 5 age matched healthy controls (HC), the values from 6 samples of umbilical cord blood are shown for comparison. Each symbol represents an individual donor **(E)**. The absolute numbers per ml of blood were also quantified **(F)**. LDGs as a percent of PBMCs from 31 mild,14 moderate and 9 severe COVID-19 patients based on WHO severity scale were quantified and compared to 7 healthy controls and 10 convalescent COVID-19 patients**(G)** and the absolute numbers per ml of blood **(H)**. Median with interquartile range. Kruskal-Wallis test, with post hoc analysis with Dunn's multiple comparisons. *p <0.05,**p <0.01, and ***p < 0.001.

3.3.2 CD16 expression defines subpopulations of LDGs in both AAV and COVID-19.

CD16 receptor (Fcγ receptor 111), is a low affinity receptor for IgG, expressed on neutrophils in a glycosylphosphatidyl inositol (GPI) linked form. It appears late during neutrophilic maturation. It is faintly expressed on metamyelocytes while banded and segmented stages of neutrophilic

development show the highest expression [212, 213]. Therefore, to investigate the subpopulations within the LDG fraction CD16 expression was quantified by flow cytometric analysis. LDGs and NDGs (classified as $SSC^{hi}CD15^{+}CD14^{-}$ singlets in the low density (PBMC) and high-density layer respectively were categorized as $CD16^{+}$, $CD16^{int}$ (clearly separated from $CD16^{+}$cells) and $CD16^{-}$ (defined by FMO). Representative CD16 plots from LDGs (**Figure 3.3 2 A, C**) and NDGs (**Figure 3.3.2 B, D)** in AAV and COVID-19 respectively, illustrate the difference in CD16 expression between the fractions and disease states. In AAV there was a significant increase of $CD16^{int/-}$ cells in both the acute AAV patients 42.24% (IQR 24.62-52.15) and DC patients 40.24% (IQR 28.89-56.19) compared to HC 18.31% (IQR 11.48-24.03), and patients in remission AAV 33.9% (IQR 24.22-43.16), indicating that this population of neutrophils is a feature of active disease (**Figure 3.3.2E**), when the absolute $CD16^{int/-}$ cell count was calculated (**Figure3.3.2F**) this population was markedly expanded in acute AAV $8.48x10^{4}$ (IQR 5.3-$65.6x10^{4}$) $CD16^{int/-}$ cells further confirming their presence in inflammation. We hypothesise therefore that $CD16^{int/-}$ cells are a feature of inflammation and present in active disease, to further investigate a disease specific response I examined the levels of $CD16^{int/-}$ in mild moderate and severe COVID-19 patients and compared them to HC and convalescent patients. Interestingly, there was no significant differences between all cohorts in terms of percentage of $CD16^{int/-}$ however when the absolute number of cells were taken into account both moderate ($9.7x10^{5}$ $CD16^{int/-}$ cells IQR 3.4-21.1 $x10^{5}$) and severe patients ($5.1x10^{6}$ $CD16^{int/-}$ IQR 0.27-$8.5x10^{6}$) had a significant increase in $CD16^{int/-}$ cells when compared to convalescent patients ($9.7x10^{4}$ $CD16^{int/-}$ cells IQR 3.5-27.1x 10^{4}) again confirming that these cells are present in active disease but not demonstrating a disease specific response with perhaps acute granulopoiesis leading to an increase in the number of circulating neutrophils.

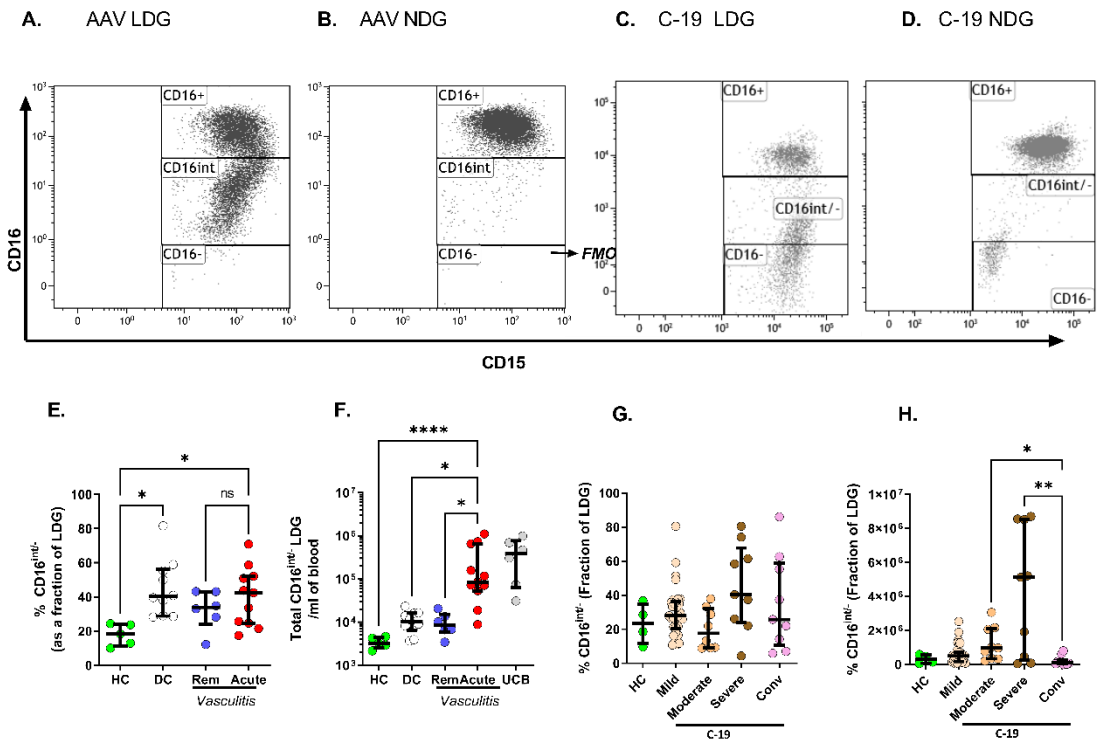

Figure 3.3.2 CD16 expression defines subpopulations of LDGs in both AAV and COVID-19.

Mixed leukocyte populations were separated by dextran sedimentation and density centrifugation. LDGs and NDGs were classified as SSC^{hi} $CD15^{+}$ $CD14^{-}$ singlets in the low-density and high-density layers respectively. LDGs and NDGs were categorised as $CD16^{+}$, $CD16^{int/-}$ and $CD16^{-}$ (FMO, fluorescence minus one) with a representative AAV LDG sample illustrated in (A), AAV NDG shown in (B). and COVID-19 LDG and NDGs represented in (C & D) respectively. In AAV most NDGs were CD16+ whereas CD16int/- cells were approximately one third of LDGs (E). The percentage (E) and absolute number (F) of CD16int/- cells were compared across disease phenotypes in AAV and autoimmunity. In COVID-19 LDGs showed a similar proportion of CD16int/- with higher percentage (G) and absolute number (H) being linked to severity. ANOVA with post hoc Tukey's multiple comparison test *p<0.05, **p <0.01, and ***p < 0.001.

3.3.3 Imaging flow cytometry confirms that AAV and COVID-19 LDGs are a mixed population of mature and immature cells as defined by CD16 expression and nuclear morphology.

To confirm that the $CD16^{int/-}$ are immature cells possibly representing myeloblasts, promyelocytes or metamyelocytes, I used imaging flow cytometry to further characterise the LDG subsets simultaneously by surface marker and nuclear morphology as less mature neutrophils have circular or kidney shaped nuclei with mature cells being multilobed. Gating on $CD15^{+}CD14^{-}$ LDGs and $CD16^{+}$ and $CD16^{int/-}$ were stained with nuclear stain DAPI and a panel of surface markers (**Figure 3.3.3A**). Merged images clearly show that the $CD15^{+}CD16^{+}$ have multilobed nuclei whereas the $CD15^{+}CD16^{int/-}$ have circular or kidney shaped nuclei (**Figure3. 3.3B**) To further validate these

findings we quantified the number of nuclear lobes in all cells in the $CD15^{+}CD16^{+}$ and the $CD15^{+}CD16^{int/-}$populations in both AAV and COVID-19 patients using automated analysis of an imaging cytometry dataset. In AAV, $CD15^{+}CD16^{+}$ had as median of 2 lobes, whereas the $CD15^{+}CD16^{int/-}$ cells had a median of 1 lobe confirming an immature phenotype (**Figure 3.3.3C**). In severe COVID-19 $CD15^{+}CD16^{+}$ had as median of 3 lobes, whereas the $CD15^{+}CD16^{int/-}$ cells had a median of 2 lobes (**Figure 3.3.3D**). There is a difference in the number of lobes in both diseases with higher numbers of lobes in the severe COVID-19 patients albeit the $CD16^{int/-}$ still represents an immature subtype likely to be metamyelocytes and band cells rather than the myelocytes that are predominant in the AAV patient.

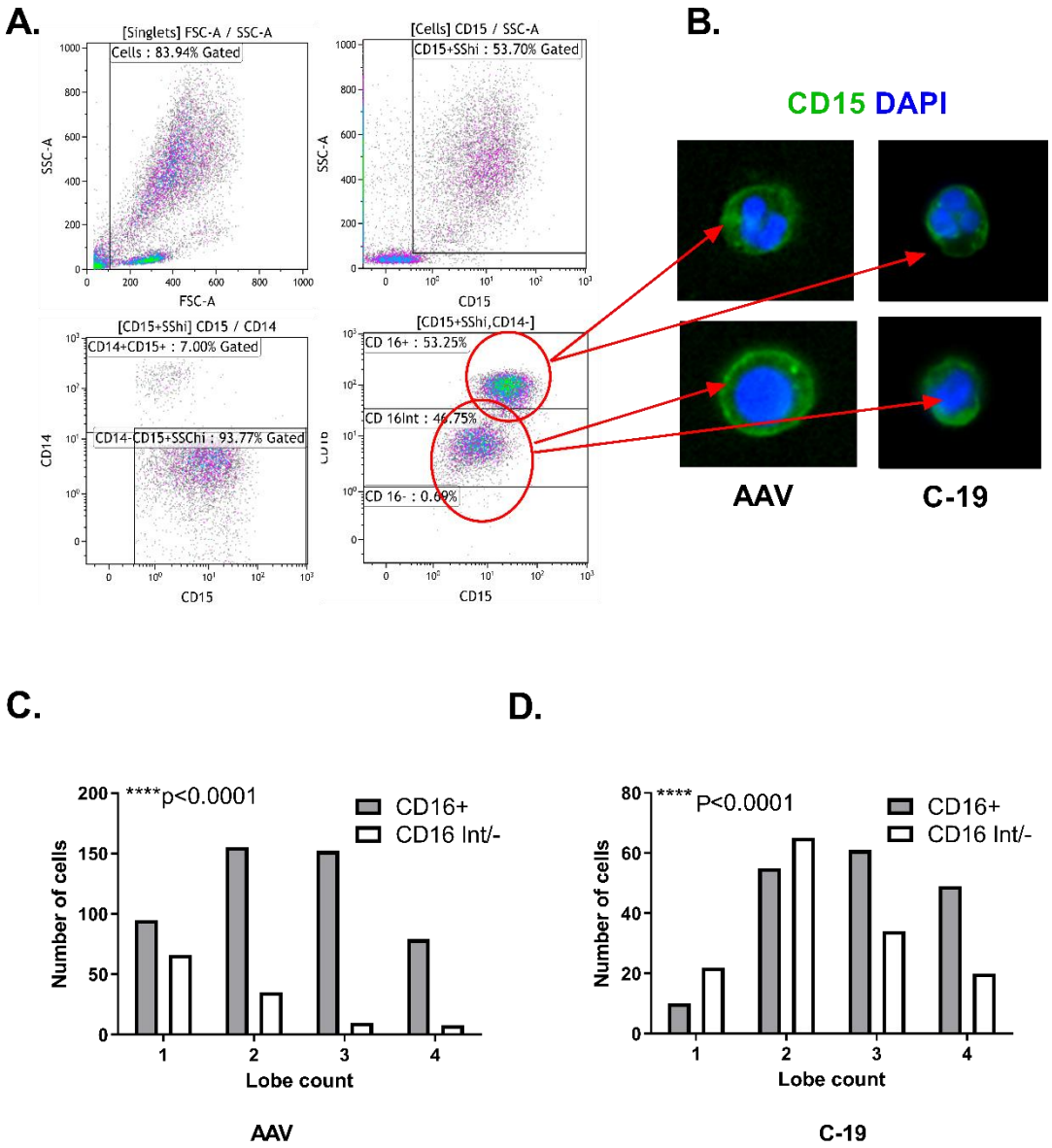

Figure 3.3.3 Imaging flow cytometry confirms that AAV and COVID-19 LDGs are a mixed population of mature and immature cells as defined by CD16 expression and nuclear morphology

Gating strategy for identification of LDG subsets by traditional and Imaging flow cytometry (A.) After gating on SSC^{hi} $CD15^{+}$ $CD14^{-}$ cells, LDG subsets were defined as $CD16^{+}$ and $CD16^{int/-}$. Representative images of LDG subsets shown Images obtained at 60X magnification on ImageStream MK11 using DAPI nuclear stain (blue) and CD15 (green), merged images show the multilobed $CD16^{+}$ population and the circular immature nuclei of the $CD16^{int/-}$ subpopulations. (B.) LDG subsets can be identified by their nuclear lobe count, a marker of neutrophil maturity. $CD16^{+}$ LDGs have predominantly multilobed nuclei while the $CD16^{int/-}$ have mostly single lobed nuclei. Chi squared test. (C.)

3.3.4 CD10 and CD16 define maturity in neutrophil subsets with both markers identifying mature and immature LDGS by flow cytometry.

Having established that LDGs in both AAV and COVID-19 are heterogenous based on nuclear morphology and CD16 expression. It is important to verify that the low level of observed CD16 expression is due to neutrophil immaturity rather than the shedding of this Fc receptor due to activation or apoptosis [214]. Whilst the nuclear morphology confirms immaturity, the expression of CD10, an established marker of neutrophil maturity expressed at the segmented stage of neutrophil development is particularly relevant [215]. To address the hypothesis that these cells are immature neutrophils I determined the correlation of CD16 with CD10 and found that CD10 correlates closely with CD16 expression in LDGs in both AAV (r^2=0.7153) and COVID-19 (r^2=0.7339) (A.B). This was confirmed by Imaging flow cytometry with the pattern of nuclear and surface marker expression of CD10 mimicking that of CD16, merged images show the multilobed $CD16^+$ population and the circular shaped nuclei of the $CD16^{int/-}$population and the CD10 staining of the CD16 subpopulations (**Figure 3.3.4 E**). Representative flow plots demonstrate the bimodal expression of both CD10 and CD16 in the LDG population whereas the NDG population display a unimodal expression of both markers' representative of mature neutrophils (**Figure 3.3.4 C**). It could be suggested that this expansion of $CD16^{int/-}$ population is as a result of emergency granulopoiesis in response to inflammation in both AAV and COVID-19 [216]. To test this hypothesis G-CSF was administered to mice with a humanized immune system; this caused a dramatic reduction of peripheral blood CD 16^+ neutrophils from 62.8± 4.7 to 12±2.8%, with a concomitant increase in $CD16^{int/-}$ neutrophils (**Figure 3.3.4 D).** (Human mouse model work was carried out by Alice Coughlan in our group). Imaging flow cytometry confirms the CD10 as a marker of mature neutrophils (**Figure 3.3.4 E**)

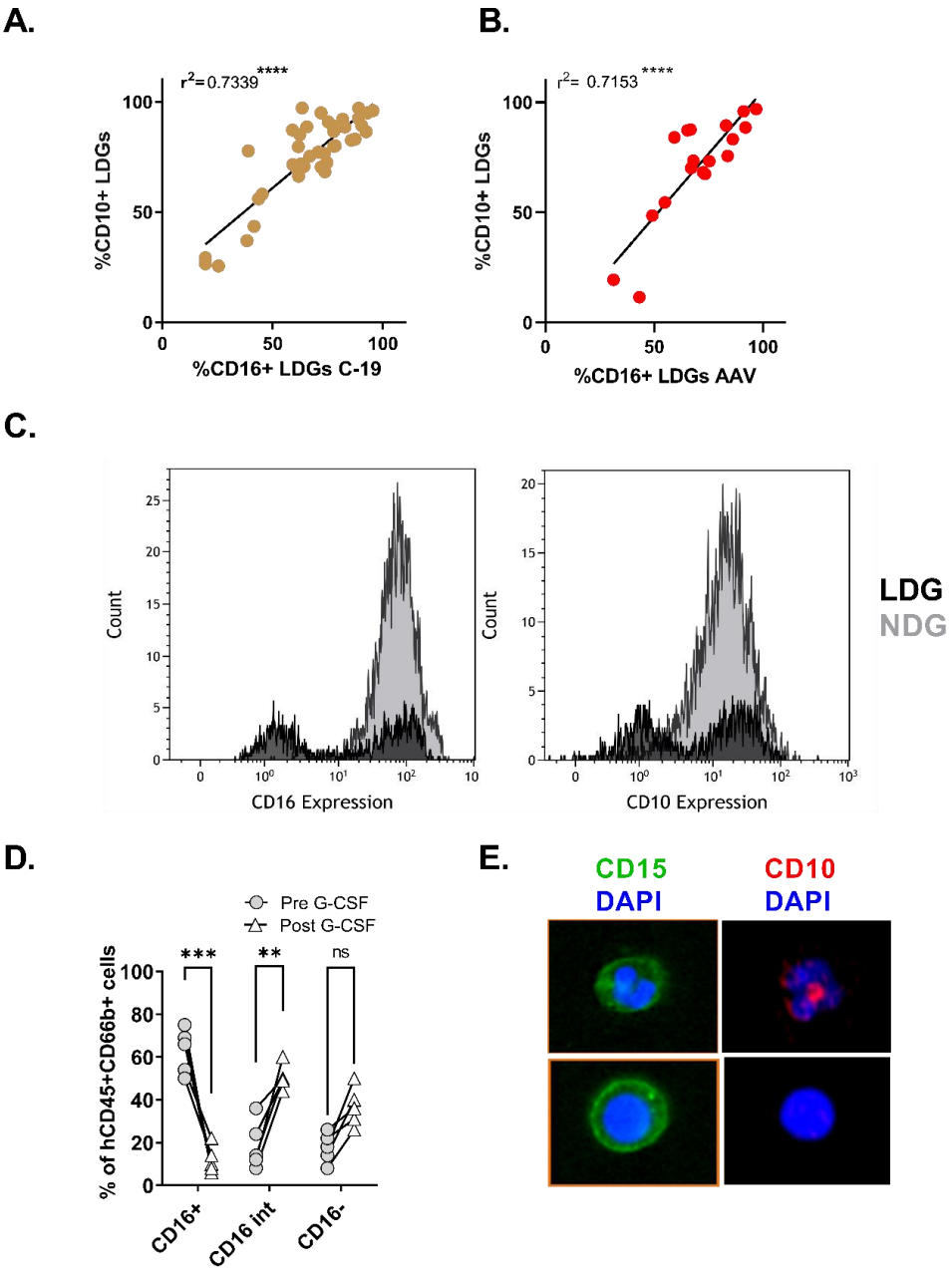

Figure 3.3.4 CD10 and CD16 define maturity in neutrophil subsets with both markers identifying mature and immature LDGS by flow cytometry

CD10 expression correlates closely with CD16 expression in both AAV and COVID-19 Spearman correlation p<0.0001 ****(A,B.) Representative MFI plots identify LDG populations as defined by CD10 and CD16 high and low expression as mature and immature respectively with NDGs being a single population of CD10 and CD16 high mature neutrophils **(C.)** Administration of G-CSF to mice with a humanized immune system caused a dramatic reduction in peripheral blood $CD16^{+}$, with an associated increase in $CD16^{int/-}$neutrophils. 2-way ANOVA and Sidak's multiple comparison test **p <0.01, *** p< 0.001 **(D).** Representative images of AAV LDG subsets shown. Images obtained at 60X magnification on ImageStreamX Mk11 using DAPI nuclear stain (blue), CD15 (green) and CD10 (red). Merged images show the multilobed $CD16^{+}$ population and the circular shaped nuclei of the $CD16^{int/-}$population and the CD10 staining of the CD16 subpopulations **(E).**

3.3.5 In AAV imaging Flow cytometry allows definitive phenotyping of PBMC populations.

Representative images are shown of various cell populations from a patient with active AAV, with each row illustrating the separate channels, alongside merged images (A). Rows 1-4 show $CD15^{+}CD16^{+}$ granulocytes, rows 5-8 $CD15^{+}CD16^{-}$ granulocytes, row 8 eosinophils and row 10 monocytes. Having established that LDGs are heterogenous based on their nuclear morphology and their CD16/CD10 expression, I then sought to link nuclear morphology to additional surface markers to more accurately define LDGs in the context of the PBMC population and to confirm that the $CD16^{-}$populations are not eosinophils, which are also $CD15^{+}CD16^{-}$. I found that the putative myeloid-derived suppressor cell marker LOX-1[90] had a low expression on $CD15^{+}CD16^{-}CD10^{+}$ cells with multilobed nuclei (**Figure 3.3.5A**). Conversely, the corresponding $CD16^{int/-}$ LDG population with round or kidney shaped nuclei had high LOX-1 expression. Eosinophils, with their distinctive classic hinged nuclei, were clearly identified as Siglec-8 positive and, like monocytes were distinct from $CD15^{+}CD16^{-}$ LDGs. (**Figure 3.3.5A A, Rows 9 &10**).

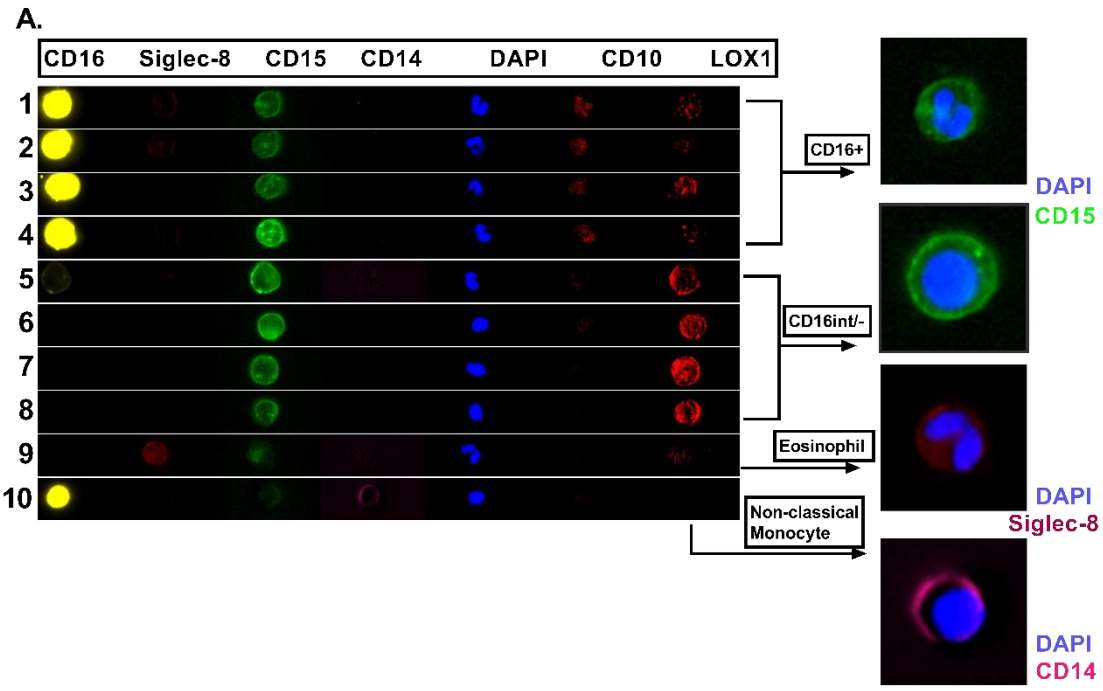

Figure 3.3.5 AAV imaging Flow cytometry allows definitive phenotyping of PBMC populations.

Representative images are shown of various cell populations from a patient with active AAV, with each row illustrating the separate channels, alongside merged images (**Figure 3.3.5A A**). Rows 1-4 show $CD15^{+}CD16^{+}$ granulocytes, Rows 5-8 $CD15^{+}CD16^{-}$ granulocytes, Row 9 eosinophils and Row 10 monocytes.

3.3.6 Surface marker expression varies according to cell fraction and disease state.

To further characterize the LDG and NDG fractions in both AAV and COVID-19 and determine if there were disease specific changes in surface marker expression, I focused on the expression of pan granulocyte marker CD15 and maturity markers CD16 and CD10 (**Figure 3.3.6 A.B.C**) using traditional flow cytometry. Interestingly, CD15 was consistently significantly elevated in the LDG fraction in all COVID-19 patients regardless of severity ($P< 0.0001$) whereas in AAV patients there was no significant increase in CD15 expression in fact some patients had lower expression not linked to acute or remission cases. Reports of altered CD15 expression on neutrophils in TB and in healthy human pregnancy suggest that CD15 expression may be altered due to activation states in different conditions [54, 217]. CD16 is expressed on maturing neutrophils faintly on metamyelocytes while banded and segmented stages show the highest expression, as I have already established that LDGs are a heterologous population of mature and immature cells in both AAV and COVID-19. There is a significant decrease in CD16 expression in both COVID-19 ($P< 0.0001$), and AAV ($P< 0.001$), the corresponding MFI flow cytometry plot clearly shows the heterogenous nature of the LDG population in its bimodal peaks, whereas the NDG population consists of a single peak, this is representative of both COVID-19 and AAV CD16 expression. CD10 is also a maturity marker for neutrophils and although there is a trend towards decreased expression on both the LDG and NDG fractions in both COVID-19 and AAV it is not statistically significant this may be partly due to the fact that CD10 is expressed later that CD16 in the maturation process of neutrophils [213]. Again, the MFI flow plot confirms the existence of a bimodal population in the LDG faction compared to the NDG fraction albeit not as clearly separated as the CD16 plot reflecting their different maturation expression patterns (the fact that CD10 is expressed later that CD16 in the maturation process of neutrophils.

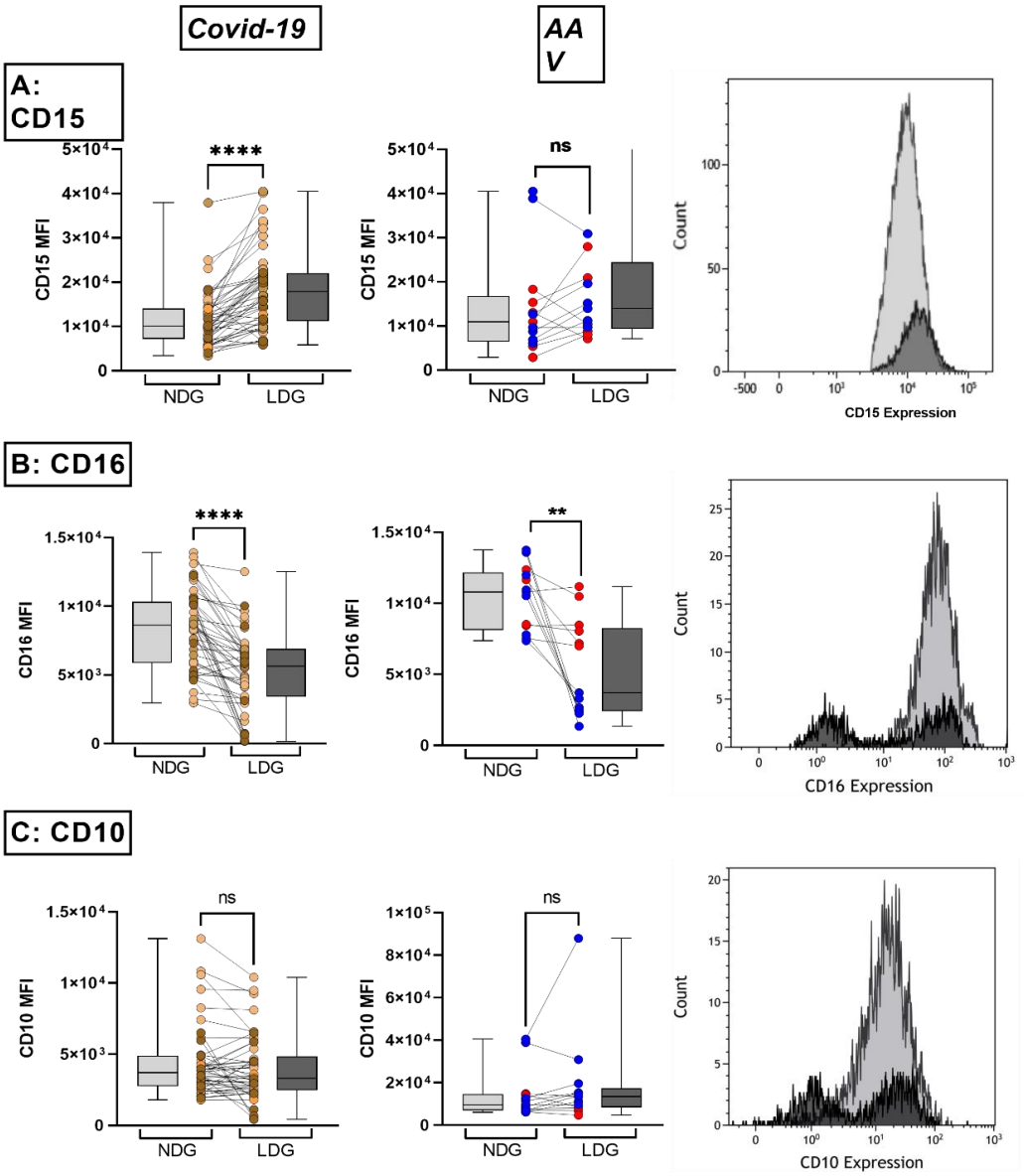

Figure 3.3.6 Surface marker expression varies according to cell fraction and disease state.

Surface marker expression of CD15 (**A**), CD16 (**B**), and CD10 (**C**) in LDG and NDG subsets and representative flow plots showing the MFI of the surface marker in both the LDG (dark grey) and NDG (light grey) fractions of COVID-19 patients. Tables analysed using Wilcoxon matched-pairs signed rank test. *p<0.05, **p <0.01, and ***p < 0.001.

3.3.7 Activation markers CD62l and myeloid marker CD33 expression on LDG and NDG fractions in AAV and COVID-19.

To further determine the phenotype of LDGs in AAV and COVID-19, the expression of activation markers CD62l and myeloid marker CD33 expression on LDG and NDG fractions were measured by flow cytometry. CD62l expression is significantly lower on LDG than NDG fractions in COVID-19 (P< 0.0001) and this lower expression is seen also in both active and remission AAV (P=0.0002),

indicating an activated cell phenotype (**Figure 3.3.7A**). A single population of lower CD62L expression is evident in the histogram of CD62L MFI, that is not bimodal suggesting that the shedding of CD62l, may not be directly linked to maturity as was the case with CD16 and CD10 (**Figure 3.3.6**)

CD33 is a myeloid marker strongly expressed on monocytes and with lower expression of neutrophils and used as a marker of PMN MDSCs [75]. In COVID-19 there is a significant reduction in CD33 expression in LDGS compared to NDGs (P< 0.0001), which may in fact be the opposite of the expected phenotype [218]. The pattern of CD33 surface staining is less clear in AAV possibly due to limited N numbers (N=13) although there is a trend towards significance (p=0.0574).

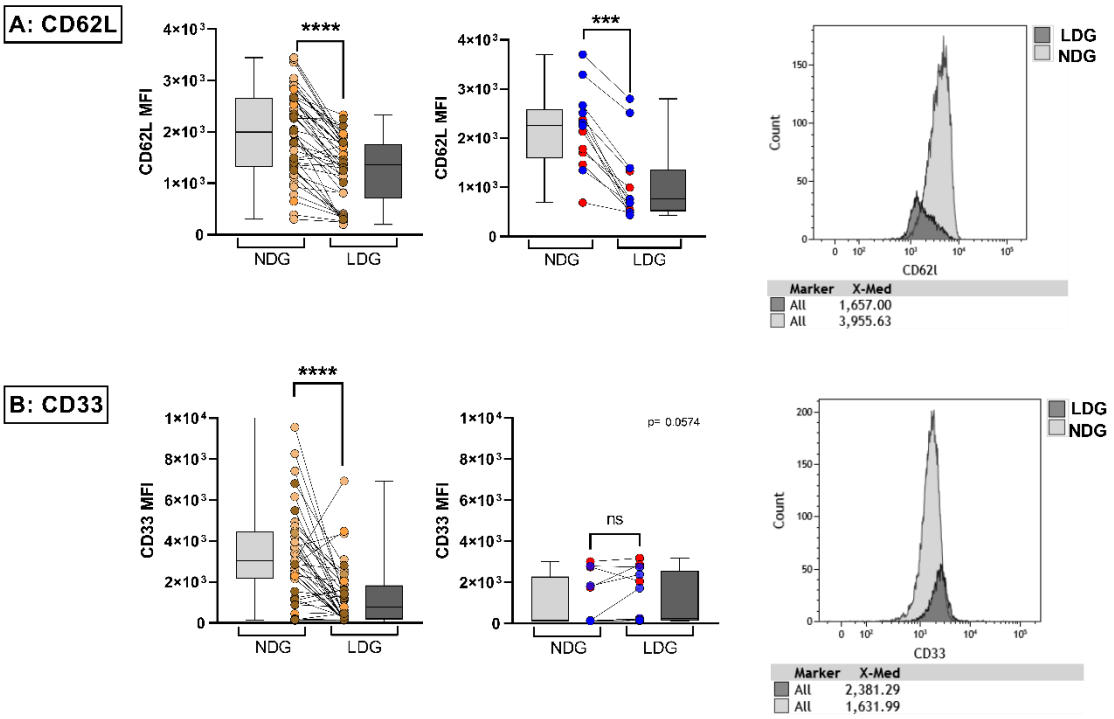

Figure 3.3.7 Activation markers CD62l and myeloid marker CD33 expression on LDG and NDG fractions in AAV and COVID-19

CD62l expression is significantly lower on LDG than NDG fractions in both AAV and COVID-19 indicating an activated cell phenotype. CD33 expression is significantly lower on LDGs in COVID-19 with the same trend approaching significance p= 0.0574 in AAV. Representative flow plots showing the MFI of the surface marker in both the LDG (dark grey) and NDG (light grey) fractions of COVID-19 patients. Tables analysed using Wilcoxon matched-pairs signed rank test. *p<0.05, **p <0.01, and ***p < 0.001.

3.4 Discussion

Low Density Granulocytes that appear in the PBMC layer of peripheral blood after density gradient centrifugation have been identified in many disease states as diverse as autoimmunuity, cancer,

sepsis and viral infection. With the onset of the SARS CoV 2 pandemic the opportunity to directly compare these cells with those already identified in ANCA vasculitis was a boon to further our understanding of the origin and phenotype of this neutrophil subset. At first glance the etiology of these diseases appears to be very different, but the systemic nature of both diseases leads to remarkably similar symptoms from glomerulonephritis to lung involvement in severe cases. Interestingly, one reported study misdiagnosed ANCA vasculitis as Covid -19 [210]. As the pandemic progresses more reports of COVID-19 patients presenting with glomerulonephritis and positive ANCA titres have been published [219, 220]. In fact these two conditions could have a closer pathophysiology that initially thought, as patients with no history of AAV or any renal dysfunction have developed positive ANCA titres [220]. Although the association between COVID-19 infection and the development of glomerulonephritis may be currently obscure it is possible that an altered response to infection in COVID-19 could give rise to AAV. The presence of NETs from neutrophils that could serve as a source of the autoantigens MPO and PR3 and NETs are reported in AAV and postulated to be involved in the pathogenesis of COVID-19 [107, 221]. Understanding therefore the key neutrophil involvement in both COVID-19 and AAV will clearly further our understanding of the etiology of both diseases.

In order to elucidate the role of LDGs in both AAV and COVID-19. I first divided the AAV patients into those with active disease and those that were in remission based on the hypothesis that those in active disease could be compared directly with patients with active COVID-19. The COVID-19 cohort were divided into mild moderate and severe cases based on the WHO severity scale classification. I found that low density granulocytes are elevated in patients with acute AAV and in patients with COVID-19 and are linked to severity in COVID-19 patients with the highest levels found in severe disease. I found that LDGs in AAV were increased compared to healthy controls but importantly were increased in comparison to disease controls, which were a mix of patients with renal impairment and non-AAV systemic inflammation. This indicates that this cell type is specifically expanded in AAV patients and therefore may play a role in the pathophysiology or disease pathogenesis of AAV. In COVID-19 there were significantly higher levels of LDGs in in moderate and severe cases when compared to healthy controls and these cells were not evident in convalescent cases highlighting their link to severity and their link to a putative role in active disease. There is a notable spread of data in COVID-19 patients in particular the moderate and severe patients this is also evident in Acute AAV this could be due in part to the systemic nature of the diseases and in COVID-19 the presence of underlying comorbidities which are a risk factor for severe disease [222]. There are reports citing elevated low-density neutrophils in COVID-19 but no accounts of a comparison between COVID-19 and AAV LDGs [223, 224].

CD16 is a low affinity receptor for IgG that is expressed on neutrophils in the latter stages of neutrophils maturation, faintly expressed on metamyelocytes whilst banded and segmented neutrophils have the highest expression [212, 213]. We have previously reported that LDGS are a mixed population of mature and immature neutrophils in AAV [49] and there are reports of LDGs in COVID-19 being a heterologous population of mature and immature cells [223]. To investigate the subpopulations CD16 expression was quantified by flow cytometry in both AAV and COVID-19 with $CD16^{+}$ representing the mature fraction and $CD16^{int/-}$ representing the immature cells. In AAV there was a significant increase in immature cells in both acute and DC patients when compared to HC patients and patients in remission suggesting that these cells are a feature of active disease the absolute count was also significantly increased in acute disease further confirming their presence in inflammation. In COVID-19, there was no significant increase in percent of immature cells however, when absolute number of cells were taken into account both moderate and severe patients were significantly increased compared to convalescent patients again confirming that these cells are present in active disease. This non-specific expansion of the $CD16^{int/-}$ LDG fraction in both AAV and COVID-19 may be arising as a result in an extreme left shift during granulopoiesis also called emergency granulopoiesis whereas the mature fraction of $CD16^{+}$ LDGs may be result from degranulation that would lead to a loss of density both a generalized response to inflammation, both these concepts will be addressed further in Chapters 4 and 5.

To confirm that LDGs from AAV and COVID-19 are a mixed population of mature and immature cells as defined by CD16 expression and nuclear morphology I used imaging flow cytometry, which exploits the advantages of traditional flow cytometry with that of microscopy, as the morphology of the nucleus defines the maturation stage of neutrophil development. Mature cells are typically multilobed whereas immature cells have gradually increasing numbers of lobes, the most immature cells having round nuclei, progressing to kidney or bean shaped and finally multilobed nuclei. There are reports of hyper-lobed and hypo-lobed nuclei in many conditions and in response to administration of certain drug regimens so the combination of maturity markers and nuclear morphology is a vital tool in the understanding of the aberrant neutrophil populations found under the inflammatory conditions of AAV and COVID-19 [7, 225]. Imaging flow cytometry confirmed that $CD16^{int/-}$ LDGs in AAV and COVID-19 had immature round or bilobed nuclei, interestingly AAV $CD16^{int/-}$ LDGs had a predominance of single lobed cells in contrast to $CD16^{int/-}$ LDGs in COVID-19 which had more bilobed neutrophils in this population. The mature $CD16^{+}$ population were similar in both conditions with most cells having two to three lobes. I found no evidence of nuclear hyper-segmentation in either condition.

To further validate that CD16 expression reflects maturity and is not a result of shedding due to neutrophil activation or apoptosis, I looked at the correlation of CD10 a maturity marker expressed at the segmented stage of neutrophil development with CD16 expression. I found a direct correlation of CD16 and CD10 in both AAV and COVID-19 and both markers identified a bimodal population in $CD16^{int/-}$ LDGs and a single population of mature neutrophils in the CD16+ LDGs. This allows us to directly compare our data with those of other laboratories that have reported heterogenous population of LDGs based on CD10 expression [104, 215]. To determine whether the expansion of the $CD16^{int/-}$ LDGs are a result emergency granulopoiesis, I re-analysed data from work previously carried out in our lab on mice with a humanized immune system. G-CSF was administered and the levels of peripheral blood CD16 neutrophils were determined by flow cytometry, confirming that $CD16^{int/-}$ neutrophils were increased in this model of emergency granulopoiesis.

In AAV imaging flow cytometry allows definitive phenotyping of the LDG population. Having determined that LDGs are a heterogenous cell population based on their nuclear morphology and CD10/CD16 expression I linked nuclear morphology in the context of additional surface markers and to confirm that the $CD16^{-}$ population are not eosinophils. Nuclear morphology and combinations of surface markers such as CD10 LOX-1 and Siglec 8 clearly reveal that the $CD16^{int/-}$ populations have a distinct phenotype that could allow identification of these cells in whole blood. This confirms that the LDG population has a distinct phenotype in AAV not just linked to maturity for example, LOX-1 expression has been mooted as a marker for MDSCs in cancer [90]. An extended panel of markers including LOX-1 is currently being investigated by a colleague in the context of COVID-19.

To establish how surface marker expression is influenced by cell fraction and in the context of COVID-19 and AAV, I focused on the expression on pan-granulocyte marker CD15 and maturity markers CD10 and CD16. CD15 revealed upregulation on LDGs is significant in COVID-19 but not in AAV, alterations in CD15 expression is reported in conditions such as TB and healthy human pregnancy and may reflect altered activation states in different disease settings [54, 217]. Increased expression of CD15 on LDGs could be due to upregulation of this molecule in response to degranulation and activation [226]. Both CD10 and CD16 have similar bimodal LDG populations reflecting a heterogenous population of mature and immature neutrophils the mature cells likely a result of emergency granulopoiesis, CD10 expression however is not statistically significant this could be in part to the later expression of CD10 than CD16 in the neutrophil maturation process and suggests that CD16 is a more suitable marker for neutrophil maturation in this scenario. In both conditions CD62L is downregulated in LDGs suggesting activation [162]. CD33 is significantly

reduced in COVID-19 LDGs and may be a useful marker for the identification of these neutrophils in whole blood, Alberca et al use CD33 to identify gMDSCs in COVID-19 [227].

In conclusion, despite the very different etiology of COVID-19 and AAV and with the emergence of LDGS being a common feature, I set about defining a disease specific response. In both diseases LDGs are elevated and linked to severity. However, both LDG populations have remarkable similarities with respect to immature populations likely due to extreme left shift from emergency granulopoiesis. The mature $CD16^{+}$ cells in both diseases again have remarkably similar surface marker expression and nuclear morphology. Indeed, it would appear that the LDGs in AAV and COVID-19 are a general response to inflammation and in fact not a result of disease specific triggers.

Chapter 4

Immunomodulatory Arginase expression in Neutrophil Subsets

4 Immunomodulatory Arginase expression in Neutrophil Subsets

4.1 Introduction - the concept of Arginase 1-mediated immunosuppression

In Chapter 3 of this work, I focused on the phenotype of LDGs in both COVID-19 and AAV based on surface marker expression and nuclear morphology. In this chapter I will focus on a functional aspect of these cells, arginase-mediated immunosuppression. The theory of arginase-1 related immunosuppression is not a new one, over 40 years ago a seminal study demonstrated that depletion of l-arginine in an arginase dependent mechanism suppressed cells in culture [170]. The initial work was focused on macrophage subsets but more recently arginase 1 expression in neutrophil subsets has garnered attention. In neutrophils arginase 1 is produced by the gelatinase granules, in steady state conditions arginase 1 is released intracellularly to combat microbial attack [176]. In disease states however there is evidence to suggest that arginase 1 is released extracellularly **(Figure 4.1.1).** This is particularly well studied in the tumour microenvironment, where neutrophils infiltrating solid lung tumours were found to have decreased intracellular arginase-1 indicating that arginase had been released into the tumour microenvironment [180]. Another study elegantly demonstrated that an increase of serum arginase 1 was associated with an expansion of degranulated neutrophils and led to suppressed T cell function *in vitro* [181]. Increased arginase 1 has subsequently been linked to disease activity in several disease states including sepsis, viral infection and cancer [46, 90, 191].

A key hallmark of neutrophilic arginase 1 is the impaired proliferation of T cells and immunosuppressive functions, it follows then that I would focus on the expression of arginase-1 in COVID-19 patients and in AAV patients in order to establish if there are specific response in these diseases. In the short time since the emergence of SARS CoV-2 there are several papers focusing on the gene expression of arginase 1 [184, 185]. There are no reports of increased arginase 1 in AAV.

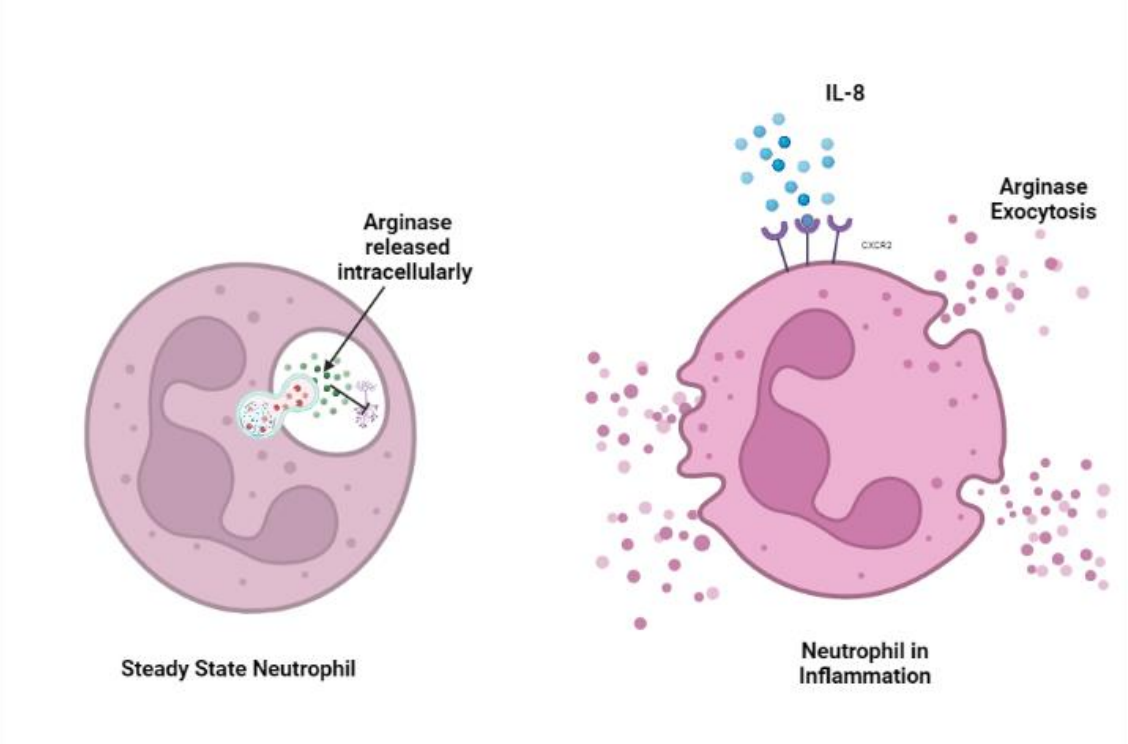

Figure 4.1.1 Arginase in steady state neutrophils and in inflammation

4.2 Design and Rationale

4.2.1 Hypothesis

We have shown that LDGs are elevated in both AAV and COVID-19. Arginase 1 released from neutrophil subsets is linked to immunosuppression. I hypothesized that

- Arginase 1 would be released by LDGs and not NDGs in both diseases
- Arginase 1 release would be linked to outcome
- Arginase 1 serum levels would be elevated in COVID-19 patients
- Neutrophil culture supernatants would suppress T cells *in vitro*

4.2.2 Methods

Patients and controls were recruited from two cohorts, COVID-19 patients as outlined in Chapter 2.3. There were 7 acute AAV patients and 6 remission patients recruited to the criteria and consents of the RKD biobank as outlined in Chapter 2.3

Flow cytometry and imaging flow cytometry and T cell suppression, Arginase 1 ELISA and activity assays as outlined in Chapter 2.4, 2.5, 2.6, 2.7.

4.3 Results

An imbalance between pro and anti-inflammatory effector systems accounts for a wide variety of autoimmune and chronic inflammatory diseases [228]. A key feature of inflammation-triggered immune dysfunction is a dramatic impairment of T-cell mediated responses [229]. To provide evidence of neutrophil plasticity in inflammation and to elucidate a mechanism whereby neutrophils can direct other cells behaviour, in particular T cells and to contradict the paradigm that neutrophils are simple bags of enzymes that are mobilized to respond to inflammation before the adaptive immune arm moves in, I set about characterizing intracellular arginase levels in AAV and COVID-19. Arginase is present in the gelatinase granules of neutrophils and its release is linked with a decrease in arginine which is required for the expression of the T cell receptor zeta chain and proliferation of T cells, resulting in immunosuppression [168, 175].

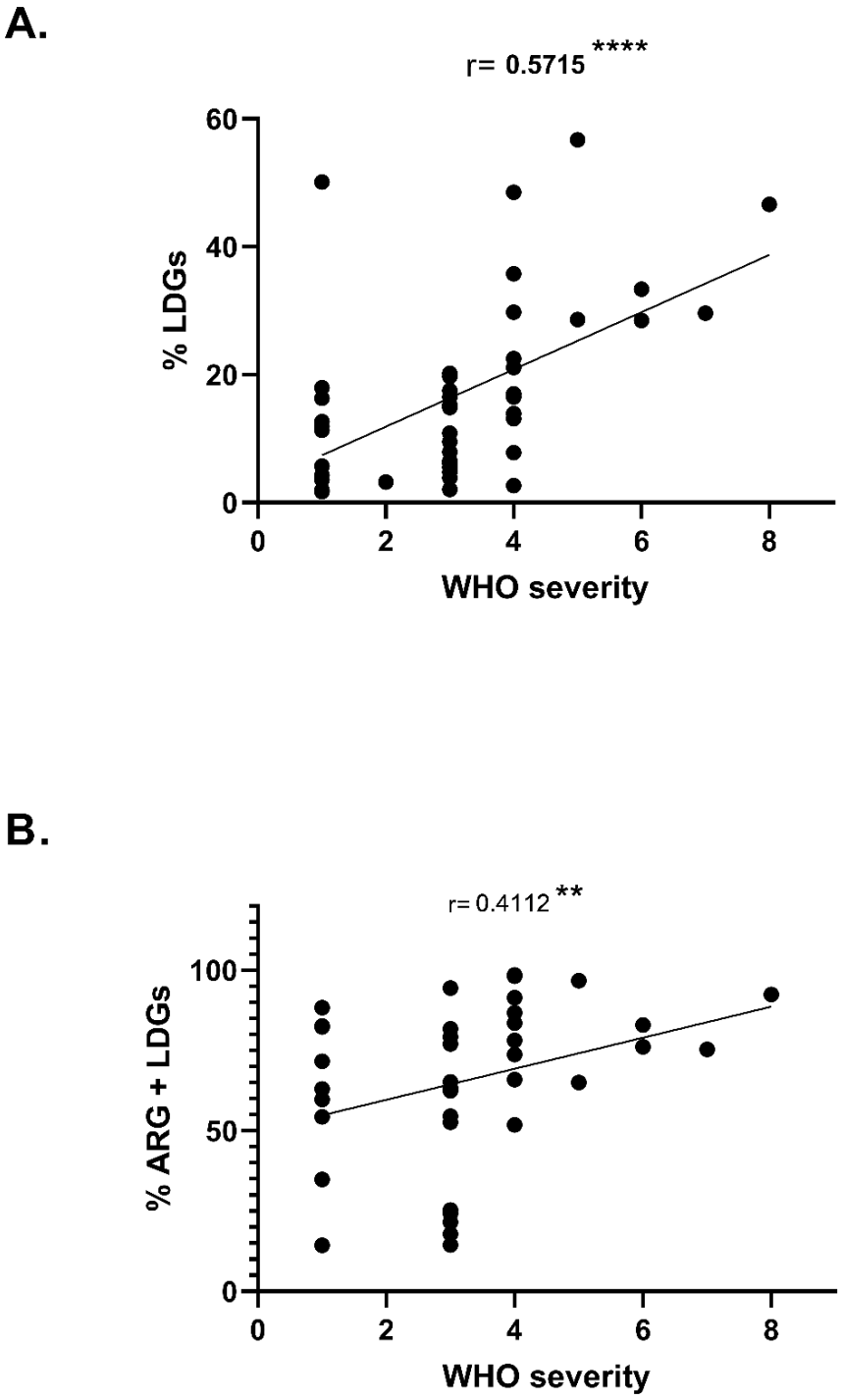

Figure 4.3.1 The percentage of LDGs in COVID-19 are elevated and linked to severity. Percentage arginase 1 positive LDGs are also linked to severity in COVID-19

PBMC were isolated from peripheral blood of patients with COVID-19, LDGs as a percent of $CD15^+$ $CD14^-$ PBMCs from 31 mild,14 moderate and 9 severe COVID-19 patients based on WHO severity scale were quantified. Arginase positive cells were classified as $CD15^+$ $CD14^-$ $Arg1^+$ singlets. Each symbol represents an individual donor. LDG percentages in PBMCS correlate closely with WHO severity. *Spearman correlation* **(A).** Arginase 1 positive cells also correlate with WHO severity with higher percentages linked to severe disease **(B).** *Spearman correlation* *p<0.05, **p <0.01, and ***p < 0.001. ****p < 0.0001**.**

4.3.1 The percentage of LDGs in COVID-19 are elevated and linked to severity. Percentage arginase 1 positive LDGs are also linked to severity in COVID-19

Low density granulocytes in the PBMC of percoll separated blood were phenotypically examined by flow cytometry in COVID-19 patient peripheral blood. LDGs as a percent of $CD15^+$ $CD14^-$PBMCs from 31 mild, 14 moderate and 9 severe COVID-19 patients based on WHO severity scale were quantified (**Table 4.1**). The percentage of LDGs in COVID-19 are significantly correlated to severity in COVID-19 with a spearman coefficient of 0.5715 (**Figure 4.3.1 A**). Having permeabilized the LDGs and stained for intracellular arginase 1, the percentage arginase 1 positive cells ($CD15^+$ $CD14^-$ $Arg1^+$ singlets) as defined by the FMO also significantly correlated with WHO severity in COVID-19 with a spearman coefficient of r=0.4112 (**Figure 4.3.1 B**). Despite the spread of data in the more severe cases, the results demonstrate a significant trend in both percentages of LDGs and arginase 1 positive cells, and likely the spread reflects the emergence of these cells in extreme inflammatory conditions. The results suggest that arginase 1 release from LDGs in mild cases of COVID-19 correlates with better outcome and prompt further investigation of arginase levels in LDG subsets.

Patient State	Treatment	WHO score
Uninfected	No clinical or virological evidence of infection	0
Ambulatory	No limitation of activities	1
	limitation of activities	2
Hospitalised	Hospitalised, no oxygen therapy	3
Mild disease	Oxygen by mask or nasal prongs	4
Hospitalised	Non-invasive ventilation or high-flow oxygen	5
Severe disease	Intubation and mechanical ventilator	6
	Ventilation and additional organ support-pressors RRT, ECMO	7
Death	Death	8

Table 4.1 WHO Severity Score

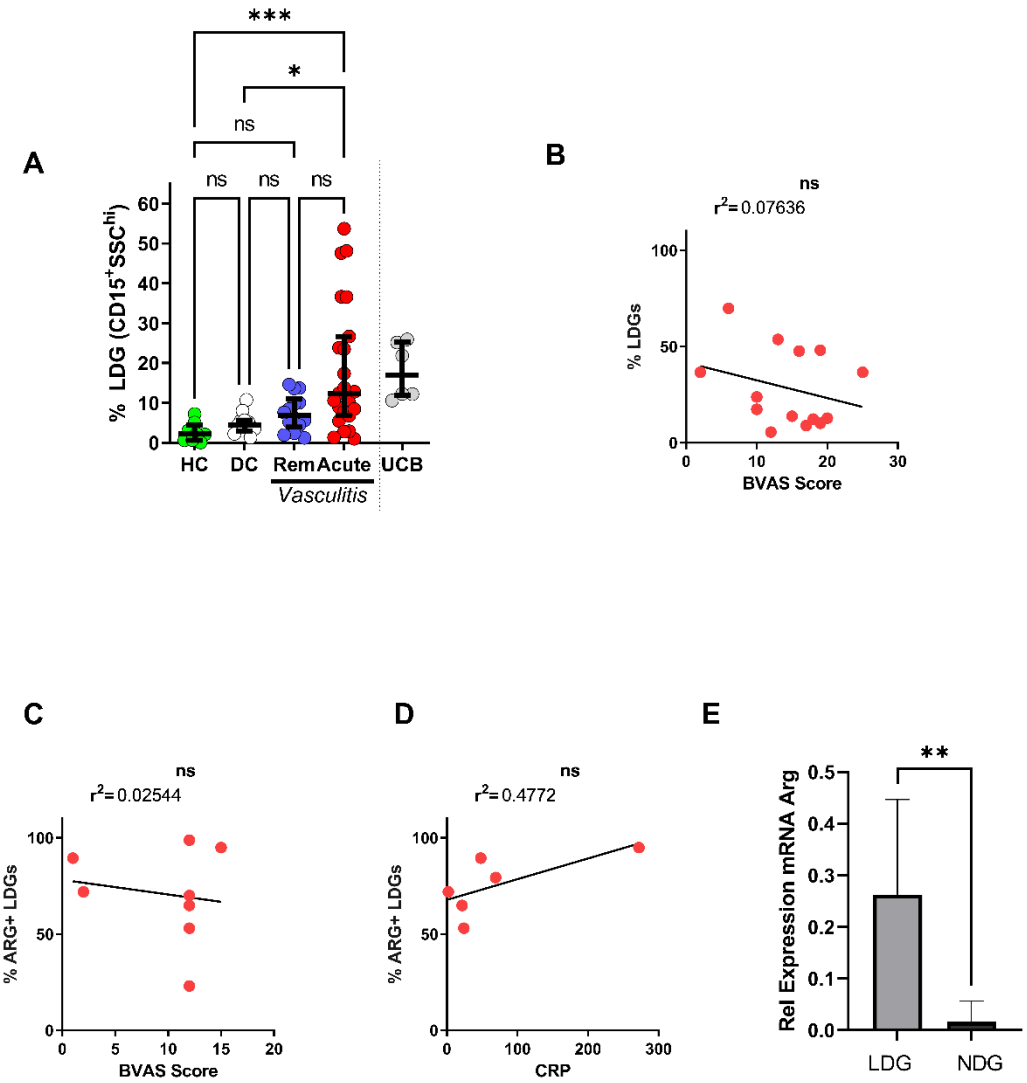

Figure 4.3.2 LDGs are elevated in patients with Acute AAV compared to those in remission. BVAS scores do not correlate with percent LDGs or percent Arg positive LDGs

PBMC were isolated from peripheral blood of patients with Acute AAV by density gradient centrifugation. LDGs were quantified as the percentage of PBMC in the peripheral blood of 23 acute AAV patients,14 remission(rem), 11 disease controls (DC) and 5 age matched healthy controls (HC), the values from 6 samples of umbilical cord blood are shown for comparison. Each symbol represents an individual donor **(A).** %LDGs does not correlate with BVAS scores in acute AAV **(B).** Arginase 1 positive LDGs do not correlate with BVAS **(C),** in fact a closer correlation was found between CRP levels and Arg + LDGs than the reported BVAS score **(D)**. rtPCR analysis shows increased arginase 1 transcription in LDGs compared to NDGs in AAV (**E**). *Spearman correlation. Median with interquartile range. Kruskal-Wallis test, with post hoc analysis with Dunn's multiple comparisons. *p <0.05,**p <0.01, and ***p < 0.001.*

rtPCR data from Dr M Lizardo

4.3.2 LDGs are elevated in patients with Acute AAV compared to those in remission. BVAS scores do not correlate with percent LDGs or percent Arg positive LDGs

In order to determine whether the arginase correlation is a disease specific phenomenon, firstly to establish that LDGs are linked to severity in AAV, LDGs were quantified as the percentage of PBMC in the peripheral blood of 23 acute AAV patients, 14 remission (rem), 11 disease controls (DC) and 5 age matched healthy controls (HC), the values from 6 samples of umbilical cord blood are shown for comparison. Each symbol represents an individual donor (**Figure 4.3.2 A**). However, whilst there is a trend towards higher percentages in acute patients than in remission the result is not significant (Median with interquartile range. Kruskal-Wallis test, with post hoc analysis with Dunn's multiple comparisons). The COVID-19 patients correlated with an established index of COVID-19 as set out by WHO guidelines (**Table 4.1**). The equivalent index of severity for AAV is the Birmingham Vasculitis Activity Score (BVAS)[230]. The percentage of LDGs does not correlate with AAV as determined by the BVAS AAV score r= 0.076 (Spearman coefficient), in fact the correlation appears to be negative. I then correlated the percentage Arg positive cells with the BVAS score and again the correlation was not significant (**Figure 4.3.2 C**). To determine if the arginase 1 positive cells correlated with a readout of inflammation I correlated the arginase 1 positive cells with the CRP levels and in fact there was a closer correlation to CRP r= 0.477 than the reported BVAS score, albeit is not significant (**Figure 4.3.2 D**). rtPCR analysis highlights an increased transcription of Arg 1 in the LDG fraction of AAV patient blood compared to the NDG fraction (**Figure 4.3.2 E**) this work was carried out by Dr Maria Lizardo under my supervision. Therefore, as the n numbers of AAV patients are low and there is not an equivalent comparable vasculitis activity score to determine disease severity, I concentrated on COVID-19 LDGs for initial characterisation of the LDG arginase 1 profile.

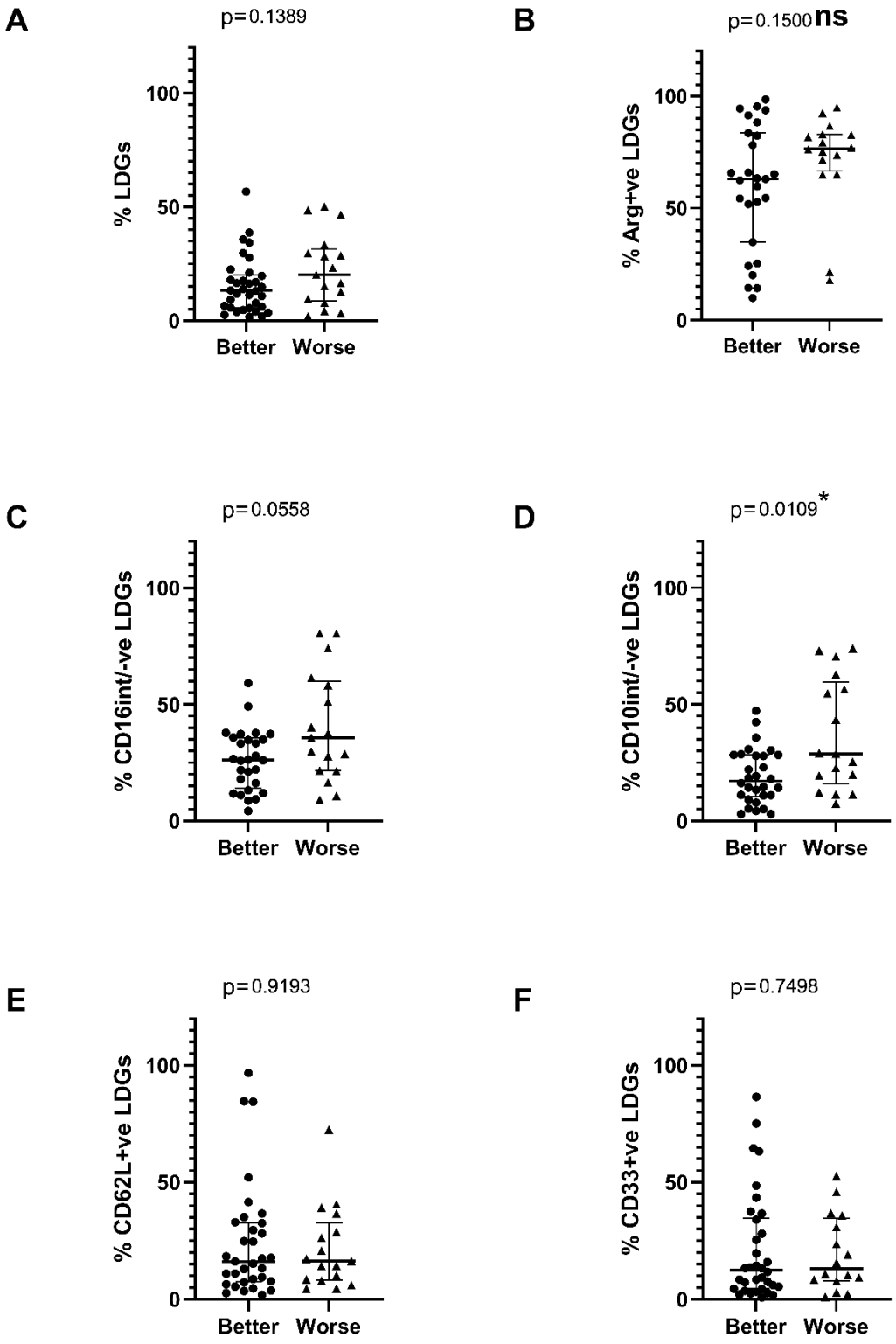

Figure 4.3.3 An expansion of immature LDGs as defined by maturation markers CD10 and CD16 are linked to outcome in COVID-19

LDGs were phenotyped using a panel of surface markers and intracellular arginase in COVID-19 patient peripheral blood. LDGS as $CD15^{+}$ $CD14^{-}$ singlets as a percentage of PBMCs levels in patients that improved (solid circle) and deteriorated (solid triangle) **(A),** intracellular arginase was determined following

permeabilization of PBMCs linked to outcome **(B)**. Percentages of maturation markers CD16 and CD10 linked to outcome **(C&D).** Percentages of activation maker CD62L **(E)** and myeloid marker CD33 **(F)** do not show significantly changed percentages when linked to outcome. *Mann-Whitney t test, P values as indicated on graph* ***p<0.05**.

4.3.3 An expansion of immature LDGs as defined by maturation markers CD10 and CD16 are linked to outcome in COVID-19

Having shown that LDGs and arginase correlate with WHO severity (**Figure 4.3.1**), with higher levels of both readouts correlating with more severe disease I hypothesised that percentage of arginase may be linked to outcome. I stratified the COVID-19 patient cohort based on outcome with those that improved and with those that deteriorated and with a panel of markers including Arg and maturation markers CD10 and CD16, and activation marker CD62l and a marker of suppressive cells myeloid marker CD33. Interestingly, percent LDGs did not significantly differ between outcomes (**Figure 4.3.3 A**). Although not significant there was a trend towards percent Arginase 1 positive cells correlating with outcome with higher levels being associated with poorer outcome (**Figure 4.3.3 B**). Both markers of maturity were increased in patients with deteriorating disease, with $CD16^{low}$ LDGs approaching significance p=0.058 and $CD10^{low}$ LDGs being significantly increased p=0.01 (**Figure 4.3.3 C, D**). Percentages of activation maker CD62L and myeloid marker CD33 did not show significantly changed percentages when linked to outcome (**Figure 4.3.3 E, F**).

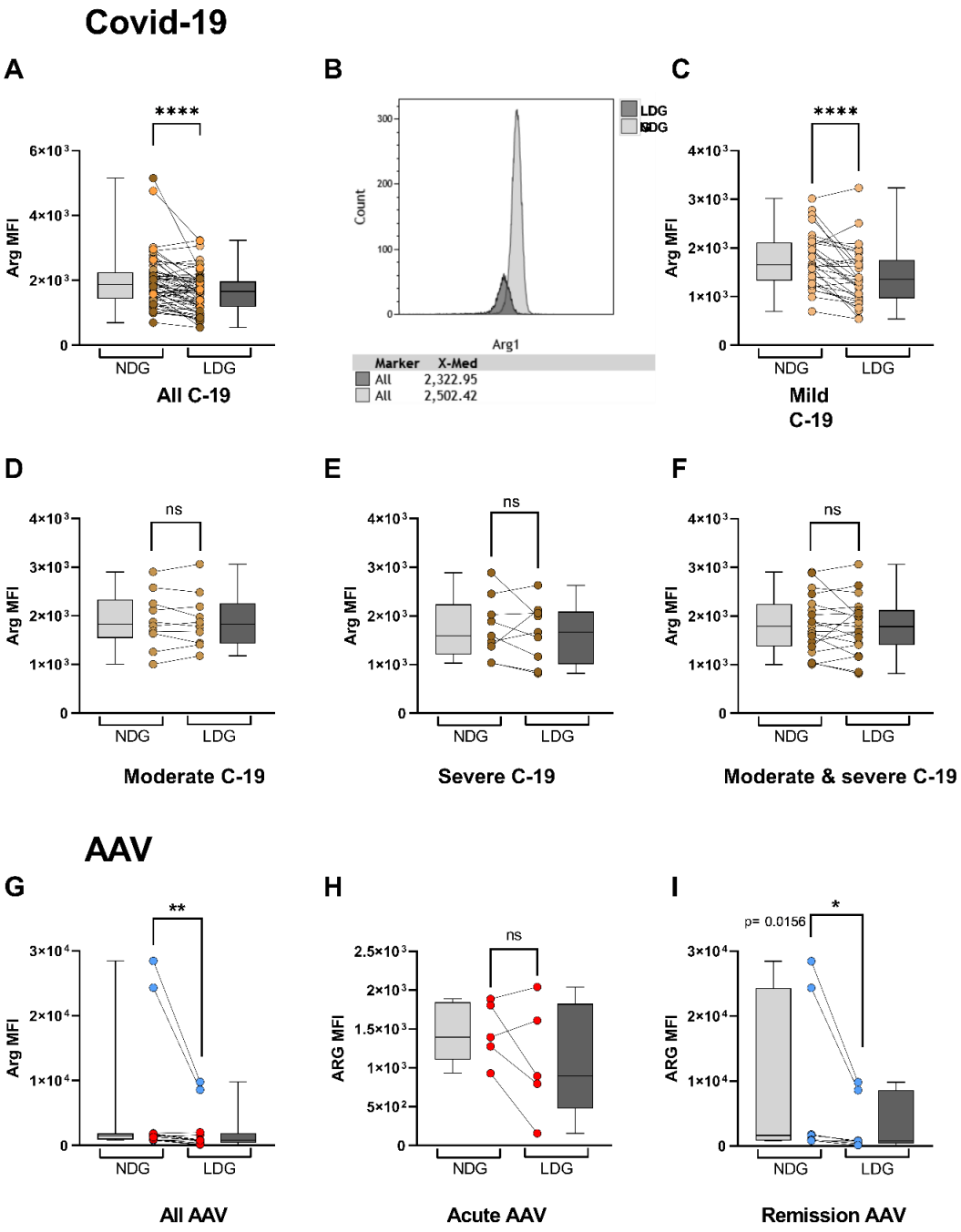

Figure 4.3.4 NDG arginase levels are inversely linked to severity in COVID-19

Whilst overall there is a difference in MFIs between LDGS and NDGs in both COVID-19 and AAV **(A, G),** milder disease displays significant differences in Arginase MFI between NDGs and LDGs, with LDGs having lower MFIs whereas this trend is not observed in moderate or severe COVID-19 or acute AAV. Intracellular Arginase MFIs were determined by flow cytometry in LDGs (dark grey) and NDGs (light grey) in mild moderate and severe COVID-19 (light mid and dark brown respectively) COVID-19 **(C, D, E)** and in acute (red) and remission (blue) AAV **(H, I).** Moderate and severe COVID-19 have no significant differences between cell fractions compared to Mild COVID-19 **(C, F).** Representative histogram flow plots showing the MFI of intracellular arginase in both LDG (dark grey) and NDG (light grey) fractions (**B**). Tables analysed using Wilcoxon matched-pairs signed rank test. ***p<0.05, **p <0.01, and ***p < 0.001.**

4.3.4 NDG arginase 1 levels are inversely linked to severity in COVID-19

To determine if there was a link between arginase release in LDGs and NDGs I looked at the paired MFIs of arginase 1 in NDGs and LDGs in both AAV and COVID-19 to determine if there were disease specific arginase response. I hypothesised that as normal healthy control NDGs have close to high levels of arginase 1 that their matched LDGs would have lower arginase 1 MFIs and that the paired MFI may reflect severity. I measured paired arginase 1 MFIs in 31 mild, 14 moderate and 9 severe COVID-19 patients based on WHO severity scale and in 7 acute and 8 remission AAV patients. Overall, there is a difference in MFIs between LDGs and NDGs with LDGs having lower MFIs in both COVID-19 (NDG MFI 1875, IQR 1434-2257, LDG MFI 1660, IQR 1180-1971) and AAV (NDG 932, IQR 1502-1866, LDG 802, IQR 441-1933) (**Figure 4.3.4 A, G**). COVID-19 patients with milder disease display significant differences in arginase 1 MFI between NDGs and LDGs (NDG 1657, IQR 1325-2111, LDG 1354, IQR 964-1753) (**Figure 4.3.4 C**) with LDGs having lower MFIs whereas this trend is not observed in moderate or severe COVID-19 where the MFIs are almost identical (NDG 1790, IQR 1376-2252, LDG 1782, IQR 1409-2121) (**Figure 4.3.4 D, E, F**) or acute AAV (NDG 1394, IQR 1102-1846, LDG 894,IQR 476-1836) (**Figure 4.3.4 H**). Intracellular arginase 1 MFIs were determined by flow cytometry in LDGs (dark grey) and NDGs (light grey) in mild moderate and severe COVID-19 (light mid and dark brown respectively) COVID-19 **(Figure 4.3.4 C, D, E)** and in acute (red) and remission (blue) AAV **(Figure 4.3.4 H, I).** Moderate and severe COVID-19 have no significant differences between cell fractions compared to Mild COVID-19 and remission AAV **(Figure 4.3.4 C, F).** Arginase 1 release by NDGs may lead to a poor outcome in both AAV and COVID-19.

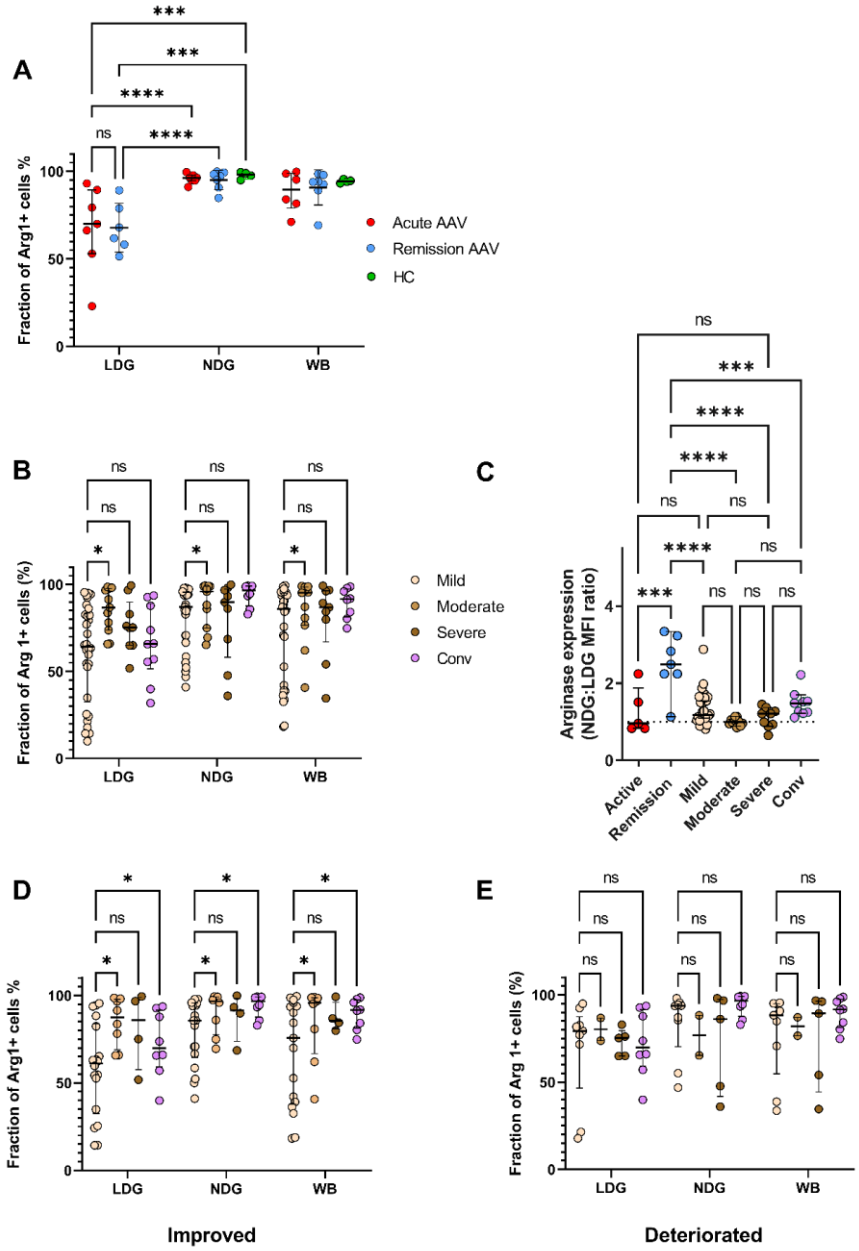

Figure 4.3.5 Arginase 1 is differentially expressed in cell fractions from AAV and COVID-19 displaying disease specific differences

Focusing on the expression of CD16 as a maturation marker for neutrophils the percentages of mature arginase 1 positive cells in each fraction LDG NDG and in whole blood (WB) in both AAV **(A)** and COVID-19 **(B)** were determined by flow cytometry. Neutrophils clearly display disease specific responses with neutrophils in the NDG fraction and in WB having significantly higher percent arginase in AAV than in COVID-19 **(A)**. Focusing on the differences in arginase expression between LDG and NDG fractions, NDG:LDG MFI ratios were calculated for AAV and COVID-19 cohorts. There is a significant difference in MFI ratio between active and remission that is not evident in the COVID-19 samples regardless of WHO severity**(C)**. As there is a broad spread of values in the COVID-19 I questioned whether arginase expression could predict outcome. Patients with improved outcome have a significant difference in arginase expression between mild and moderate and mild and convalescent samples in all fractions **(D)**, whereas patients whose condition deteriorated had no significant differences regardless of severity or fraction **(E)**. Differences between AAV and COVID-19 cell fractions were analysed using a 2-way ANOVA with Tukey's multiple comparisons test. ***p<0.05, **p <0.01, and ***p < 0.001.**

4.3.5 Arginase 1 is differentially expressed in cell fractions from AAV and COVID-19 displaying disease specific differences

To further investigate the release of arginase by LDGs and NDGs in COVID-19 and AAV I measured the percentage of arginase 1 positive cells in both fractions and diseases and stratified the results according to severity. In AAV LDGs in both Acute (70%, IQR 53-89) and remission (65%, IQR 56-81) have lower percentage arginase 1 than their equivalent NDGs, acute (96%, IQR 95-98), remission (97%, IQR 91-99). Healthy control NDGs have high percentage arginase 1 (98%, IQR 96-98) **(Figure 4.3.5 A).** This pattern of low LDG arginase 1 and high NDG arginase 1 is not evident however in COVID-19, In fact NDGs have lower percentage arginase than their AAV equivalents (**Figure 4.3.5 A, B**). Interestingly, mild cases of COVID-19 (61%, IQR 28-81) have significantly lower percentages of arginase 1 in LDGs than the moderate cases (72%, IQR 66-84) but this trend is lost in very severe disease (77%, IQR 60-97). This is observed in all three fractions, LDGs NDGs and WB. Of particular note are the convalescent fractions with LDG percentage arginase 1 (66%, IQR 52-89) being equivalent to mild COVID-19 LDGs (61%, IQR 28-81), with the NDG (97%, IQR, 88-99) fractions returning to HC levels (98%, IQR 96-98) in convalescence (**Figure 4.3.5 B**). Focusing on the differences in arginase expression between LDG and NDG fractions, NDG:LDG MFI ratios were calculated for AAV and COVID-19 cohorts. There is a significant difference in MFI ratio between active and remission AAV that is not evident in the COVID-19 samples regardless of WHO severity (**Figure 4.3.5 C**), emphasising a disease specific response. As there is a broad spread of values in the COVID-19 data I questioned whether arginase 1 expression could predict outcome. Patients with improved outcome have a significant difference in arginase 1 expression between mild and moderate and mild and convalescent samples in all fractions (**Figure 4.3.5 D**), whereas patients whose condition deteriorated had no significant differences in arginase 1 expression regardless of severity (**Figure 4.3.5 E**).

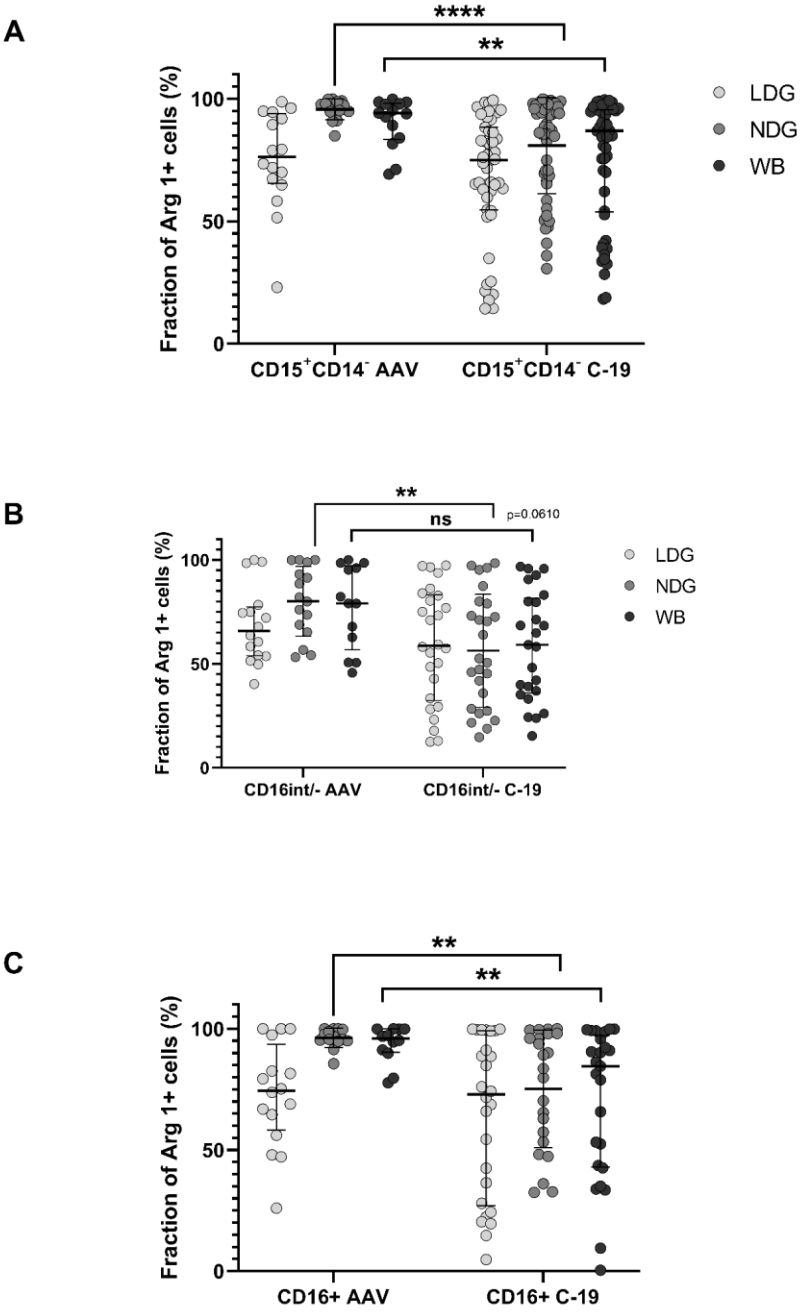

Figure 4.3.6 Arginase 1 is differentially expressed in neutrophil populations from AAV and COVID-19 with both mature and immature neutrophils having significantly less arginase 1 in COVID-19 than AAV

Whilst LDGs in both AAV and COVID-19 have similar levels of expression of arginase 1 disease specific differences are evident in the NDG fraction and also in WB with COVID-19 patients having significantly lower arginase 1 expression **(A).** When neutrophils ($CD15^+CD14^-$) are separated into mature and immature cells based on CD16 expression, I hypothesized that immature cells ($CD16^{int/-}$) would have less arginase 1 which is the case in both diseases **(B)**. Interestingly, COVID-19 immature neutrophils have significantly lower levels than AAV in the NDG fraction **(B).** Mature neutrophils ($CD16^+$) in COVID-19 have significantly lower arginase 1 than their AAV counterparts in NDG and WB **(C)**. Data was analysed using a mixed effects model with Sidak's multiple comparisons tests. ***p<0.05, **p <0.01, and ***p < 0.001.**

4.3.6 Arginase 1 is differentially expressed in neutrophil populations from AAV and COVID-19 with both mature and immature neutrophils having significantly less arginase in COVID-19 than AAV

Whilst LDGs in both AAV (76%, IQR 65-94) and COVID-19 (75%, IQR 54-88) have similar levels of expression of arginase 1, disease specific differences are evident between the NDG AAV fraction (97%, IQR 94-99) and the NDG COVID-19 fraction (88%, IQR 68-88) and also in WB with COVID-19 patients having significantly lower arginase 1 expression (87%, IQR 54-95) **(Figure 4.3.6 A)**. In Figure 4.3.3 as there was a trend towards immature neutrophils being linked to poorer outcome and as I have established that LDGs are a mixed population of mature and immature cells. in chapter three, I sought to determine the arginase 1 expression of mature and immature neutrophils. When neutrophils ($CD15^{+}CD14^{-}$) are separated into mature and immature cells based on CD16 expression, I hypothesized that immature cells ($CD16^{int/-}$) would have less arginase 1 which is the case in both AAV and COVID-19 (**Figure 4.3.6 B)**. Interestingly, COVID-19 immature neutrophils (51%, IQR 28-79) have significantly lower levels than AAV (81%, IQR 66-97) in the NDG fraction **(Figure 4.3.6 B).** Mature neutrophils ($CD16^{+}$) in COVID-19 (83%, IQR 53-98) have significantly lower arginase 1 than their AAV (96%, IQR 95-99) counterparts in NDG and is reflected in WB **(Figure 4.3.6 C)**.

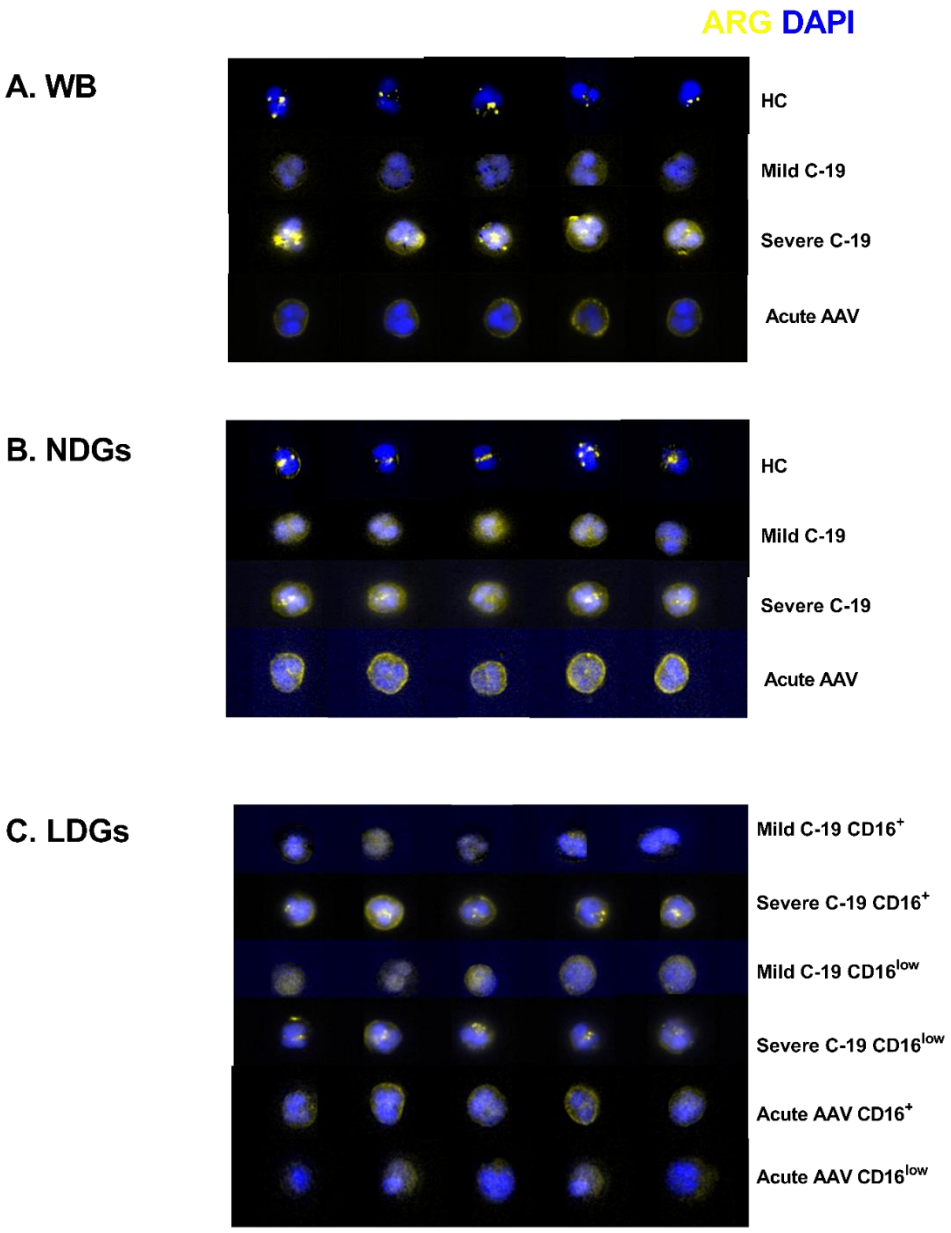

Figure 4.3.7 Imaging flow cytometry confirms disease specific intracellular arginase 1 expression in AAV and COVID-19 Neutrophils

Representative merged images of neutrophils in HC Acute AAV, mild and severe COVID-19 with DAPI stained nuclei (blue) and intracellular arginase 1 (yellow) in WB NDG and LDG fractions. In WB HC neutrophils arginase 1 are located in granules whereas in disease conditions there is a diffuse staining in the cytoplasm by contrast severe COVID-19 has a high expression of arginase 1 that appears to be both located in granules and cytoplasm. Mild COVID-19 has a very similar arginase 1 expression pattern to Acute AAV **(A).** This pattern of staining is also evident in the NDG fraction **(B)**. LDGs are subdivided into mature and immature cells based on their CD16 expression and validated by their immature round or kidney shaped nuclei (CD16 ^{low}). As in WB and NDG fractions mild and Acute COVID-19 have similar arginase 1 patterns, with the CD16^{low} immature cells having low levels of arginase 1 compared to their CD16^{+} counterparts. However, in severe COVID-19 there appears to be both a cytoplasmic and granular expression of arginase 1 suggesting either aberrant release mechanisms or increased transcription of the enzyme in severe disease **(C)**. Images obtained at 60x magnification on ImageStream X MKII.

4.3.7 Imaging flow cytometry confirms disease specific intracellular arginase 1 expression in AAV and COVID-19 Neutrophils

Arginase 1 is an intracellular enzyme and I hypothesised that as I have reported aberrant arginase 1 expression in both AAV and COVID-19 that the expression of arginase 1 could be visualised using imaging flow cytometry and may be altered in disease states. Representative merged images of neutrophils in HC Acute AAV, mild and severe COVID-19 with DAPI stained nuclei (blue) and intracellular arginase 1 (yellow) in WB NDG and LDG fractions. In WB HC neutrophils arginase 1 are located in granules whereas in disease conditions there is a diffuse staining in the cytoplasm by contrast severe COVID-19 has a high expression of arginase 1 that appears to be both located in granules and cytoplasm. Mild COVID-19 has a very similar arginase expression pattern to Acute AAV **(Figure 4.3.7 A).** This pattern of staining is also evident in the NDG fraction **(Figure 4.3.7 B)**. LDGs are subdivided into mature and immature cells based on their CD16 expression and validated by their immature round or kidney shaped nuclei (CD16 ^{low}). As in WB and NDG fractions mild and Acute COVID-19 have similar arginase 1 patterns, with the CD16^{low} immature cells having low levels of arginase 1 compared to their CD16^{+} counterparts. However, in severe COVID-19 there appears to be both a cytoplasmic and granular expression of arginase 1 suggesting either aberrant release mechanisms or increased transcription of the enzyme in severe disease **(Figure 4.3.7 C)**. Images obtained at 60x magnification on ImageStream X MKII.

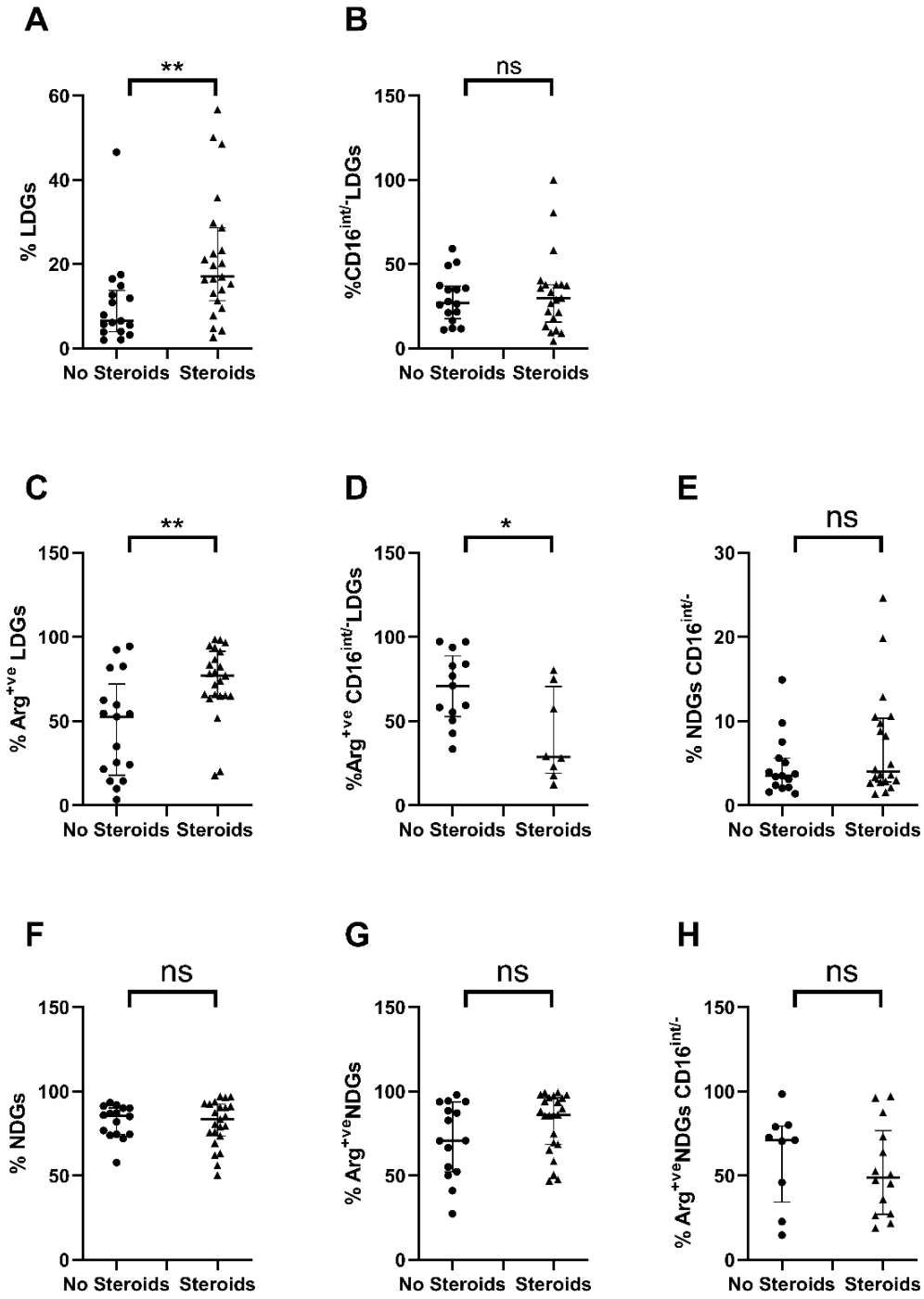

Figure 4.3.8 Steroid use is linked to phenotypic alterations in the LDG populations

The percent LDGs in COVID-19 patients with or without steroids on the day of sampling (**A**). As steroid administration is linked to increased granulopoiesis I determined the percent CD16int/- LDGs in patients with or without steroids surprisingly there was no significant increase in immature cells(**B**)..The percent Arg^{+ve} LDGs were significantly higher in steroid treated patients(**C**). Interestingly, the Arg^{+ve} $CD16^{int/-}$ LDGs were decreased in the steroid treated cohort (**D**). In the NDG fraction there was no significant difference between the steroid and non-steroid treated groups (**E,F,G,H**).

4.3.8 Steroid use is linked to phenotypic alterations in the LDG populations

As the pandemic progressed steroid use became the standard of care in hospitalised patients. My data is from late 2019 and many of my samples were steroid free. I determined the percent LDGs in COVID-19 patients with or without steroids on the day of sampling. There is a significant increase in LDGs in patients with steroids (**Figure 4.3.8 A)**. As steroid administration is linked to increased granulopoiesis I determined the percent CD16int/- LDGs in patients with or without steroids surprisingly there was no significant increase in immature cells (**Figure 4.3.8 B)**. The percent Arg^{+ve} LDGs were significantly higher in steroid treated patients (**Figure 4.3.8 C)**. Interestingly, the Arg^{+ve} $CD16^{int/-}$ LDGs were decreased in the steroid treated cohort (**Figure 4.3.8 F)**. There was no significant increase in the NDG fraction (**Figure 4.3.8 E, F, G, H**) Care is required when interpreting this result as early on in the pandemic it was only severe patients that were treated with steroids so this may skew the data.

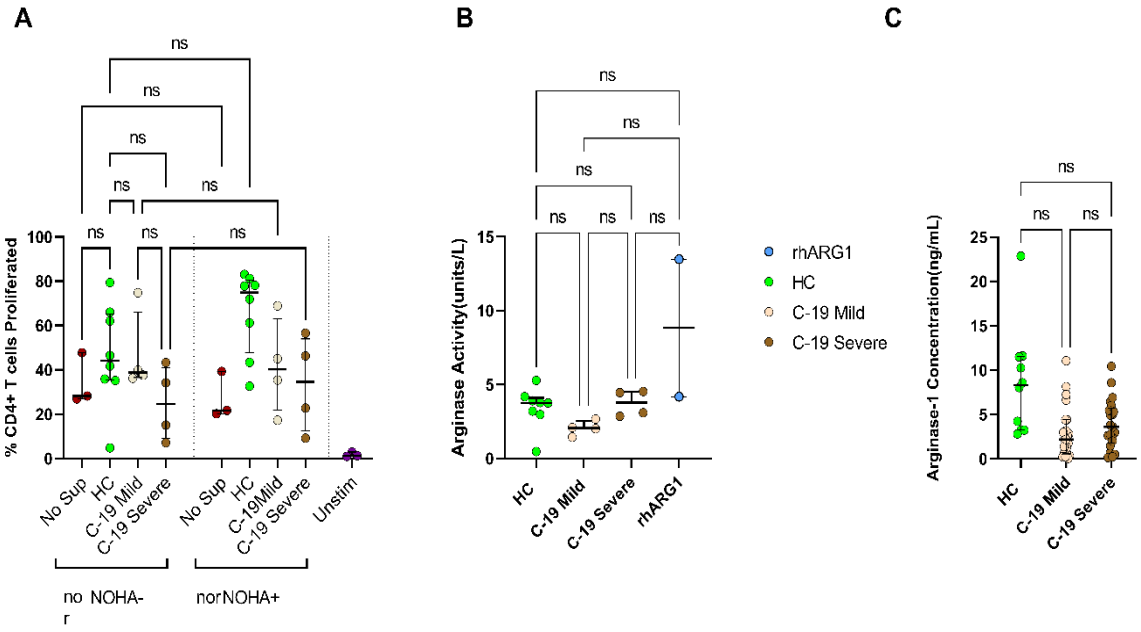

Figure 4.3.9 Severe COVID-19 neutrophil cell culture supernatant has a suppressive effect on T-cell proliferation but it is not reversed by arginase inhibitor nor-NOHA

Arginase-1 concentrations (ng/mls) are found to be elevated in serum from healthy controls in comparison to serum of COVID-19 patients. **(B)** When comparing the arginase activity levels in neutrophil supernatants from COVID-19 patients, healthy controls display higher arginase activity in comparison to both mild and severe covid. Recombinant Human Arg1 is used as a positive control at both 50 µg/mls and 10 µg/mls. **(C)** COVID-19 neutrophil supernatants were used to perform a T cell suppression assay on PBMCs from a healthy donor with/without the addition of NOHA, an arginase inhibitor. Cells were stimulated with αCD3/αCD28. Healthy controls exhibit the highest percentage of CD4+ T cell proliferation in contrast to mild and severe COVID-19. In addition, neutrophil supernatants from severe COVID-19 displayed notable suppression of CD4+ T cell proliferation.

4.3.9 Severe COVID-19 neutrophil cell culture supernatant has a suppressive effect on T-cell proliferation but it is not reversed by arginase inhibitor nor-NOHA

Having shown that LDGs and arginase 1 correlate with WHO severity (**Figure 4.3.1**), with higher levels of both readouts correlating with more severe disease I hypothesised that supernatants from COVID-19 patients would suppress T cell proliferation in an arginase dependent manner. I stratified the COVID-19 patient cohort according to severity. To characterise the suppressive capacity of neutrophil subsets, neutrophils from severe (n=4) and mild (n=4) COVID-19 patients and HC (n=8) were cultured at 37°C (5% CO_2) for 20 hours and the cell culture supernatants harvested. T cells from freshly harvested PBMCs from healthy donors were activated with CD3/CD8 beads in culture media and the supernatants added. After 4 days incubation at 37°C (5% CO_2) the samples were analysed by flow cytometry for CFSE expression to determine the number of cell divisions and proliferation index (**Figure 4.3.9 A**). Severe COVID-19 supernatants showed the greatest inhibition of T cell proliferation, although there is a large spread in the data, HC controls and mild COVID-19 did not seem to inhibit T cell proliferation compared to the control of no supernatant at all. Using nor-NOHA to determine if any suppression was linked to arginase activity the results were unexpected, HC seemed to stimulate T cells and the nor-NOHA had no effect on the COVID-19 trend of higher T cell suppression in the severe COVID-19 cohort (**Figure 4.3.9 A**). It would appear therefore that the results are not arginase mediated since the arginase inhibitor had no effect. We then measured the arginase 1 enzyme activity in the supernatants and using recombinant arginase 1 as a control there was paradoxically higher levels of enzymatic activity in the HC and lower levels in the mild than the severe COVID-19 samples (**Figure 4.3.9 B**). We then tested the levels of arginase 1 in the COVID-19 serum by ELISA, and the mild had lower levels than severe and both were lower than the HCs (**Figure 4.3.9 C**). None of these results were significant. (T-cell suppression assay and ELISA and activity assays were carried out by Makala Carroll in our lab)

4.4 Discussion

An imbalance between pro and anti-inflammatory effector systems accounts for a wide variety of autoimmune and chronic inflammatory diseases [228]. A key feature of inflammation-triggered immune dysfunction is a dramatic impairment of T-cell mediated responses [229]. To provide evidence of neutrophil plasticity in inflammation and to elucidate a mechanism whereby neutrophils can direct other cells behaviour, in particular T cells and to contradict the paradigm that neutrophils are simple bags of enzymes that are mobilized to respond to inflammation before the

adaptive immune arm moves in, I set about characterizing intracellular arginase 1 levels in AAV and COVID-19. Arginase 1 is present in the gelatinase granules of neutrophils its release is linked with a decrease in l-arginine which is required for the expression of the T cell receptor zeta chain and proliferation of T cells, resulting in immunosuppression [168, 175].

Arginase1 is constitutionally produced by the gelatinase granules of neutrophils, normal resting neutrophils do not release arginase 1, it is stored in the gelatinase granules and released intracellularly to combat microbial attack [176]. A recent study has shown that patients with colorectal cancer (CRC) had increased levels of arginase 1 activity in peripheral blood released by neutrophils during inflammation [177]. If arginase 1 is released, a lower intracellular arginase 1 would be anticipated. Rodriguez et al reported that neutrophils from renal cell carcinoma (RCC) had far lower arginase 1 activity and expression compared to those of healthy controls [92]. I hypothesized that measuring the intracellular arginase 1 levels together with maturity markers and markers of activation in both AAV and COVID-19 could give an insight into the etiology of both diseases.

I have shown that LDGs are linked to severity in COVID-19 and that percentage arginase 1 positive LDGs are also linked to severity in COVID-19. There are no reports in the literature of intracellular arginase levels in neutrophils or LDGs in COVID-19. Interestingly, despite a clear spread of data in the severe cases, the results suggest that arginase 1 release in mild cases of COVID-19 may correlate with better outcome. However, the converse is the case with moderate and severe cases having higher levels, paradoxically healthy normal neutrophils have high levels of arginase 1. While there are no reports of arginase 1 on a protein level several studies have shown increased transcription of arginase 1 in COVID-19, whole blood transcriptome analysis in COVID-19 patients reveal an upregulation of arginase 1 expression [231]. Aschenbrenner et al report that arginase gene upregulation was only found in severe COVID-19 patients. The authors also report that there was a heightened expression of immature neutrophil markers and interestingly CD15 upregulation limited to severe patients. Another study measured ARG 1 by rt PCR, there was a 2.3 fold increase in ARG 1 expression in whole blood and that ARG 1 expression could have prognostic potential for COVID-19 [184]. A bioinformatics approach identified arginase as one of the key genes in COVID-19, this study also reports that degranulation and activation of neutrophils are the most activated biological processes [185]. Despite the relative infancy of COVID-19 the abundance of studies to date is astounding. AAV by contrast is a rare condition which makes large studies particularly on neutrophils which cannot be cryopreserved very difficult. There are no reports of arginase upregulation in AAV either on a transcriptional or translational level. Dr Maria Lizardo of our lab noted that arginase 1 gene expression was increased in LDGs compared to NDGs in AAV using rtPCR.

I have shown in chapter 3 that LDGs are a feature of both diseases and that the etiology of both conditions are remarkably similar therefore the direct comparison of intracellular arginase 1 is warranted. I focused on the $CD16^{int/-}$ subsets that I had characterized in Chapter 3 to identify disease restricted differences in expression.

The main difference that I identified was the arginase 1 expression which was significantly lower in COVID-19 NDGs moderate and severe cases than the mild counterparts, suggesting that NDGs may be releasing arginase 1 in a severity related manner. In AAV by contrast NDGs appear to behave like healthy control neutrophils with arginase 1 levels remaining high in both acute AAV and patients in remission suggesting that arginase 1 is not released by these cells. This is the first disease particular finding of this work. I followed on to examine these cells by imaging flow cytometry and noted that the intracellular location of arginase differed between HC and disease states with the HC neutrophils having a distinct granular location of arginase 1 whereas in both AAV and COVID-19 mild disease have lower levels of arginase 1 and a cytoplasmic distribution. Of particular interest is the staining of the severe COVID-19 neutrophils which show a combination of granular and cytoplasmic staining. These high levels of arginase 1 are reflected in the traditional flow cytometry data and may reflect an aberrant release mechanism in severe disease or increased transcription limited to severe COVID-19 which has been reported in several recent studies [184, 185, 231]. Despite my hypothesis that there would be differences in $CD16^{int/-}$ low density subsets it was the NDG fraction that revealed disease specific behaviour. A key recent paper has highlighted that dexamethasone use modulates immature neutrophils in severe COVID-19, with this in mind I stratified the COVID-19 patients according to steroid use and noted that there was a significant increase in LDGs in steroid treated cohorts but as LDGs are linked to severity and severe patients routinely receive steroids this result needs to be interpreted with caution [232]. Following on from this I did find significantly higher percentage arginase 1 positive LDGs in the steroid treated cohort and those without were significantly lower. A key caveat to this is that the mild samples in my cohort were not treated with steroid whereas all severe patients were, so by stratifying patients into steroid treated and untreated the cohort are in reality being divided by severity and the results need to be interpreted with care. Sinha et al report in their study that dexamethasone expands immature neutrophils with high levels of arginase 1. Others have reported that ARG1 express glucocorticoid response elements which could emphasise the possibility of ARG1 gene expression as a result of dexamethasone treatment [233, 234]. My findings are that firstly there was no significant expansion of immature neutrophils in those patients on steroid treatment from those without, moreover, there was a significant decrease in arginase 1 levels in the steroid treated LDGs. This could suggest that the arginase expression is not completely linked to steroid use and that a

far more complex scenario is taking place not limited to administered drugs. As I have seen that NDGs in COVID-19 have a different arginase 1 pattern than healthy controls I also stratified NDG fractions according to their steroid treatment group and interestingly steroids had no significant influence on either the percent NDGs or the arginase positive NDGs or on the expansion of immature neutrophils or arginase 1 positive immature NDGs. One rationalization could be that immature LDGs are transcriptionally active and responsive therefore to dexamethasone treatment or other stimuli whereas the NDG fraction is transcriptionally silent and unresponsive to gene upregulation. In AAV, Ciavatta et al finds an epigenetic basis for the upregulation of MPO and PR3 in mature neutrophils and that proper silencing mechanisms must be in place to ensure that genes silenced during granulopoiesis remain silenced [99]. Using the aberrant expression of PR3 and MPO in ANCA vasculitis patients as a model, they tested whether epigenetic gene silencing processes occur in neutrophils and whether aberrant PR3 and MPO expression result from disrupted epigenetic silencing.

A key difference between both COVID-19 and AAV neutrophils was the pattern of arginase 1 expression seen by imaging flow cytometry. These cells are permeabilized and in healthy controls the staining of arginase appears to be limited to the granules, however in both AAV and COVID-19 there is a distinct diffuse arginase staining, this could reflect a cytoplasmic distribution of arginase but it could also be surface distribution of arginase 1 which is not well documented, this phenomenon of protein on the surface is a feature of activated neutrophils in AAV. In healthy individuals MPO and PR3 are stored in granules, in AAV however on activation they are mobilized to the surface allowing interaction with autoantibodies and resulting in vascular inflammation [235]. There is one report of surface arginase 1 being elevated on neutrophils activated by FMLSP and that surface arginase 1 in increased in neutrophil of patients with Cystic fibrosis [236] . This study reports that degranulation is required for surface expression of arginase 1. The triggers for neutrophil degranulation are likely to be inflammatory cytokines such as TNF alpha. The question of surface expression of arginase requires further investigation.

Lymphopenia is an established feature of COVID-19 and is linked to severity. The mechanism of how SARS-CoV-2 induces lymphopenia is unknown [224]. LDGs have been reported to suppress T cell function in many other diseases [64, 191]. I have reported that the NDG fraction of COVID-19 patients have lower arginase levels than AAV NDGs which have the same levels as HCs, I hypothesized therefore that NDGs in COVID-19 would have immunosuppressive capacity (**Figure 4.3.6A**). To test the immunosuppressive ability of COVID-19 neutrophils *ex vivo*, healthy donor T cells were activated in the presence of supernatants from a 20-hour culture of mild and severe COVID-19 neutrophils. Severe COVID-19 supernatant caused the highest levels of T cell suppression

albeit not significant, however this was not reversed by the addition of nor-NOHA as would be expected if the suppression was arginase 1 mediated. To address this the levels of arginase 1 activity in the supernatant was measured and found to have lower levels than HCs, and an Arg ELISA confirmed that indeed the serum of patients with COVID-19 was indeed lower than HCs. These results suggest that arginase 1 may have already been released in the tissues and that the peripheral blood neutrophils in disease have lower arginase 1 than their HC counterparts. These are normal density neutrophils I have excluded the low-density fraction from this experiment and it is these cells that are reported to be immunosuppressive [237]. I had hypothesized that these cells were activated based in their shedding of CD62L and did not stimulate these neutrophils. Rodriguez et al report that cells require activation to be immunosuppressive this may be a required step in this experiment [92]. The T cell suppression assay needs to be repeated with the following conditions, CD15+ cells from whole blood which would include the low-density fraction and stimulated and unstimulated supernatants. The low enzyme activity in the supernatants may be accounted for by lack of stimulation but also the release of potentially immunomodulatory arginase is tightly controlled and requires concomitant release of azurophilic granules to be enzymatically active at physiological pH [178]. It is difficult in *ex vivo* work to replicate the interactions of cells *in vivo.* The low levels of arginase 1 in the sera of COVID-19 patients were unexpected as many studies have reported that the serum of patients have high arginase activity and is linked to severity [191, 192]. Steady state neutrophils do not release arginase 1 it is stored in the gelatinase granules and released intracellularly when required to combat microbial attack. A recent study showed that in contrast to healthy controls, patients with colorectal cancer (CRC) had increased levels of arginase 1 activity in peripheral blood, released during inflammation [177]. If arginase 1 is released from neutrophils, a decrease in intracellular arginase I in these cells would be expected. Rodriguez et al reported that MDSC from RCC patients had a much lower arginase activity and expression compared with to healthy control neutrophils and autologous normal neutrophils. They reported that arginase I mRNA expression was increased in MDSC compared with healthy controls and autologous neutrophils suggesting an increase in arginase transcription to compensate for the increased release of enzyme [92].

In this chapter I have shown that there are disease specific differences in arginase 1 expression in AAV and COVID-19 most notably that COVID-19 NDGs have lower arginase 1 levels than their AAV counterparts and HCs. I have shown by imaging flow cytometry that severe -19 is characterised by a high level of cytoplasmic and granular arginase 1 compared to AAV and HC. This may be the result of an errant release mechanism and increased transcription of the enzyme that is well documented in this disease [184, 185]. Mild Covid and acute AAV have similar cytoplasmic distribution of

arginase 1 compared to the granular location of arginase 1 in HCs. The T cell suppression assay requires further optimisation to elucidate the role of arginase 1 in both AAV and COVID-19.

Chapter 5

Whole Blood Neutrophils

5 Whole Blood Neutrophils

5.1 Introduction

Density has dominated the field of neutrophil biology, since they were first described in patients with systemic lupus erythematous (SLE) there has been reports of low density neutrophils in the PBMC layer of density gradient separated blood [51]. These cells have been described in several disease and healthy states. In these conditions LDGs do not constitute a discrete population but a multitude of phenotypes that vary in their maturation stage, morphology and activation status depending on the underlying condition be it viral autoimmune, cancer, or a healthy condition such as pregnancy [54, 191, 238]. The current phenotyping of LDGs is reliant on density centrifugation, density gradient centrifugation itself may enrich for activated neutrophils and surface marker expression may be altered by shedding during the centrifugation step [239]. In this thesis I too have focused on the low-density neutrophil and its phenotype but what has become clear from this work is that all neutrophils are implicated in any immune response and to simply sideline normal density neutrophils as steady state neutrophil unworthy of further investigation may be a grievous error. The main focus of this work has been to identify any differences between neutrophils in COVID-19 and AAV. I propose in this chapter to focus on whole blood phenotyping to provide a comprehensive view of neutrophils in etiology of both these diseases.

Surface markers must identify the immature low-density fraction and the mature low- density fraction to identify these cells in whole blood. While the normal density neutrophils are predominantly CD16 positive additional markers are required to define the mature low- density cells. A 2012 study by Pillay et al identified an immunosuppressive population of $CD16^{+}CD62l^{low}$ neutrophils induced in human volunteers following injection of low dose of bacterial liposaccharide LPS, these cells suppressed T cell function, and potentially allow identification of a subtype of neutrophils that identifies the mature $CD16^{+}$ LDG phenotype [162]. To definitively define the LDG immature subset, immature neutrophil markers are necessary, Evrard's mass cytometry (CyTOF) study of the developmental analysis of bone marrow neutrophils, provided further markers to identify the subsets in whole blood, in particular Evrard used CD101 and CD49d to identify pre neutrophils in human bone marrow, and further gated on CD10 and CD16 [146]. Ng et al's definitive review compared known markers of neutrophils and suggested a panel for identification of neutrophil subpopulations combining all the published knowledge has resulted in the design of two 8 colour panels (**Table 5.1, 5.2**) [2]. Our aim is to develop a panel of markers that will allow identification of these cells in peripheral blood and ideally in tissues which would allow further insight into the role of these cells in inflammatory conditions.

With the advent of mass cytometry (CyTOF) the dimensionality of cytometry experiments keeps increasing, this enables the deep phenotyping of complex biological systems. These high dimensional data need more sophisticated techniques rather than the laborious manual gating of cells, two markers at a time. A relatively new research field is at the intersection of computational biology and immunology, this involves ways to analyse, visualise and interpret data to extract biological knowledge. I used UMAP dimension reduction and the clustering algorithm FlowSOM to identify clusters in an unsupervised manner. Other plugins such as Cluster Explorer allow further analysis through heatmaps of marker MFI and frequencies of populations. This approach is becoming established as a method of visualisation and analysis of cytometry data and should enable the identification of neutrophil subsets in whole blood [240].

5.2 Design and Rationale

5.2.1 Hypothesis

All neutrophils are implicated in the immune response to either viral infection or autoimmunity, I therefore hypothesized that

1. Neutrophil subsets will be identifiable in WB with a definitive phenotyping panel that includes sensitive markers of neutrophil maturity and activation
2. High dimensional flow analysis with cluster algorithm FlowSOM will identify populations that are implicated in the etiology of disease that may not have been identified by traditional manual gating methods

5.2.2 Specific Methods

Patients were as outlined in Chapter 2. Whole blood staining and flow cytometry were carried as outlined in Chapter 2, with the use of two whole blood phenotyping panels (**Table 5.1, 5.2**).

Antibody	Fluorophore
CD14	PE-Vio770
CD15	Per CP Cy5.5
CD16	APC Cy7
CD62l	FITC
LOX-1	APC
CD49d	PE
CD101	BV421

Table 5.1 Whole Blood Phenotyping - Panel A

Antibody	Fluorophore
CD14	PE-Vio770
CD15	Per CP Cy5.5
CD16	APC Cy7
CD62l	FITC
CD33	APC
CD66b	PE
CD10	BV421

Table 5.2 Whole Blood Phenotyping Panel B

UMAP and Clustering Analysis

Patient FCS files from COVID-19 cohort as outlined in Chapter 2.3 (mild n=4, moderate n=4, severe n=5, convalescent n=5, HC n=4) were gated on $CD15^{+}CD14^{-}$singlets, downsampled to 3000 events per patient and concatenated for dimension reduction by UMAP and clustering by FlowSOM. Results were analysed using Flowjo software.

5.3 Results

In Chapter 3 of this work I have shown that LDGs in both COVID-19 and AAV are elevated and linked to severity, I have also provided evidence of immature and activated cells in this fraction. It would seem logical therefore that these cells could be detectable in whole blood which would minimize handling and lab-based bias from the analysis. Reliance upon density to define these cells is a difficult to control variable and whole blood analysis could bring closure to the lack of consensus in the literature and also allow direct comparison across disease states.

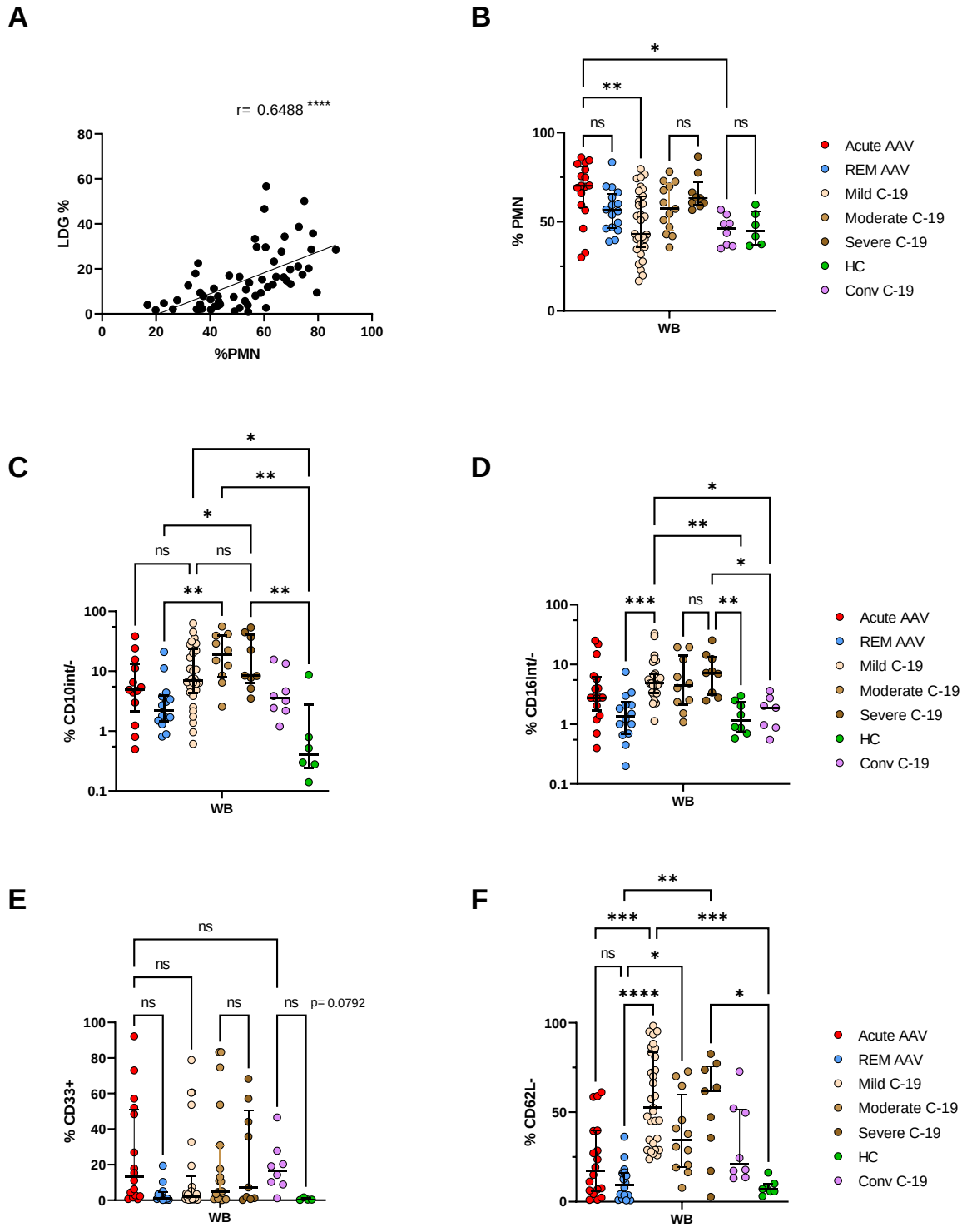

Figure 5.3.1 LDGs correlate with % PMN in whole blood In COVID-19 and Immature and activated neutrophils are significantly elevated in COVID-19 WB but not AAV

PDMCs were isolated from the peripheral blood of COVID-19 patients and LDGs as a percent of $CD15^+$ $CD14^-$ PBMCs were quantified by flow cytometry (n=54). The proportion of PMNs $CD15^+$ $CD14^-$ cells in WB was also quantified by flow cytometry. Each symbol represents an individual donor. Per cent LDGs significantly correlate with per cent PMNs in COVID-19 whole blood in COVID-19 (Spearman coefficient r=0.64) (**A**). Per cent PMNs were also calculated for acute (n=17) and remission (n=14) AAV mild (n=33) moderate (n=13) and severe COVID-19 (n=9) and for HC (n=8)

and convalescent COVID-19 patients (n=8). There is a severity related trend towards higher %PMNs in both acute AAV and moderate and severe COVID-19 although this is not significant and interestingly convalescent COVID-19 %PMN returns to HC levels. PMN are significantly increased in acute AAV compared to mild COVID-19 (**B**). Immature Neutrophils defined as $CD10^{int/-}$ $CD15^{+}$ $CD14^{-}$ cells, were quantified for the cohorts described in B, and there was a significant severity related increase in $CD10^{int/-}$ immature neutrophils in COVID-19 with moderate and severe having highest levels. In AAV patient's peripheral blood there is an increase in both acute and remission with highest in acute disease although not reaching significance, of note is that both remission and convalescent patients had a population of immature $CD10^{int/-}$neutrophils that have not returned to healthy levels(**C**). Another marker of neutrophil immaturity CD16 was quantified by flow cytometry and percent $CD16^{int/-}$ neutrophils in the WB of the patients described in B are increased and linked to severity in COVID-19 patients with convalescent levels returning to those of HCB there was no significant increase in either acute or remission AAV patients (**D**). Myeloid marker CD33 was quantified as $CD33^{+}$ $CD15^{+}$ $CD14^{-}$ cells and percent were calculated for the patient cohorts as described in B. There were higher CD33 populations in Acute AAV and mild and severe COVID-19 but these were not significant, of note is the population of $CD33^{+}$ cells in the convalescent patients that do not return to HC levels and is approaching significance (**E**). CD62L is shed on neutrophil activation. CD62L was quantified as $CD62L^{-}$ $CD15^{+}$ $CD14^{-}$ cells by flow cytometry in the same patient cohorts as B. Mild COVID-19 patients had significantly higher $CD62l^{-}$ cells than HC, Acute AAV also had high percent CD62L- cells although not significant. Again, note the population of activated cells in the convalescent patients that are not present in HCB (**F**).

5.3.1 LDGs correlate with % PMN in whole blood In COVID-19 and Immature and activated neutrophils are significantly elevated in COVID-19 WB but not AAV

I hypothesized that LDG levels would correlate with percent neutrophils in peripheral blood and be detectable in WB, per cent LDG in the PBMC layer significantly correlates with per cent PMNs in COVID-19 whole blood in C19 (Spearman coefficient r=0.64) (**Figure 5.3.1 A**). Per cent PMNs were also calculated for acute (n=17) and remission (n=14) AAV mild (n=33) moderate (n=13) and severe COVID-19 (n=9) and for HC (n=4) and convalescent COVID-19 patients (n=8). There is a severity related trend towards higher % PMNs in both acute AAV and moderate and severe COVID-19 although this is not significant and interestingly, convalescent % PMN returns to HC levels (**Figure 5.3.1B**). Immature neutrophils defined as $CD10^{int/-}$ $CD15^{+}$ $CD14^{-}$ cells, were quantified for the cohorts described in B, and there was a significant increase in $CD10^{int/-}$ immature neutrophils in COVID-19 that was not evident in AAV patient's peripheral blood, of note is that 2 convalescent patients had a population of immature $CD10^{int/-}$neutrophils (**Figure 5.3.1C**). Another marker of neutrophil immaturity CD16 was quantified by flow cytometry and percent $CD16^{int/-}$ neutrophils in the WB of the patients described in B are increased and linked to severity in COVID-19 patients with convalescent levels returning to those of HCB there was no significant increase in either acute or remission AAV patients (**Figure 5.3.1D**). Although both CD10 and CD16 are both markers of mature neutrophils the expression of CD16 occurs at an earlier stage of development. According to Elghetany CD16 is expressed at low levels at the metamyelocyte stage increasing at band stage and

highest on segmented neutrophils, CD10 expression is limited to the segmented mature neutrophil. This could explain the different levels of immature cells particularly in the moderate and severe fractions and convalescent cohorts, identified in each fraction as defined by these subtly different differentiation markers (**Figure 5.3.1 C,D**)[212]. CD33 is a myeloid marker expressed on cell of myeloid linage highly on monocytes and dendritic cells it has been mooted as a marker for PMN-MDSC, as it has a low expression on these cells and not on mature steady state neutrophils [145]. CD33 was quantified as $CD33^{+}$ $CD15^{+}$ $CD14^{-}$ cells and percent were calculated for the patient cohorts as described in B. There were higher CD33 populations in Acute AAV and mild and severe COVID-19 but these were not significant, of note is the population of $CD33^{+}$ cells in the convalescent COVID-19 patients that do not return to HC levels (**Figure5.3.1E**). CD62L is shed on neutrophil activation [241]. CD62L was quantified as $CD62L^{+}$ $CD15^{+}$ $CD14^{-}$ cells by flow cytometry in the same patient cohorts as B. Mild COVID-19 patients had significantly higher $CD62^{-}$ cells than HC and although not significant Acute AAV had a high percentage of $CD62L^{-}$ cell. There are significantly higher numbers of activated cells in the COVID-19 cohort than the AAV samples indicating perhaps that all neutrophils are in the immune response and not limited to the low-density fraction. Again, note the population of activated cells in the convalescent patients that are not present in HCB. (**Figure 5.3.1F**).

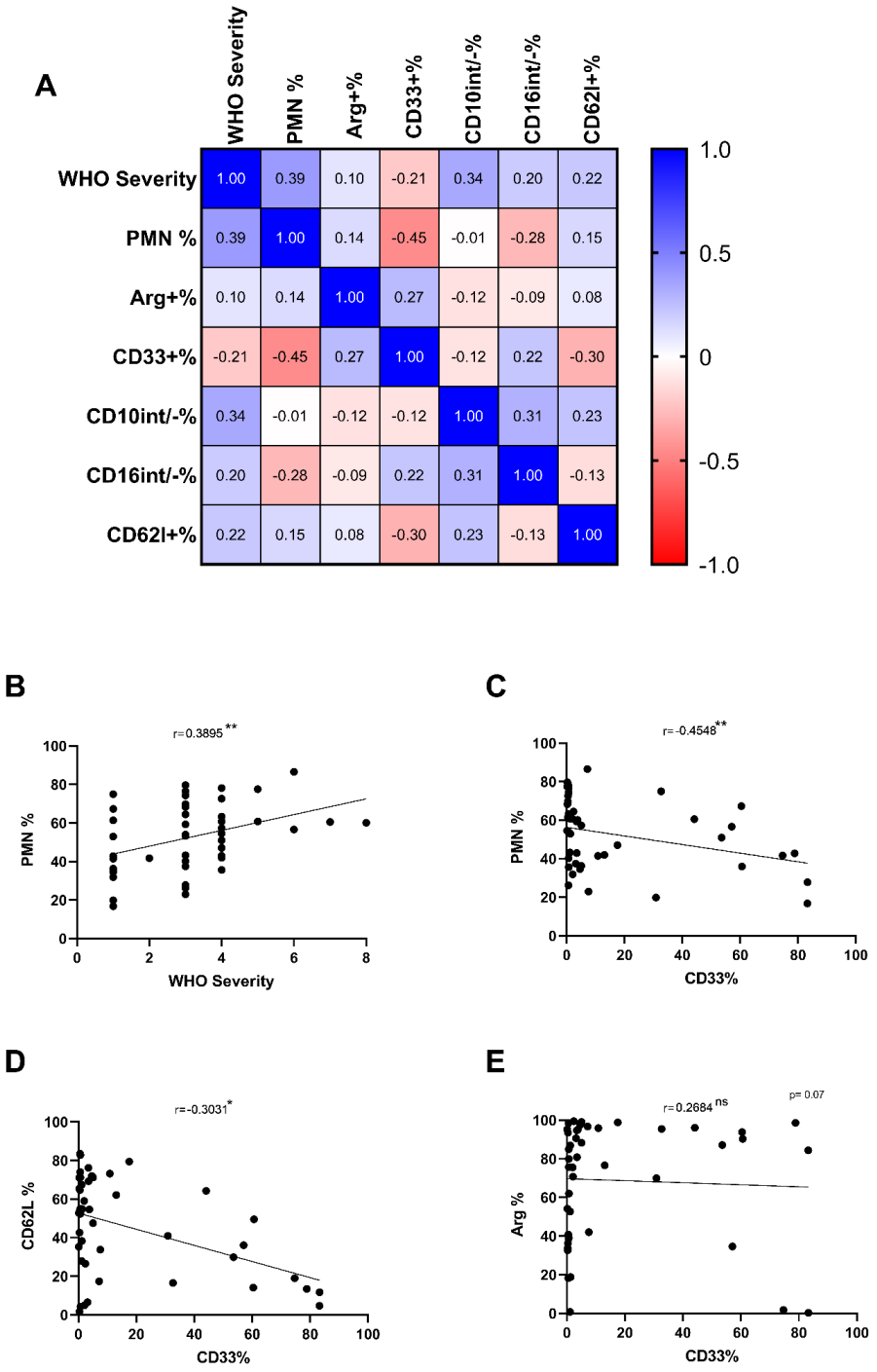

Figure 5.3.2 Levels of neutrophils correlate with WHO severity in COVID-19 whole blood, CD33 and CD62L are identified as key markers in whole blood

Heat map correlation matrix of spearman coefficients of 45 mild moderate and severe COVID-19 patients with percent of maturation markers CD10 and CD16, activation markers CD62L and suppressive markers Arg 1 and CD33 in peripheral whole blood(**A**). Markers with significant correlations are plotted below There is a significant correlation % PMN with WHO severity score (**B**). There is an inverse correlation between %PMN and $CD33^{+}$ $CD15^{+}$ $CD14^{-}$ cells (**C**). There is an inverse correlation between activation marker CD62L and myeloid marker CD33(**D**). CD33 has a weak correlation with suppressive marker Arg 1 (**E**). *Spearman correlation* *p<0.05, **p <0.01, and ***p < 0.001. ****p < 0.0001**.**

5.3.2 Levels of neutrophils correlate with WHO severity in COVID-19 whole blood, CD33 and CD62L are identified as key markers

As numbers are limited for AAV samples I will focus on identifying COVID-19 neutrophils in WB. I used a heat map correlation matrix of spearman coefficients of mild moderate and severe COVID-19 patients with percent of maturation markers, activation markers, suppressive markers whole blood to identify relationships between these markers and WHO severity and each other (**Figure 5.3.2 A**) There is a significant correlation % PMN with WHO severity score as previously discussed (**Figure 5.3.2 B**). There is an inverse correlation between %PMN and $CD33^{+}$ $CD15^{+}$ $CD14^{-}$ cells (**Figure 5.3.2 C**). There is an inverse correlation between activation marker CD62L and myeloid marker CD33 (**Figure 5.3.2 D**). CD33 has a weak correlation with suppressive marker Arg 1 (**Figure 5.3.2E**). Using the correlation matrix to identify trends facilitates the finding of activated and suppressive ($CD33^{+}$) cells in WB in COVID-19 (**Figure 5.3.1)** and their link to disease severity.

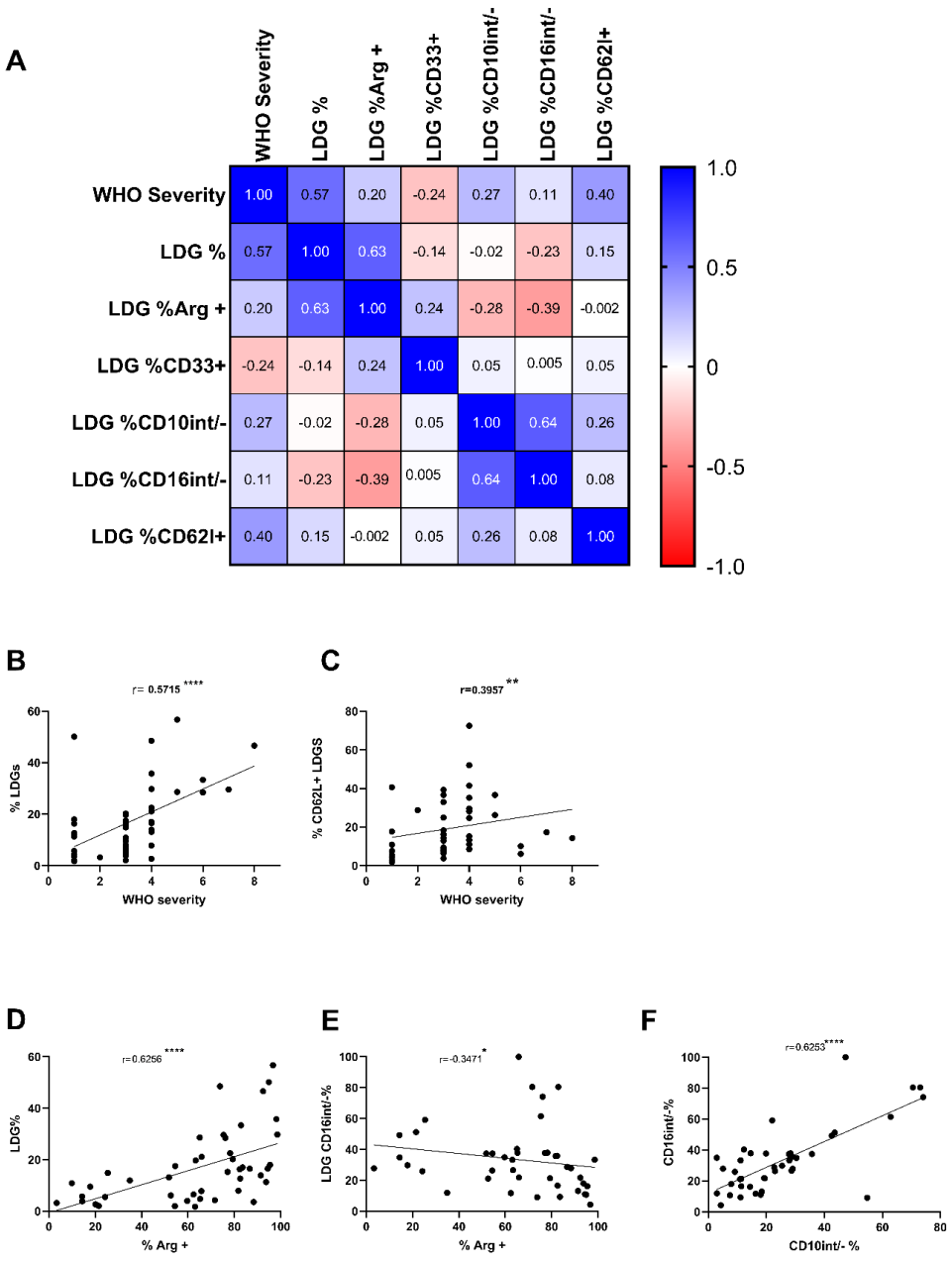

Figure 5.3.3 LDGs correlate with WHO severity, immature activated and potentially suppressive neutrophils are identified in LDG fraction

Heat map correlation matrix of spearman coefficients of 45 mild moderate and severe COVID-19 patients with percent of maturation markers CD10 and CD16, activation markers CD62L and suppressive markers Arg 1 and CD33 in the PBMC fraction of density separated peripheral blood(**A**). Markers with significant correlations are plotted below There is a significant strong correlation %LDG with WHO severity score (**B**). There is a significant correlation between WHO severity and $CD62L^{+}$ $CD15^{+}$ $CD14^{-}$ cells but not between percent LDG and $CD62L^{+}$ (**A, C**). There is a clear association between %LDG and % arginase positive cells (**D**). A less pronounced but significant association between immature cells as defined by $CD16^{int/-}$ and arginase (**E**). Although this is not reflected in the CD10int/- cells clearly there is a strong correlation between both maturity markers (**F**)*Spearman correlation* *p<0.05, **p <0.01, and ***p < 0.001. ****p < 0.0001**.**

5.3.3 LDGs correlate with WHO severity, immature activated and potentially suppressive neutrophils are identified in LDG fraction

A heat map summary of correlation matrix showing spearman coefficients of mild moderate and severe COVID-19 patients with percent of maturation markers, activation markers and suppressive markers in the PBMC fraction of density separated peripheral blood was used to identify significant markers and their correlation with severity (**Figure 5.3.3 A**). There is a significant strong correlation % LDG with WHO severity score that corroborates the link between LDGs and disease severity discussed in Chapter 3 (**Figure 5.3.3 B**). There is a significant correlation between WHO severity and $CD62L^{+}$ $CD15^{+}$ $CD14^{-}$ cells but not between percent LDG and $CD62L^{+}$ (**Figure 5.3.3 A, C**). There is a clear association between % LDG and % arginase positive cells (**Figure 5.3.3 D**). A less pronounced but significant association between immature cells as defined by $CD16^{int/-}$ and arginase (**Figure 5.3.3 E**). Although this is not reflected in the CD10int/- cells clearly there is a strong correlation between both maturity markers (**Figure 5.3.3 F**). There is a clear discrepancy between the finding in the LDG fraction than in WB with respect to CD33 which was not significantly correlated with severity or % LDG.

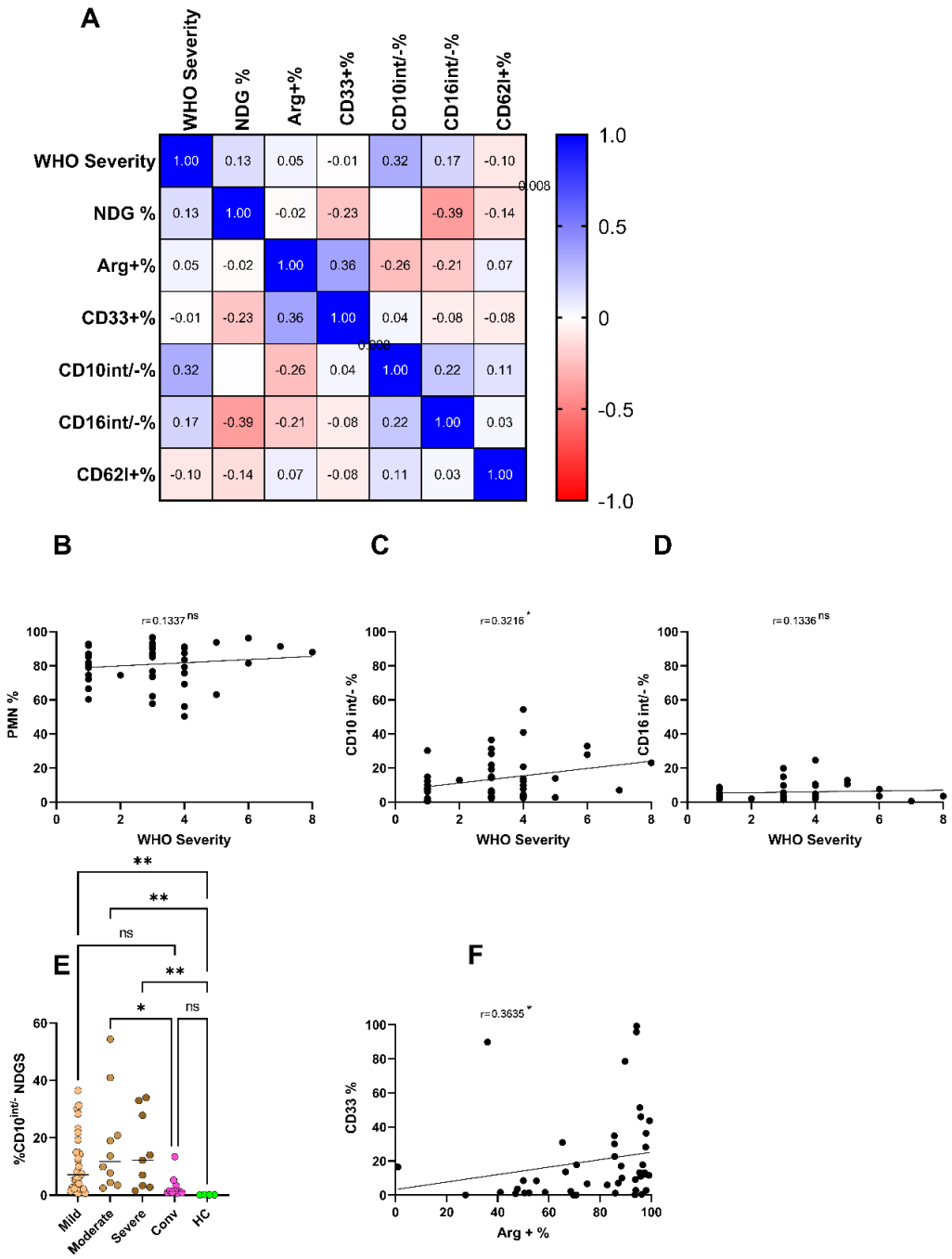

Figure 5.3.4 NDGs do not correlate with WHO severity, suppressive markers CD33 and Arg 1 have a weak association and there is a clearly population of CD10int/- NDGs that correlate with severity the pattern is not repeated with CD16int/- NDGs

Heat map correlation matrix of spearman coefficients of 45 mild moderate and severe COVID-19 patients with percent of maturation markers CD10 and CD16, activation markers CD62L and suppressive markers arginase 1 and CD33 in the NDG fraction of density separated peripheral blood(**A**). There is no significant correlation between %NDGs and WHO severity score (**B**). An immature population as defined by CD10 correlates with WHO severity (**C**). This is not evident in immature cells defined by CD16 (**D**). There is a significant correlation between Arg 1 positive NDGs and $CD33^{+}$ NDGs (**E**) *Spearman correlation* *p<0.05, **p <0.01, and ***p < 0.001. ****p < 0.0001**.**

5.3.4 NDGs do not correlate with WHO severity, suppressive markers CD33 and Arg 1 have a weak association and there is a clearly population of CD10int/- NDGs that correlate with severity the pattern is not repeated with CD16int/- NDGs

Summary heat map of correlation matrix of spearman coefficients of mild moderate and severe COVID-19 patients with percent of maturation markers CD10 and CD16, activation markers CD62L and suppressive markers Arg 1 and CD33 in the NDG fraction of density separated peripheral blood was used to identify correlations between WHO score and expression of markers (**Figure 5.3.4 A**). There is no significant correlation between % NDGs and WHO severity score which reflects the fact that this is a fraction of only neutrophils and therefore there is no expansion of this population relative to other immune cells unlike the LDGs in the PBMC layer or neutrophils in WB (**Figure 5.3.4 B**). Interestingly, an immature population as defined by CD10 correlates with WHO severity. CD16 is expressed on metamyeocytes and band stage whereas CD10 is expression is limited to the segmented stage of neutrophil development, the later expression of CD10 on mature neutrophils may account for a population of immature cells in the normal density fraction (**Figure 5.3.4 C**)[212]. There is a significant correlation between arginase 1 positive NDGs and $CD33^{+}$ NDGs which is notable because both are markers linked to suppressive function and not expected in the NDG fraction (**Figure 5.3.4 E**).

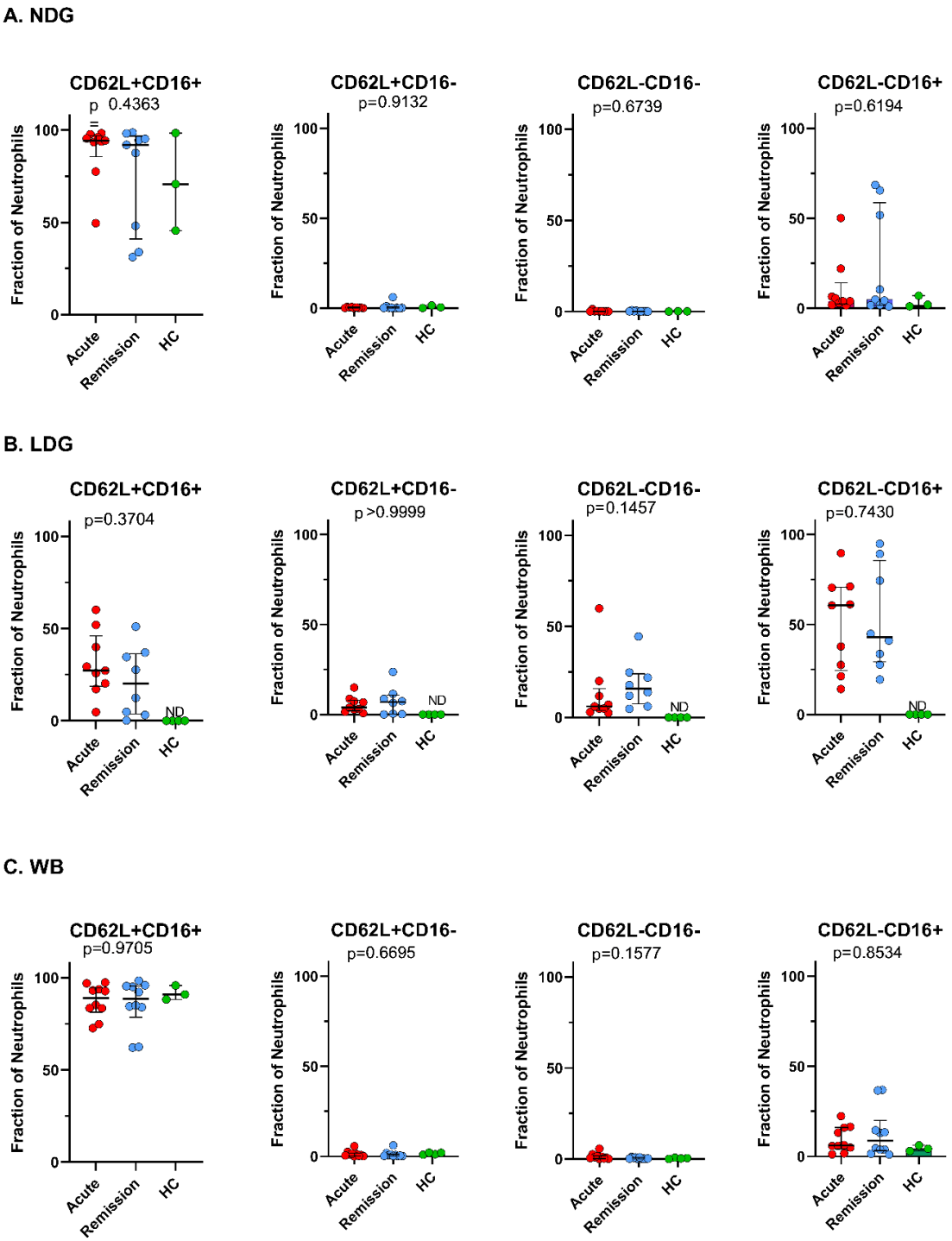

Figure 5.3.5 Phenotyping of neutrophil subsets using CD62l and CD16 does not identify a disease specific cell population in AAV

Density gradient separated blood from patients with acute or remission AAV, and healthy controls, were compared to whole blood (WB) using surface staining for CD62L and CD16. The results according to the four fluorochrome combinations are depicted for NDG (**A**), LDG (**B**) and whole blood (WB) (**C**) fractions. The distribution of surface staining is different in LDGs compared to NDGs and Whole blood, but this does not correlate with disease activity. ND= not detected. P values were determined using the Mann-Whitney test and are shown for acute versus remission patient samples.

5.3.5 Phenotyping of neutrophil subsets using CD62l and CD16 does not identify a disease specific cell population in AAV.

Traditional flow cytometric surface markers used to identify granulocytic subpopulations include CD66b CD15 CD11b and CD16, however expression of these markers may be altered by neutrophil activation and density gradient centrifugation. Currently there is not a definitive panel of markers to identify these cells in whole blood. Previous work has shown that CD62L and CD16 are differentially expressed on low density neutrophil subsets, on the basis of this, four subsets based on expression of these markers were analysed by flow cytometry [49, 162]. The patients were divided into acute (n=9) and remission (n=10) AAV and age matched healthy control blood (n=4). The samples were separated by density gradient centrifugation and LDG NDG and WB were stained for two phenotyping panels (**Table 5.1, 5.2**). In NDGS and whole blood (WB) the predominant subsets are $CD16^+$ $CD62L^+$ > 90% in both groups and HCB (Acute, 94.4%,IQR 85.5-97.0, Rem 92% IQR 41.2-96.7)(**Figure 5.3.5 A,C**), in LDGs however this subset is reduced and only < 30% of Acute and Rem LDGs are $CD16^+$ $CD62L^+$ (Acute:27.2% IQR 18.75-46, Rem:20.1% IQR 3.6-36.4) Whilst the $CD16^-$ $CD62L^+$ population were elevated in LDG (Acute:60.6% IQR24.4-70.8, Rem:43.0% IQR 29-85) compared to NDG (Acute:4% IQR2.3-14.3, Rem 4.9%IQR 1.75-38.7) (**Figure 5.3.5 A, B**) this subset was not statistically elevated in WB acute 6.1% IQR 4.1-16.1 and remission 8.7% IQR 3.15-20.0 versus HCB 4.3% IQR 3-6.2(**Figure 5.3.5 C**). None of the CD16 CD62l subsets showed statistically significant differences between acute AAV and remission AAV. Pillay et al have reported that this subpopulation $CD62l^-$ $CD16^+$ are capable of suppressing T cell function and as $CD16^+$ cells are part of our heterogenous LDG sample (**Figure 3.3.3**), identifying a marker that could detect these cells in whole blood seemed achievable with CD62l. Disappointingly the CD16 CD62l subsets were not identifiable in whole blood, and perhaps further fuels concerns over the artefactual nature of density gradient centrifugation these results suggest that the $CD62l^-$ population could be a result of shedding of l-selectin during the isolation procedure and not a bona-fide subgroup in whole blood. A recent study found that neutrophils from dextran sedimentation had a significant increase in cell surface CD11b expression and CD62L shedding and a marked increase in adhesion [239]. These findings suggest that care needs to be taken in choosing the method of neutrophil purification for functional studies and further underlines the need for a definitive whole blood panel for the identification of neutrophil subsets.

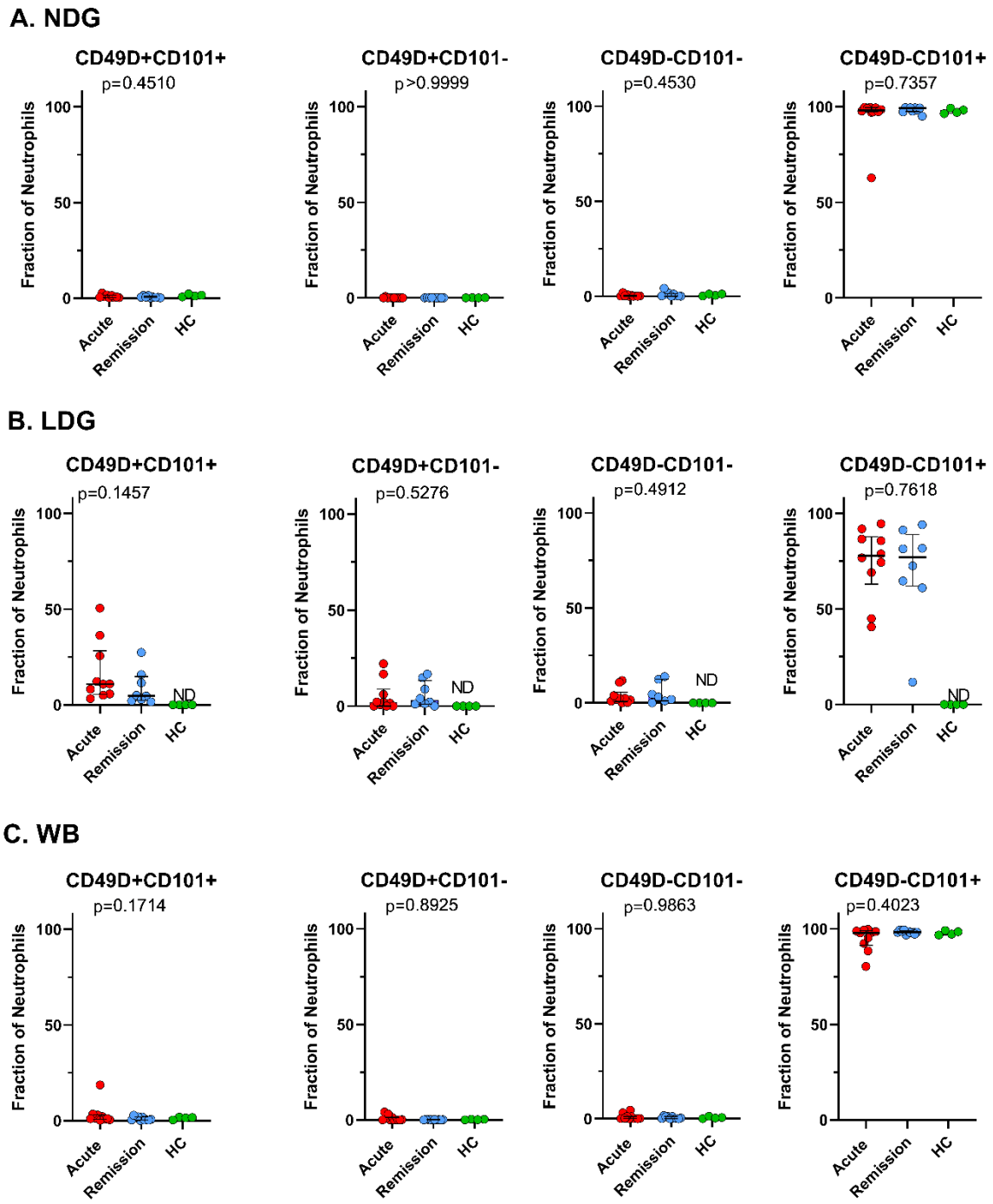

Figure 5.3.6 Phenotyping of Neutrophil subsets using CD49d and CD101 does not identify subsets that correlate with disease activity

Density gradient separated blood from patients with acute or remission AAV, and healthy controls, were compared to whole blood (WB) using surface staining for CD49d and CD101. The results according to the four fluorochrome combinations are depicted for NDG (**A**), LDG(**B**) and whole blood fractions(**C**). The distribution of surface staining is different in LDGs compared to NDGs and Whole blood, but this does not correlate with disease activity. P values were determined using the Mann-Whitney test and are shown for acute versus remission patient samples.

5.3.6 Phenotyping of Neutrophil subsets using CD49d and CD101 does not identify subsets that correlate with disease activity

My previous work has shown that LDGs are a heterogenous population of mature and immature cells with CD16+ cells defining the mature cells and CD16int/- the immature cell subset (**Figures 3.3.2, 3.3.3**). In order to further define the immature population a study by Evrard et al had highlighted CD49d and CD101 suitable markers of immature and mature neutrophils respectively [146]. Density gradient separated blood from patients with acute or remission AAV, and healthy controls, were compared to whole blood (WB) using surface staining for CD49d and CD101. The results according to the four fluorochrome combinations are depicted for NDG, LDG and whole blood fractions (**Figure 5.3.6**)**.** The distribution of surface staining is different in LDGs compared to NDGs and Whole blood, but this does not correlate with disease activity, p values were determined using the Mann-Whitney test and are shown for acute versus remission patient samples. The predominant subset in NDGs (Acute: 98.2%, IQR 97.28-99.55, Rem: 99.3% IQR 97.5-99.5, HCB:97.7% IQR 96.5-99.0) and WB (Acute:98.0% IQR 91.4-99.0, Rem:98.2% IQR 97.8-98.8, HCB: 97.2% IQR 96.9-98.9) are $CD49d^{-}$ $CD101^{+}$ reflecting the mature nature of these cells (**Figure 5.3.6 A, C**). Interestingly, this population is decreased in the LDG fraction (Acute:77.8% IQR 63.0-87.9, Rem: 77% IQR 62.0-88.9) corresponding to an increase in the $CD49d^{+}$ $CD101^{+}$ fraction (LDG Acute: 10.8% IQR 5.5-28.2, Rem: 4.8% IQR 2.2-14.8,) compared to NDG (Acute: 0.7% IQR 0.2-0.7, Rem 0.5%IQR 0.3-1.0, HCB 1.8% IQR 0.8-2.1) and WB (Acute 1.2% IQR 0.7-3.0, Rem:0.6% IQR 0.3-0.6, HCB ;1.6% 0.7-1.7) (**Figure 5.3.6 A, B, C**). This population is reported by Evrard to be present in the bone marrow but not in whole blood suggesting perhaps that these cells are a result of an extreme left shift emergency granulopoiesis in acute AAV. *In vivo* work in our group by Alice Coughlan has shown that G-CSF administered to humanised mice resulted in a dramatic reduction in $CD16^{+}$ neutrophils (mature) and a corresponding increase in $CD16^{int/-}$ neutrophils suggesting that emergency granulopoiesis leads to an increase in number of circulating immature neutrophils (**Figure 3.3.4**)[49]. However, these cells are not increased compared to the healthy controls in WB (**Figure 5.3.6 C**). Both $CD101^{-}$ subsets are upregulated in LDGs but not in WB and with no significant difference between acute and remission samples. Stratifying the samples according to CD16 expression could be useful to further characterise these subsets.

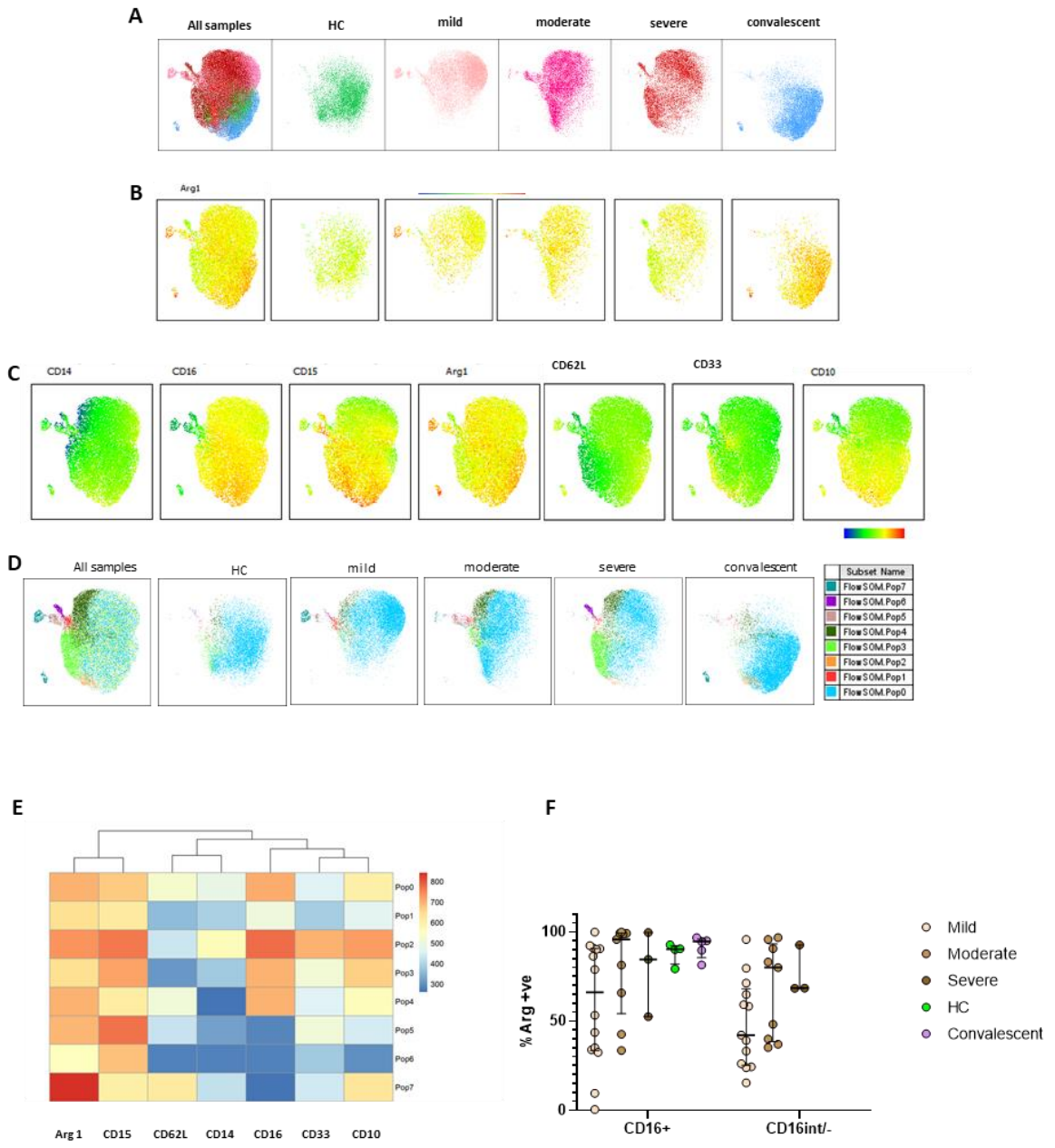

Figure 5.3.7 Altered composition of neutrophil populations is associated with disease severity in COVID-19 Whole Blood

Results were obtained through unsupervised subset identification based on UMAP projection on concatenated files of mild (n=4) moderate (n=4) and severe (n=4) and convalescent COVID-19 (n=5) patients and healthy controls (n=3) **(A)**. MFI heatmaps of the phenotyping panel in the UMAP as described **(A)** demonstrate the expression of intracellular arginase in the samples **(B)**. MFI heatmaps of the phenotyping panel in the UMAP as described **(A)** demonstrate the expression of cell surface markers and intracellular arginase in the samples **(C).** FlowSOM hierarchical clustering identify eight populations in the concatenated files **(D)**. Population heatmap showing the relative expression of each marker in each population defines neutrophil subsets that have differential expression according to disease severity**(E)**. Traditional gating on immature neutrophils based on CD16 expression show a trend towards higher arginase levels in moderate/severe cases although it is not significant **(F)**. *ANOVA with post hoc Tukey's multiple comparisons test*

5.3.7 Altered composition of neutrophil populations is associated with disease severity in COVID-19 Whole Blood

Rather than traditional flow cytometry gating a high-dimensional profiling approach was used to identify putative neutrophil sub populations in whole blood. Fresh peripheral blood was obtained from mild moderate severe convalescent and healthy controls and analysed by flow cytometry the resulting flow files were downsampled to contain equal numbers of cells and then concatenated. Data from $CD15^{+}CD14^{-}$ singlets were dimensionally reduced by Uniform Manifold Approximation and projection (UMAP) and clustered by FlowSOM. The resulting analysis reveal that mild moderate and severe COVID-19 patients to have clearly distinct populations from the HC and interestingly convalescent patients reveal distinct populations from HC and diseased samples (**Figure 5.3.7 A**). Individual marker expression is shown on the concatenated samples and reveal areas of high and low expression that can be mapped to to the corresponding severity level (**Figure 5.3.7 B, C**). FlowSOM identified eight clusters that differ in their marker expression (**Figure 5.3.7 D**). A heatmap of the MFIs of the markers in each cluster enables detailed phenotyping of the clusters expressed at varying stages of severity (**Figure 5.3.7 E**). Population 4 in dark green gradually increases with severe samples having the largest proportion of this cluster this is characterised by mid CD62l and high CD16 and mid Arg expression (**Figure 5.3.7 D**). Population 7 is found in mild and convalescent cases this cluster is characterised by high Arginase, mid CD62L, low CD16 and interestingly mid CD10 it is also low for CD33 (**Figure 5.3.7 E**). Another cluster that only appears in severe cases, population 3 in bright green, this population is characterised by low CD62L (activated) and mature CD16 high MFIs. This may be the population of cells I tried unsuccessfully to identify in whole blood of AAV patients and that Pillay et al report to be immunosuppressive[162]. It is interesting that they are only evident in severe disease. A population of interest is population 2 in orange present only in convalescent and a very low levels in severe cases is a population of high Arg, CD15, low CD62L, high CD16 and of particular interest high CD33 (**Figure 5.3.7 D, E**). This corroborates our finding of a $CD33^{high}$ population in WB analysis of convalescent patients (**Figure 5.3.1**). Of note also is the $CD16^{low}$ population found in mild moderate and severe that is not present in HC or convalescent samples populations 1.5,6 and 7 highlighting that immature cells are a feature of disease states. Using traditional gating methods, I focused on the $CD16^{int/-}$ expression of arginase 1 and there is less intracellular arginase 1 in immature neutrophils as defined by $CD16^{int/-}$, this is seen in population 6 in severe in particular (**Figure 5.3.7 F).** It is difficult to interpret all the perturbations that are possible but this technique could potentially uncover an important phenotype heretofore overlooked by traditional gating strategies.

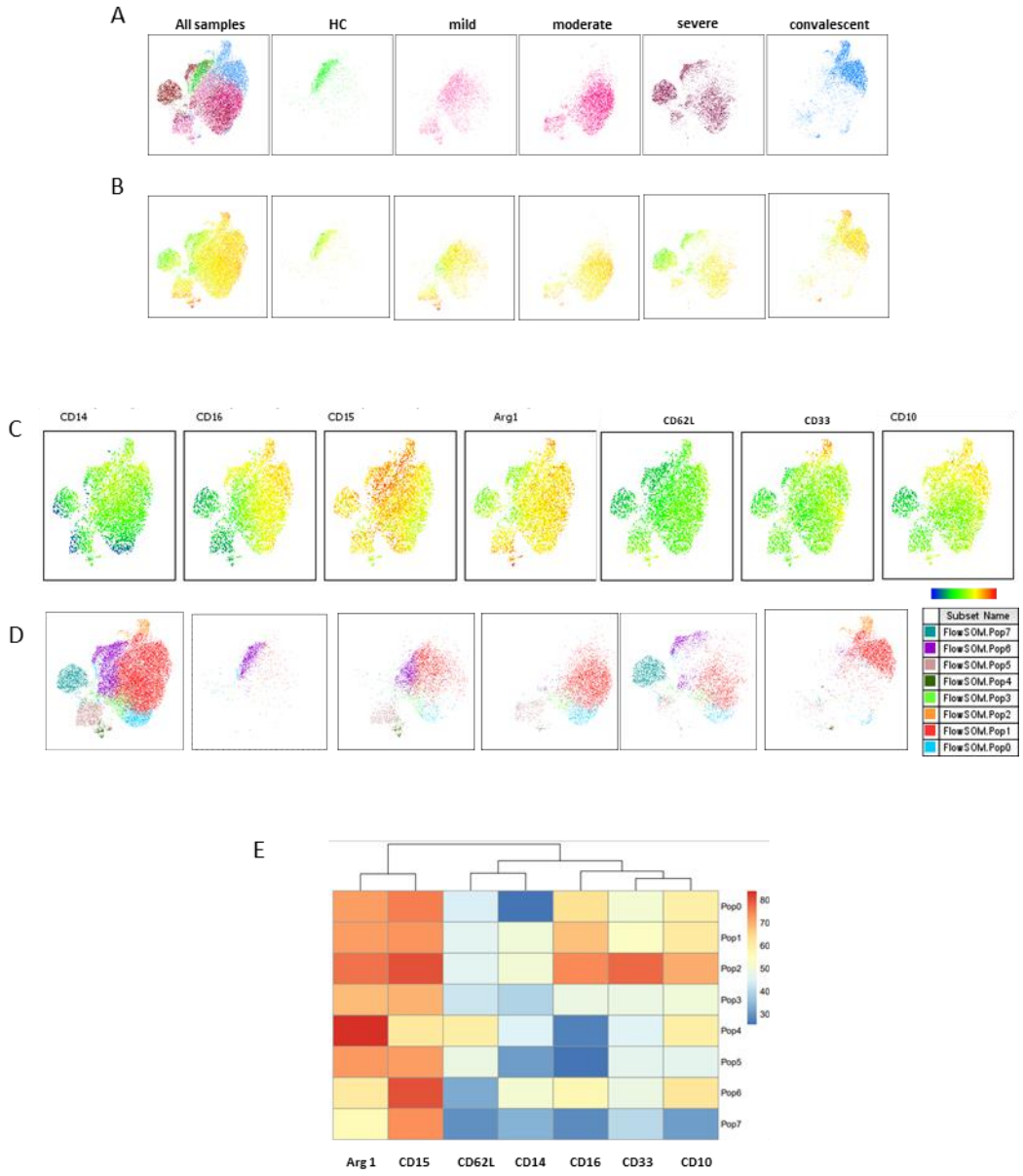

Figure 5.3.8 UMAP analysis of LDGs reveals severity related populations and convalescent populations that differ from healthy controls

Results were obtained through unsupervised subset identification based on UMAP projection on concatenated files of mild (n=4) moderate (n=4) and severe (n=4) and convalescent COVID-19 (n=5) patients and healthy controls (n=3) **(A)**. MFI heatmaps of the UMAP as described **(A)** demonstrate the expression of intracellular arginase in the samples stratified by severity**(B)**. MFI heatmaps of the phenotyping panel in the UMAP as described **(A)** demonstrate the expression of cell surface markers and intracellular arginase in the samples **(C).** FlowSOM hierarchical clustering identify eight populations in the concatenated files **(D)**. Population heatmap showing the relative expression of each marker in each population defines neutrophil subsets that have differential expression according to disease severity **(E)**.

5.3.8 UMAP analysis of LDGs reveals severity related populations and convalescent populations that differ from healthy controls

As I am particularly interested in neutrophil subsets in inflammatory states and the focus of a lot of my initial work was on the low-density subsets, I used the same approach that I had used for whole blood and applied it to LDGs in order to phenotype the clusters that are present in the low density fraction to compare to those found in whole blood. Data from $CD15^{+}CD14^{-}$ singlets were dimensionally reduced by UMAP and clustered by FlowSOM. The resulting analysis reveal that mild moderate and severe COVID-19 patients have clearly distinct populations from the HC and interestingly convalescent patients reveal distinct populations from HC and diseased samples reflecting the same findings in WB (**Figure 5.3.7**). What is clear here is the large expansion of immature neutrophils as defined by CD10 and CD16, indicative of emergency granulopoiesis and evident particularly in severe disease (**Figure 5.3.8 C**). The FlowSOM population 7 is particularly increased in severe disease and has low levels of all markers except CD15 which increases expression on activation and therefore this cells maybe immature activated cells. Of note is a CD33 high population that is only present in convalescent patients FlowSOM population 2 in orange, that was noted in my whole blood analysis (**Figure 5.3.8 D, E**). This population is a high arginase mature cell with low CD62L. The expansion of immature neutrophils is evident in the heatmap and (**Figure 5.3.8C**) and with these cells having low CD62L. What is clear from the individual marker heatmaps (**Figure 5.3.8 C**) is that there is a greater variability in the marker expression than in WB.

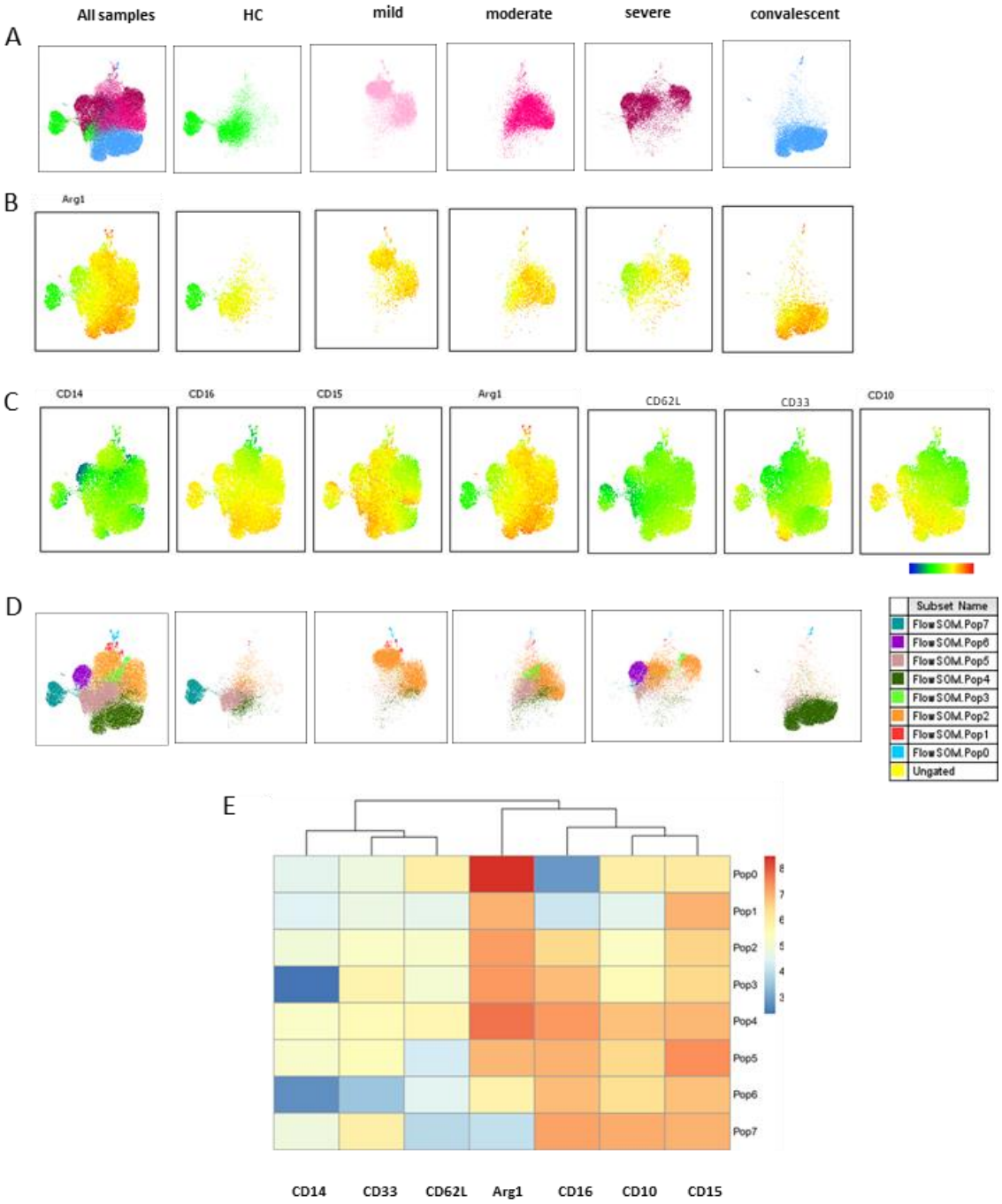

Figure 5.3.9 UMAP analysis of NDG identify neutrophil populations that are associated with disease severity in COVID-19 and in convalescence

Results were obtained through unsupervised subset identification based on UMAP projection on concatenated files of mild (n=4) moderate (n=4) and severe (n=4) and convalescent COVID-19 (n=5) patients and healthy controls (n=3) **(A)**. MFI heatmaps of the UMAP as described **(A)** demonstrate the expression of intracellular arginase in the samples stratified by severity**(B)**. MFI heatmaps of the phenotyping panel in the UMAP demonstrate the expression of cell surface markers and intracellular arginase in the samples **(C).** FlowSOM hierarchical clustering identify eight populations in the concatenated files **(D)**. Population heatmap showing the relative expression of each marker in each population defines neutrophil subsets that have differential expression according to disease severity **(E)**.

5.3.9 UMAP analysis of NDG identify neutrophil populations that are associated with disease severity in COVID-19 and in convalescence.

In chapter four, I noted there was a difference between Arg expression in NDGs in AAV, COVID-19 and HCs. There are no AAV samples in this cohort but as AAV NDGs appeared phenotypically as HC neutrophils a comparison of COVID-19 NDGs and HC NDGs is warranted. Data from $CD15^{+}CD14^{-}$ singlets in the NDG fraction of density gradient separated blood of the cohort described in 5.7 were concatenated and dimensionally reduced by UMAP and clustered by FlowSOM. The resulting analysis reveal that mild moderate and severe COVID-19 patients have clearly distinct populations from the HC and again as in WB and LDG convalescent patients, reveal distinct populations from HC and COVID-19 samples. One would expect fewer immature cells in the NDG fraction and there are far less immature populations as defined by CD10 and CD16 in this normal density fraction. CD33 overall has low MFI but again the main convalescent population 4 (dark green) has a mid-level expression in combination with a high arginase and mature phenotype (**Figure 5.3.9 D**, **E**). Levels of arginase 1 in the healthy controls appear to be lower than the COVID-19 samples and the convalescent patients, perhaps this a reflection of increased transcription in the COVID-19 patients relative to the healthy controls.

5.4 Discussion

Density has dominated the field of neutrophil biology. Since they were first described in patients with systemic lupus erythematous there have been reports of low density neutrophils in the PBMC layer of density gradient separated blood in cancer autoimmunity viral and bacterial infection and sepsis [51]. To date, most of the studies of neutrophil subsets in disease have focused on low density subsets, as I have shown in chapter four of this work there are differences in what have heretofore been referred to as normal density neutrophils (NDG) or normal steady state neutrophils with respect to arginase 1 expression in AAV and COVID-19. It is imperative therefore, in light of this finding that a study of all neutrophils in disease conditions are the subject of renewed focus. To achieve this objective, I have focused on the whole blood analysis of both COVID-19 and AAV patients.

In this chapter, I have used three approaches to interrogate the phenotype of neutrophils in whole blood. Firstly, I directly compared the frequency of immature and activated subsets in both AAV and COVID-19 using traditional flow gating techniques. The hypothesis behind this approach is that the low-density subsets are a mixed population of mature and immature cells with the immature cells resulting from emergency granulopoiesis and the mature cells in the low-density fraction are activated degranulated neutrophils. By focusing therefore on immature activated neutrophils, these cells should be identifiable in whole blood. I highlighted that there was an expansion of immature neutrophils in COVID-19 WB compared to AAV, there were also differences in the frequencies of activated subsets based on CD62L expression with significantly more activated cells being found in COVID-19 patient peripheral blood. The finding that CD33 cells were elevated in COVID-19 convalescent patients and not in AAV remission points to underlying differences in the neutrophils in both diseases and warrants further investigation. In fact, the finding that these subsets are present in a non-inflammatory state such as convalescent COVID-19 and not remission AAV points to a disease specific longlasting population The opportunity to compare these two systemic diseases has highlighted differences in the neutrophil population between both cohorts and suggests that neutrophils are a plastic population responding to their environment.

For my second approach, I focused on neutrophil subpopulations in WB of AAV patients and directly compared frequencies of these subpopulations with those in the low density and normal density fractions of the same patients. The development of two panels to accommodate as many markers as possible with 8 colour flow cytometry was based on our results that show that LDGs are a mixed population of mature and immature cells based on CD15 and CD16 expression and their nuclear morphology as determined by imaging flow cytometry in Chapter 3 of this work. To identify these cells in whole blood, surface markers would have to define the immature low-density fraction and

the mature low-density fraction whereas the normal density neutrophils are predominantly CD16 positive additional markers are required to define the mature low-density cells. A study by Pillay et al identified an immunosuppressive population of $CD16^{+}CD62l^{low}$ neutrophils induced in human volunteers following injection of a low dose of bacterial liposaccharide LPS, these cells inhibited T cell function, and these potentially allow identification of a subtype of neutrophils that may reflect the mature LDG phenotype (CD16+) [162]. To categorically define the LDG immature subset, markers of immature neutrophils are necessary, Evrard's mass cytometry (CyTOF) study of the developmental analysis of bone marrow neutrophils, provided additional markers to identify the subpopulations in whole blood, in particular Evrard used CD49d and CD101 to identify pre neutrophils in human bone marrow[146]. This combination of markers could therefore identify very immature neutrophils released during emergency granulopoiesis. The results however did not define the subsets. This could be due to low n numbers within the study. The division of the patient cohort into remission and acute did not show any differences between the subsets. Subsets were defined in LDGs and are different from NDGs however, these subsets were not detectable in whole blood. LDG subpopulations could be in part an artefactual result of processing. Neutrophil purification for *in vitro* studies can be challenging as they may be easily activated during *ex vivo* handling. However, the practice of erythrocyte sedimentation using dextran and subsequent density gradient centrifugation remains very widely practiced. Our results highlight the disparity between separated and whole blood. Populations are present in LDGs that are not detectable in whole blood. This could be due to the low percentage of cells in LDG subsets in PBMC that do not translate into a detectable population in whole blood. An alternative theory to explain the disparity is that certain surface markers are shed during purification. In a recent study by Quach et al the authors examined neutrophils purified by dextran sedimentation and density gradient and density gradient alone and found that cells from the dextran sedimented procedure had increased CD11b levels -linked to activation- and CD62l shedding [239]. Interestingly, the authors depleted monocytes lymphocytes and platelets before sedimentation and deduced that monocytes were the responsible cell type for neutrophil activation. This work could explain why LDGs in the PBMC layer shed CD62l and those in the NDG layer have high levels. Our results failed to identify LDGs in whole blood, this further underlines the necessity for a definitive whole blood panel to identify these putative subsets and reinforces the necessity of a reclassification of neutrophil subsets and a move away from reliance of density gradient classification[242].

The third approach was to focus on a more automated approach to the analysis of the flow cytometry data. The manual downstream analysis of flow cytometry data is arduous, frequently insufficient and user biased [243]. With the advent of mass cytometry (CyTOF) the dimensionality keeps increasing and this has led to the development of computational flow cytometry techniques

[240]. Even with relatively few markers the permutations of markers and subsets are many and require more sophisticated analytical techniques than the traditional gating of two markers at a time. The UMAP and subsequent clusters identified by FlowSOM reveal the changes in marker distribution as the disease progresses. One of the key findings of the whole blood analysis is the phenotype of the convalescent patients which is clearly separate from the healthy control patients. One of the key clusters has high arginase 1 low CD62l and high CD33 which corroborates our finding in traditional whole blood analysis. The power of this approach is that allows us to directly compare populations that would be otherwise overlooked. Focusing then on the LDG fraction, again severity related populations are identified, but the key finding is that the $CD33^{+}$ population identified in whole blood analysis is also identifiable in the low-density fraction. The expansion of immature neutrophils activated neutrophils are also evident in the LDG layer. The NDG fraction had fewer immature populations as would be expected with the immature cells remaining in the low-density fraction. Again, there is a population of CD33 mid expression in the NDG fraction of convalescent patients. The clearly different clusters identified by this technique in particular in the convalescent patients has demonstrated the power of this analysis. Convalescent patients do not have the same neutrophil marker profile as the healthy controls. This is a notable result as the phenotype of these cells as low CD62L high arginase 1 and CD33, could link them to having an immunosuppressive function [145]. The presence of these subsets in a non-inflammatory state such as convalescence is a key finding and their absence in healthy controls. Future work examining subsets in the two other non-inflammatory states HC and AAV remission is justified. The current gold standard for quantification of inflammation is BVAS in AAV and WHO classification in COVID-19 and perhaps further work would benefit from using c-reactive protein (CRP) levels to reflect inflammation. CRP is routinely tested in the hospital setting and may be a good surrogate for inflammation in both diseases.

Chapter 6

General Discussion

6 General Discussion

The paradigm of neutrophils as a uniform short-lived and functionally restricted population of innate immune cells is being robustly challenged. Evidence suggests that they feature a plasticity that allows them to respond and adapt to different disease situations [52, 244, 245]. These plastic neutrophil subsets suggest roles beyond acute infection and their classic function to kill invading pathogens that challenge the conventional concept of neutrophils and have been the focus of this work. I endeavoured to establish whether these subsets are a generic response to inflammation or disease specific immunomodulatory subsets that demonstrates neutrophil plasticity in inflammatory settings.

Using COVID-19 and AAV as models of viral and autoimmune disease respectively, I set about defining a disease specific response. In both diseases LDGs are elevated and linked to severity. Both LDG populations have remarkable similarities with respect to immature populations likely due to extreme left shift from emergency granulopoiesis. There were subtle differences in the nuclear lobe counts between the conditions suggesting that AAV neutrophils were more immature. The mature $CD16^{+}$ cells in both diseases again have remarkably similar surface marker expression and nuclear morphology. CD33 as a MDSC marker was highlighted as having different expression between the diseases. It would appear that the LDGs in AAV and COVID-19 are a general response to inflammation and in fact not a result of disease specific triggers.

To investigate the immunomodulatory role of neutrophils I focused on arginase 1, an established mechanism of T cell suppression. I have established that there are disease specific differences in arginase 1 expression in AAV and COVID-19, most notably that COVID-19 NDGs have significantly lower arginase levels than their AAV counterparts and healthy controls. AAV NDGs are almost identical to healthy control NDGs. I have shown by imaging flow cytometry that severe COVID-19 is characterised by a high level of cytoplasmic and granular arginase compared to AAV and HC. This may be the result of an errant release mechanism and increased transcription of the enzyme that is well documented in this disease[184, 185]. Mild Covid and acute AAV have similar cytoplasmic location of arginase compared to the granular location of arginase in HCs.

Heretofore the study of neutrophil subsets has been largely based on the concept of density, density gradient centrifugation itself may enrich for activated neutrophils and surface markers may be altered by shedding during the centrifugation step[239]. Having established that the key differences between COVID-19 and AAV were in the NDG fraction and not limited to the low-density fraction it followed that I would focus on the identification of neutrophil subsets in whole blood. There was an expansion of immature neutrophils in COVID-19 WB compared to AAV, there were also differences in the frequencies of activated subsets based on CD62L expression with

significantly more activated cells being found in COVID-19 patient peripheral blood. The finding that CD33 cells were elevated in COVID-19 convalescent patients and not in AAV remission points to underlying differences in the neutrophils in both diseases. Using UMAP and FlowSOM clustering, novel subsets were identified in each fraction, of particular note was the CD33 high population that was present consistently in the convalescent patients, this population had a high arginase 1 expression and low CD62L. CD33 has been highlighted as a disease specific difference in all chapters and its link with CD62L and arginase 1 suggests that it may fit the phenotype of MDSCs. A recent paper has reported that high levels of G-MDSCs as defined by $CD15^{+}$ $CD14^{-}$ and $CD33^{+}$ in whole blood were elevated in severe COVID-19 and high levels predicted fatal outcome[246]. This is in direct contrast to my finding that these CD33+ cells are present in convalescent patients. This finding raises many questions.

6.1 Unanswered questions

1. **Convalescent CD33+ neutrophil subset**
    - Are these cells protective or detrimental to the patient?
    - Are these cells present in all convalescent COVID-19 patients?
    - Are they a long-lived phenomenon or transient (patients were less than 3 months post COVID-19)?
    - If they are immunosuppressive would that have an effect on future vaccine responses?
    - Could they be a feature in the pathogenesis of long COVID-19

I propose that longitudinal studies be carried out on convalescent COVID-19 patients, to answer the above questions. There is a weekly post COVID-19 clinic in SJH, comparing their neutrophil phenotype with clinical readouts could give us an insight into the relevance of this subset. A clear issue would be in recruiting healthy controls as many individuals normally in this category are currently convalescent COVID-19.

2. **Aberrant arginase 1 expression in severe COVID-19**

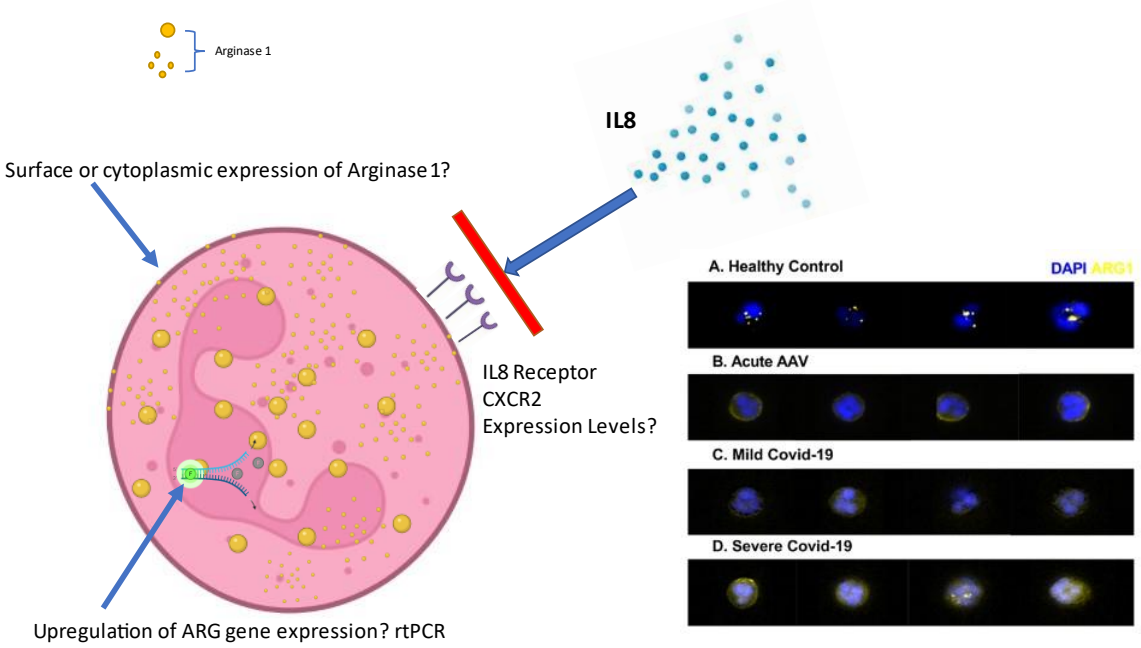

Figure 6.1.1 Investigation of the aberrant expression of Arginase 1 in Severe COVID-19.

Schematic outlining key points to investigate the aberrant expression of Arginase 1 in COVID-19. Arginase has a cytoplasmic and granular distribution in Severe Covid 19 (**D**). IL8 is required for the exocytosis of arginase 1. Representative merged images are shown of whole blood neutrophils in mild and severe COVID-19 Acute AAV and HC using DAPI nuclear stain (blue) and Arginase 1 (yellow) (**A-D**). Images obtained at 60X magnification on ImageStream X Mk 11.

Imaging flow cytometry and traditional flow cytometry data has highlighted that arginase is differentially expressed in COVID-19. To investigate this, key questions must be addressed.

1. IL8 is required for the exocytosis of arginase from neutrophils[179]. To investigate an aberrant release of arginase in these cells, levels of CXCR2, the receptor for IL8, would be determined by flow cytometry in severe COVID-19 and compared with mild COVID-19 and HC. IL8 levels in serum could be determined by ELISA in mild and severe and HC to determine if there is a lower IL8 expression.
2. Neutrophils in this experiment are permeabilized to access intracellular arginase, it is possible that arginase has also translocated to the cell surface, to investigate this permeabilized and non-permeabilised neutrophils from COVID-19 and HC would be stained with arginase 1. BD FACs lyse used to lyse RBCs would be replaced by a lysing buffer that does not contain permeabilizing agents. This would address the cellular location of the diffuse arginase in the images.

3. The increased arginase 1 in the severe samples could be due to increased transcription and this could be determined by rtPCR and compared to mild COVID-19 and HC (**Figure 6.1.1**).

6.2 Future Work

The work presented in this thesis has helped to establish that disease specific responses are a feature of neutrophils in inflammation. The key finding that all neutrophils are implicated in COVID-19 whereas AAV neutrophil differences are limited to the low-density fraction suggest that neutrophils are a plastic population responding to different triggers in diverse inflammatory setting. The identification however, of a neutrophil subset in convalescent patients that are otherwise healthy, supports the concept of a bona fide subset not just a result of neutrophil plasticity in response to inflammation. The finding of this subset in whole blood further emphasises the need to move away from density gradient as a standard for defining these subsets and underlines the need for a complete reassessment of neutrophil nomenclature as outlined in our recent paper[213]. Elucidating the differences in these subsets would be greatly aided by the development of the addition of new markers to the panel this would not only help in the understanding of neutrophils subsets in this field but in other areas such as sepsis and cancer where these cells are also a focus of study. I propose that in addition to the current marker panel that additional markers such as PD L1 (T cell suppression) LOX-1 (MDSC marker) be included as well as chemokines such as CXCR 1,2 and 4 [90, 247, 248]. This would allow more detailed phenotypes to be identified. This in combination with readouts of neutrophil function such as netosis, phagocytosis and ROS production would greatly improve our understanding of these cells.

Arginase 1 has been identified in this work as a key player in these diseases, however work remains to establish a working T cell suppression assay. I propose using neutrophils from whole blood (mixed leukocyte preparation) in the assay as opposed to only NDGs, which was our initial approach in this work, this would ensure that any low-density cells would be included. These cells would then be cocultured with T cells. Having a working T cell suppression assay, $CD33^{+}$ neutrophils could be isolated by flow sorting and this subset cocultured with T cells, to determine if this specific population is immunosuppressive.

6.3 Translational relevance

This work is of importance if neutrophils are to be targeted therapeutically, it is unclear if neutrophil subsets exist that could be targeted. If two subsets circulate in the bloodstream then targeting one would have avoid the other critical subset. If, however, all neutrophils are the same in blood but have the potential to perform different functions in different environments, then immunomodulation on a local level may be a therapeutic strategy. The targeting of all neutrophils

would lead to immunocompromise and resulting infections from neutropenia. Careful targeting of subsets and the mediators such as arginase 1, that they release may be necessary[249].

6.4 Final remarks

The differing roles of neutrophils in inflammation is likely to be a complex multifactorial one which depends on disease type, patient age, underlying comorbidities and stage of the disease and ongoing medications. In this thesis I have attempted to advance our knowledge of neutrophils in inflammatory settings and how they respond in different conditions. These are the first steps in unravelling the immunomodulatory potential of these heretofore understudied and much misunderstood cell type. This work has identified some key results which are outlined,

- LDGs are increased and linked to severity in AAV and COVID-19
- LDGs are a mixed population of mature and immature neutrophils in both AAV and COVID-19
- Arginase 1 is differentially expressed on NDGs from COVID-19 when compared to AAV, displaying a disease-specific response that is not limited to the low-density fraction
- Arginase 1 in healthy controls is located in granules whereas in COVID-19 and AAV there is a cytoplasmic distribution. Severe COVID-19 has a marked increase in cytoplasmic and granular arginase.
- WB analysis of COVID-19 neutrophils reveals immature activated subsets
- AAV LDGs are not identifiable in whole blood underlining the necessity to move away from reliance on density gradient separation
- The urgency of standardised neutrophil subset nomenclature in all fields is highlighted
- UMAP and clustering algorithms reveal severity-related populations in COVID-19
- Convalescent patients have a different profile from HC and active COVID-19, a neutrophil subset with high CD33 was identified which may be a bona fide neutrophil subset as it is not linked to systemic inflammation

I have shown that neutrophils display a plasticity in inflammatory settings and have explored the concept of true immunomodulatory subsets. These results have added to our general understanding of neutrophils in inflammation and have highlighted new directions for future studies both in neutrophil biology and in the etiology of AAV and COVID-19.

References

1. Mayadas, T.N., X. Cullere, and C.A. Lowell, *The Multifaceted Functions of Neutrophils.* Annual review of pathology, 2014. **9**: p. 181-218.
2. Ng, L.G., R. Ostuni, and A. Hidalgo, *Heterogeneity of neutrophils.* Nat Rev Immunol, 2019. **19**(4): p. 255-265.
3. Kolaczkowska, E. and P. Kubes, *Neutrophil recruitment and function in health and inflammation.* Nature Reviews Immunology, 2013. **13**(3): p. 159-175.
4. Bratton, D.L. and P.M. Henson, *Neutrophil clearance: when the party is over, clean-up begins.* Trends in Immunology, 2011. **32**(8): p. 350-357.
5. von Vietinghoff, S. and K. Ley, *Homeostatic Regulation of Blood Neutrophil Counts.* The Journal of Immunology, 2008. **181**(8): p. 5183.
6. Görgens, A., et al., *Revision of the Human Hematopoietic Tree: Granulocyte Subtypes Derive from Distinct Hematopoietic Lineages.* Cell Reports, 2013. **3**(5): p. 1539-1552.
7. Rosales, C., *Neutrophil: A Cell with Many Roles in Inflammation or Several Cell Types?* Front Physiol, 2018. **9**: p. 113.
8. Hong, C.-W., *Current Understanding in Neutrophil Differentiation and Heterogeneity.* Immune network, 2017. **17**(5): p. 298-306.
9. Ohls, R.K., A. Maheshwari, and R.D. Christensen, *Hematology, Immunology and Genetics*. Third ed. 2019: Elsevier.
10. Bjerregaard, M.D., et al., *The in vivo profile of transcription factors during neutrophil differentiation in human bone marrow.* Blood, 2003. **101**(11): p. 4322-32.
11. Benarafa, C., et al., *SerpinB1 protects the mature neutrophil reserve in the bone marrow.* Journal of leukocyte biology, 2011. **90**(1): p. 21-29.
12. Peters, A.M., *Just How Big is the Pulmonary Granulocyte Pool?* Clinical Science, 1998. **94**(1): p. 7-19.
13. Borregaard, N. and J.B. Cowland, *Granules of the human neutrophilic polymorphonuclear leukocyte.* Blood, 1997. **89**(10): p. 3503-21.
14. Rørvig, S., et al., *Proteome profiling of human neutrophil granule subsets, secretory vesicles, and cell membrane: correlation with transcriptome profiling of neutrophil precursors.* Journal of Leukocyte Biology, 2013. **94**(4): p. 711-721.
15. Cowland, J.B. and N. Borregaard, *Granulopoiesis and granules of human neutrophils.* Immunol Rev, 2016. **273**(1): p. 11-28.
16. Lawrence, S.M., R. Corriden, and V. Nizet, *The Ontogeny of a Neutrophil: Mechanisms of Granulopoiesis and Homeostasis.* Microbiol Mol Biol Rev, 2018. **82**(1).
17. Borregaard, N., et al., *Regulation of human neutrophil granule protein expression.* Curr Opin Hematol, 2001. **8**(1): p. 23-7.
18. Korkmaz, B., T. Moreau, and F. Gauthier, *Neutrophil elastase, proteinase 3 and cathepsin G: Physicochemical properties, activity and physiopathological functions.* Biochimie, 2008. **90**(2): p. 227-242.
19. Glenthøj, A., et al., *Processing of Neutrophil α-Defensins Does Not Rely on Serine Proteases In Vivo.* PloS one, 2015. **10**(5): p. e0125483-e0125483.
20. Gardiner, E.E., et al., *Regulation of P-selectin binding to the neutrophil P-selectin counter-receptor P-selectin glycoprotein ligand-1 by neutrophil elastase and cathepsin G.* Blood, 2001. **98**(5): p. 1440-1447.
21. Ragland, S.A. and A.K. Criss, *From bacterial killing to immune modulation: Recent insights into the functions of lysozyme.* PLoS pathogens, 2017. **13**(9): p. e1006512-e1006512.

22. Li, R.H.L. and F. Tablin, *A Comparative Review of Neutrophil Extracellular Traps in Sepsis.* Front Vet Sci, 2018. **5**: p. 291.
23. Fuchs, T.A., et al., *Novel cell death program leads to neutrophil extracellular traps.* Journal of Cell Biology, 2007. **176**(2): p. 231-241.
24. Papayannopoulos, V., et al., *Neutrophil elastase and myeloperoxidase regulate the formation of neutrophil extracellular traps.* Journal of Cell Biology, 2010. **191**(3): p. 677-691.
25. Warnatsch, A., et al., *Neutrophil extracellular traps license macrophages for cytokine production in atherosclerosis.* Science, 2015. **349**(6245): p. 316.
26. Sollberger, G., et al., *Gasdermin D plays a vital role in the generation of neutrophil extracellular traps.* Science Immunology, 2018. **3**(26): p. eaar6689.
27. Klausen, P., et al., *On mouse and man: neutrophil gelatinase associated lipocalin is not involved in apoptosis or acute response.* Eur J Haematol, 2005. **75**(4): p. 332-40.
28. Boström, E.A., A. Tarkowski, and M. Bokarewa, *Resistin is stored in neutrophil granules being released upon challenge with inflammatory stimuli.* Biochimica et Biophysica Acta (BBA) - Molecular Cell Research, 2009. **1793**(12): p. 1894-1900.
29. Liu, W., et al., *Olfactomedin 4 inhibits cathepsin C-mediated protease activities, thereby modulating neutrophil killing of Staphylococcus aureus and Escherichia coli in mice.* J Immunol, 2012. **189**(5): p. 2460-7.
30. Stroncek, D.F., K.M. Skubitz, and J.J. McCullough, *Biochemical characterization of the neutrophil-specific antigen NB1.* Blood, 1990. **75**(3): p. 744-55.
31. Häger, M., J.B. Cowland, and N. Borregaard, *Neutrophil granules in health and disease.* J Intern Med, 2010. **268**(1): p. 25-34.
32. Chavakis, E., E.Y. Choi, and T. Chavakis, *Novel aspects in the regulation of the leukocyte adhesion cascade.* Thrombosis and haemostasis, 2009. **102**(08): p. 191-197.
33. Scheiermann, C., et al., *Adrenergic nerves govern circadian leukocyte recruitment to tissues.* Immunity, 2012. **37**(2): p. 290-301.
34. Stark, M.A., et al., *Phagocytosis of apoptotic neutrophils regulates granulopoiesis via IL-23 and IL-17.* Immunity, 2005. **22**(3): p. 285-294.
35. Adrover, J.M., J.A. Nicolás-Ávila, and A. Hidalgo, *Aging: A Temporal Dimension for Neutrophils.* Trends in Immunology, 2016. **37**(5): p. 334-345.
36. Cerutti, A., I. Puga, and G. Magri, *The B cell helper side of neutrophils.* Journal of Leukocyte Biology, 2013. **94**(4): p. 677-682.
37. Hampton, H.R. and T. Chtanova. *The lymph node neutrophil*. in *Seminars in immunology*. 2016. Elsevier.
38. Massena, S., et al., *Identification and characterization of VEGF-A–responsive neutrophils expressing CD49d, VEGFR1, and CXCR4 in mice and humans.* Blood, The Journal of the American Society of Hematology, 2015. **126**(17): p. 2016-2026.
39. Buckley, C.D., et al., *Identification of a phenotypically and functionally distinct population of long-lived neutrophils in a model of reverse endothelial migration.* J Leukoc Biol, 2006. **79**(2): p. 303-11.
40. Ji, J. and J. Fan, *Neutrophil in Reverse Migration: Role in Sepsis.* Front Immunol, 2021. **12**: p. 656039.
41. Tecchio, C., A. Micheletti, and M.A. Cassatella, *Neutrophil-derived cytokines: facts beyond expression.* Frontiers in immunology, 2014. **5**: p. 508-508.
42. Tecchio, C. and M.A. Cassatella, *Uncovering the multifaceted roles played by neutrophils in allogeneic hematopoietic stem cell transplantation.* Cellular & molecular immunology, 2021. **18**(4): p. 905-918.

43. Nauseef, W.M. and N. Borregaard, *Neutrophils at work.* Nat Immunol, 2014. **15**(7): p. 602-11.
44. Gordon, S., *Elie Metchnikoff, the Man and the Myth.* Journal of Innate Immunity, 2016. **8**(3): p. 223-227.
45. Kay, A.B., *Paul Ehrlich and the Early History of Granulocytes.* Microbiol Spectr, 2016. **4**(4).
46. Darcy, C.J., et al., *Neutrophils with myeloid derived suppressor function deplete arginine and constrain T cell function in septic shock patients.* Crit Care, 2014. **18**(4): p. R163.
47. Sagiv, J.Y., S. Voels, and Z. Granot, *Isolation and Characterization of Low- vs. High-Density Neutrophils in Cancer.* Methods Mol Biol, 2016. **1458**: p. 179-93.
48. Cloke, T., et al., *Phenotypic alteration of neutrophils in the blood of HIV seropositive patients.* PLoS One, 2013. **8**(9): p. e72034.
49. Ui Mhaonaigh, A., et al., *Low Density Granulocytes in ANCA Vasculitis Are Heterogenous and Hypo-Responsive to Anti-Myeloperoxidase Antibodies.* Frontiers in Immunology, 2019. **10**(2603).
50. Cuartero, M.I., et al., *N2 neutrophils, novel players in brain inflammation after stroke: modulation by the PPARγ agonist rosiglitazone.* Stroke, 2013. **44**(12): p. 3498-508.
51. Hacbarth, E. and A. Kajdacsy-Balla, *Low density neutrophils in patients with systemic lupus erythematosus, rheumatoid arthritis, and acute rheumatic fever.* Arthritis Rheum, 1986. **29**(11): p. 1334-42.
52. Denny, M.F., et al., *A distinct subset of proinflammatory neutrophils isolated from patients with systemic lupus erythematosus induces vascular damage and synthesizes type I IFNs.* Journal of immunology (Baltimore, Md. : 1950), 2010. **184**(6): p. 3284-3297.
53. Cloke, T., et al., *Characterization of a Novel Population of Low-Density Granulocytes Associated with Disease Severity in HIV-1 Infection.* PLOS ONE, 2012. **7**(11): p. e48939.
54. Ssemaganda, A., et al., *Characterization of Neutrophil Subsets in Healthy Human Pregnancies.* PLOS ONE, 2014. **9**(2): p. e85696.
55. Porntrakulpipat, S., K.R. Depner, and V. Moennig, *Are Low-Density Granulocytes the Major Target Cells of Classical Swine Fever Virus in the Peripheral Blood?* Journal of Veterinary Medicine, Series B, 2001. **48**(8): p. 593-602.
56. Hoffmann, M.H., et al., *The cathelicidins LL-37 and rCRAMP are associated with pathogenic events of arthritis in humans and rats.* Annals of the Rheumatic Diseases, 2013. **72**(7): p. 1239.
57. Dean, M.J., et al., *Severe COVID-19 Is Characterized by an Impaired Type I Interferon Response and Elevated Levels of Arginase Producing Granulocytic Myeloid Derived Suppressor Cells.* Frontiers in Immunology, 2021. **12**(2726).
58. Ui Mhaonaigh, A., et al., *Low Density Granulocytes in ANCA Vasculitis Are Heterogenous and Hypo-Responsive to Anti-Myeloperoxidase Antibodies.* Frontiers in Immunology, 2019. **10**: p. 2603.
59. Wright, H.L., et al., *Low-density granulocytes: functionally distinct, immature neutrophils in rheumatoid arthritis with altered properties and defective TNF signalling.* Journal of Leukocyte Biology, 2016. **101**(2): p. 599-611.
60. Lin, A.M., et al., *Mast cells and neutrophils release IL-17 through extracellular trap formation in psoriasis.* J Immunol, 2011. **187**(1): p. 490-500.

61. Villanueva, E., et al., *Netting neutrophils induce endothelial damage, infiltrate tissues, and expose immunostimulatory molecules in systemic lupus erythematosus.* J Immunol, 2011. **187**(1): p. 538-52.
62. Carmona-Rivera, C. and M.J. Kaplan, *Low-density granulocytes: a distinct class of neutrophils in systemic autoimmunity.* Seminars in Immunopathology, 2013. **35**(4): p. 455-463.
63. Cochrane , C.G., E.R. Unanue , and F.J. Dixon *A ROLE OF POLYMORPHONUCLEAR LEUKOCYTES AND COMPLEMENT IN NEPHROTOXIC NEPHRITIS.* The Journal of Experimental Medicine, 1965. **122**(1): p. 99-116.
64. Denny, M.F., et al., *A distinct subset of proinflammatory neutrophils isolated from patients with systemic lupus erythematosus induces vascular damage and synthesizes type I IFNs.* J Immunol, 2010. **184**(6): p. 3284-97.
65. Mistry, P., et al., *Transcriptomic, epigenetic, and functional analyses implicate neutrophil diversity in the pathogenesis of systemic lupus erythematosus.* Proceedings of the National Academy of Sciences, 2019: p. 201908576.
66. Rahman, S., et al., *Low-density granulocytes activate T cells and demonstrate a non-suppressive role in systemic lupus erythematosus.* Annals of the Rheumatic Diseases, 2019. **78**(7): p. 957.
67. Sagiv, J.Y., et al., *Phenotypic diversity and plasticity in circulating neutrophil subpopulations in cancer.* Cell Rep, 2015. **10**(4): p. 562-73.
68. Kusmartsev, S.A., Y. Li, and S.H. Chen, *Gr-1+ myeloid cells derived from tumor-bearing mice inhibit primary T cell activation induced through CD3/CD28 costimulation.* J Immunol, 2000. **165**(2): p. 779-85.
69. Keskinov, A.A. and M.R. Shurin, *Myeloid regulatory cells in tumor spreading and metastasis.* Immunobiology, 2015. **220**(2): p. 236-42.
70. Gabrilovich, D.I., et al., *The terminology issue for myeloid-derived suppressor cells,* in *Cancer Res*. 2007. p. 425; author reply 426.
71. Pillay, J., et al., *Immune suppression by neutrophils and granulocytic myeloid-derived suppressor cells: similarities and differences.* Cellular and molecular life sciences : CMLS, 2013. **70**(20): p. 3813-3827.
72. Raber, P.L., et al., *Subpopulations of myeloid-derived suppressor cells impair T cell responses through independent nitric oxide-related pathways.* Int J Cancer, 2014. **134**(12): p. 2853-64.
73. Rosales, C., *Neutrophil: A Cell with Many Roles in Inflammation or Several Cell Types?* Frontiers in physiology, 2018. **9**: p. 113-113.
74. Grecian, R., M.K.B. Whyte, and S.R. Walmsley, *The role of neutrophils in cancer.* British Medical Bulletin, 2018. **128**(1): p. 5-14.
75. Dumitru, C.A., et al., *Neutrophils and granulocytic myeloid-derived suppressor cells: immunophenotyping, cell biology and clinical relevance in human oncology.* Cancer Immunol Immunother, 2012. **61**(8): p. 1155-67.
76. Favaloro, J., et al., *Myeloid derived suppressor cells are numerically, functionally and phenotypically different in patients with multiple myeloma.* Leuk Lymphoma, 2014. **55**(12): p. 2893-900.
77. Jacobsen, L.C., et al., *Arginase 1 is expressed in myelocytes/metamyelocytes and localized in gelatinase granules of human neutrophils.* Blood, 2006. **109**(7): p. 3084-3087.
78. Rodriguez, P.C., D.G. Quiceno, and A.C. Ochoa, *l-arginine availability regulates T-lymphocyte cell-cycle progression.* Blood, 2006. **109**(4): p. 1568-1573.

79. Feldmeyer, N., et al., *Arginine deficiency leads to impaired cofilin dephosphorylation in activated human T lymphocytes.* International Immunology, 2012. **24**(5): p. 303-313.
80. Sionov, R.V., Z.G. Fridlender, and Z. Granot, *The Multifaceted Roles Neutrophils Play in the Tumor Microenvironment.* Cancer Microenviron, 2015. **8**(3): p. 125-58.
81. Shaul, M.E., et al., *Tumor-associated neutrophils display a distinct N1 profile following TGFβ modulation: A transcriptomics analysis of pro- vs. antitumor TANs.* Oncoimmunology, 2016. **5**(11): p. e1232221-e1232221.
82. Fridlender, Z.G., et al., *Polarization of tumor-associated neutrophil phenotype by TGF-beta: "N1" versus "N2" TAN.* Cancer Cell, 2009. **16**(3): p. 183-94.
83. Jablonska, J., et al., *Neutrophils responsive to endogenous IFN-beta regulate tumor angiogenesis and growth in a mouse tumor model.* J Clin Invest, 2010. **120**(4): p. 1151-64.
84. Hietbrink, F., et al., *Kinetics of the innate immune response after trauma: implications for the development of late onset sepsis.* Shock, 2013. **40**(1): p. 21-7.
85. Fridlender, Z.G. and S.M. Albelda, *Tumor-associated neutrophils: friend or foe?* Carcinogenesis, 2012. **33**(5): p. 949-55.
86. Sagiv, Jitka Y., et al., *Phenotypic Diversity and Plasticity in Circulating Neutrophil Subpopulations in Cancer.* Cell Reports, 2015. **10**(4): p. 562-573.
87. Deng, Y., et al., *Low-Density Granulocytes Are Elevated in Mycobacterial Infection and Associated with the Severity of Tuberculosis.* PLOS ONE, 2016. **11**(4): p. e0153567.
88. Cassetta, L., et al., *Deciphering myeloid-derived suppressor cells: isolation and markers in humans, mice and non-human primates.* Cancer immunology, immunotherapy : CII, 2019. **68**(4): p. 687-697.
89. Brandau, S., et al., *Myeloid-derived suppressor cells in the peripheral blood of cancer patients contain a subset of immature neutrophils with impaired migratory properties.* J Leukoc Biol, 2011. **89**(2): p. 311-7.
90. Condamine, T., et al., *Lectin-type oxidized LDL receptor-1 distinguishes population of human polymorphonuclear myeloid-derived suppressor cells in cancer patients.* Science Immunology, 2016. **1**(2): p. aaf8943.
91. Nan, J., et al., *Endoplasmic reticulum stress induced LOX-1+ CD15+ polymorphonuclear myeloid-derived suppressor cells in hepatocellular carcinoma.* Immunology, 2018. **154**(1): p. 144-155.
92. Rodriguez, P.C., et al., *Arginase I-producing myeloid-derived suppressor cells in renal cell carcinoma are a subpopulation of activated granulocytes.* Cancer Res, 2009. **69**(4): p. 1553-60.
93. Marini, O., et al., *Mature CD10⁺ and immature CD10[−] neutrophils present in G-CSF–treated donors display opposite effects on T cells.* Blood, 2017. **129**(10): p. 1343.
94. Schonermarck, U., E. Csernok, and W.L. Gross, *Pathogenesis of anti-neutrophil cytoplasmic antibody-associated vasculitis: challenges and solutions 2014.* Nephrol Dial Transplant, 2015. **30 Suppl 1**: p. i46-52.
95. Booth, A.D., et al., *Outcome of ANCA-associated renal vasculitis: a 5-year retrospective study.* American Journal of Kidney Diseases, 2003. **41**(4): p. 776-784.
96. Falk, R.J. and J.C. Jennette, *Anti-Neutrophil Cytoplasmic Autoantibodies with Specificity for Myeloperoxidase in Patients with Systemic Vasculitis and Idiopathic Necrotizing and Crescentic Glomerulonephritis.* New England Journal of Medicine, 1988. **318**(25): p. 1651-1657.

97. Williams, R.C., et al., *Epitopes on proteinase-3 recognized by antibodies from patients with Wegener's granulomatosis.* The Journal of Immunology, 1994. **152**(9): p. 4722.
98. Jones, B.E., et al., *Gene-Specific DNA Methylation Changes Predict Remission in Patients with ANCA-Associated Vasculitis.* Journal of the American Society of Nephrology, 2017. **28**(4): p. 1175.
99. Ciavatta, D.J., et al., *Epigenetic basis for aberrant upregulation of autoantigen genes in humans with ANCA vasculitis.* J Clin Invest, 2010. **120**(9): p. 3209-19.
100. Schreiber, A., et al., *C5a receptor mediates neutrophil activation and ANCA-induced glomerulonephritis.* J Am Soc Nephrol, 2009. **20**(2): p. 289-98.
101. Lyons, P.A., et al., *Novel expression signatures identified by transcriptional analysis of separated leucocyte subsets in systemic lupus erythematosus and vasculitis.* Ann Rheum Dis, 2010. **69**(6): p. 1208-13.
102. Cheadle, C., et al., *Transcription of proteinase 3 and related myelopoiesis genes in peripheral blood mononuclear cells of patients with active Wegener's granulomatosis.* Arthritis and rheumatism, 2010. **62**(6): p. 1744-1754.
103. Grayson Peter, C., et al., *Neutrophil-Related Gene Expression and Low-Density Granulocytes Associated With Disease Activity and Response to Treatment in Antineutrophil Cytoplasmic Antibody–Associated Vasculitis.* Arthritis & Rheumatology, 2015. **67**(7): p. 1922-1932.
104. Endo, A., et al., *Two distinct subsets of LDGs (low density granulocytes) in ANCA-associated vasculitis.* Modern Rheumatology, 2021: p. 1-25.
105. Cavalcante-Silva, L.H.A., et al., *Neutrophils and COVID-19: The road so far.* International Immunopharmacology, 2021. **90**: p. 107233.
106. Liu, Y., A.H. Sawalha, and Q. Lu, *COVID-19 and autoimmune diseases.* Current opinion in rheumatology, 2021. **33**(2): p. 155-162.
107. Barnes, B.J., et al., *Targeting potential drivers of COVID-19: Neutrophil extracellular traps.* Journal of Experimental Medicine, 2020. **217**(6).
108. Reizine, F., et al., *SARS-CoV-2-Induced ARDS Associates with MDSC Expansion, Lymphocyte Dysfunction, and Arginine Shortage.* Journal of Clinical Immunology, 2021.
109. Thierry, A. and B. Roch, *NETs By-Products and Extracellular DNA May Play a Key Role in COVID-19 Pathogenesis: Incidence on Patient Monitoring and Therapy.* MEDICINE & PHARMACOLOGY, 2020.
110. Leppkes, M., et al., *Vascular occlusion by neutrophil extracellular traps in COVID-19.* EBioMedicine, 2020. **58**: p. 102925.
111. Thierry, A.R., *Anti-protease Treatments Targeting Plasmin(ogen) and Neutrophil Elastase May Be Beneficial in Fighting COVID-19.* Physiological reviews, 2020. **100**(4): p. 1597-1598.
112. Torres-Ruiz, J., et al., *Neutrophil Extracellular Traps Contribute to COVID-19 Hyperinflammation and Humoral Autoimmunity.* Cells, 2021. **10**(10): p. 2545.
113. Yang, A.-P., et al., *The diagnostic and predictive role of NLR, d-NLR and PLR in COVID-19 patients.* International immunopharmacology, 2020. **84**: p. 106504-106504.
114. Morrissey, S., et al., *Emergence of Low-density Inflammatory Neutrophils Correlates with Hypercoagulable State and Disease Severity in COVID-19 Patients*. 2020.
115. Daamen, A.R., et al., *Comprehensive Transcriptomic Analysis of COVID-19 Blood, Lung, and Airway.* bioRxiv, 2020: p. 2020.05.28.121889.

116. Carmona-Rivera, C. and M.J. Kaplan, *Low density granulocytes: a distinct class of neutrophils in systemic autoimmunity.* Seminars in immunopathology, 2013. **35**(4): p. 455-463.
117. Blanco-Melo, D., et al., *Imbalanced Host Response to SARS-CoV-2 Drives Development of COVID-19.* Cell, 2020. **181**(5): p. 1036-1045.e9.
118. Wu, D. and X.O. Yang, *TH17 responses in cytokine storm of COVID-19: An emerging target of JAK2 inhibitor Fedratinib.* Journal of Microbiology, Immunology and Infection, 2020. **53**(3): p. 368-370.
119. Agrati, C., et al., *Expansion of myeloid-derived suppressor cells in patients with severe coronavirus disease (COVID-19).* Cell Death & Differentiation, 2020.
120. Parackova, Z., et al., *Disharmonic Inflammatory Signatures in COVID-19: Augmented Neutrophils' but Impaired Monocytes' and Dendritic Cells' Responsiveness.* Cells, 2020. **9**(10): p. 2206.
121. Cabrera, L.E., et al., *Characterization of low-density granulocytes in COVID-19.* PLOS Pathogens, 2021. **17**(7): p. e1009721.
122. Mackey, J.B.G., S.B. Coffelt, and L.M. Carlin, *Neutrophil Maturity in Cancer.* Front Immunol, 2019. **10**: p. 1912.
123. Veda, P., *Why are Neutrophils Polymorphonuclear?* European Journal of Inflammation, 2011. **9**(2): p. 85-93.
124. Olins, A.L. and D.E. Olins, *Cytoskeletal influences on nuclear shape in granulocytic HL-60 cells.* BMC Cell Biol, 2004. **5**: p. 30.
125. Elghetany, M.T., *Surface antigen changes during normal neutrophilic development: a critical review.* Blood Cells Mol Dis, 2002. **28**(2): p. 260-74.
126. Davoine, F., et al., *Expression of FcγRIII (CD16) on human peripheral blood eosinophils increases in allergic conditions.* Journal of Allergy and Clinical Immunology, 2002. **109**(3): p. 463-469.
127. Haziot, A., B.Z. Tsuberi, and S.M. Goyert, *Neutrophil CD14: biochemical properties and role in the secretion of tumor necrosis factor-alpha in response to lipopolysaccharide.* J Immunol, 1993. **150**(12): p. 5556-65.
128. Elghetany, M.T., et al., *CD87 as a marker for terminal granulocytic maturation: assessment of its expression during granulopoiesis.* Cytometry B Clin Cytom, 2003. **51**(1): p. 9-13.
129. Terstappen, L., M. Safford, and M. Loken, *Flow cytometric analysis of human bone marrow. III. Neutrophil maturation.* Leukemia : official journal of the Leukemia Society of America, Leukemia Research Fund, U.K, 1990. **4**: p. 657-63.
130. Elghetany, M.T., et al., *Flow cytometric study of neutrophilic granulopoiesis in normal bone marrow using an expanded panel of antibodies: correlation with morphologic assessments.* J Clin Lab Anal, 2004. **18**(1): p. 36-41.
131. Liu, M., et al., *Flow cytometric analysis of CD64 expression pattern and density in the diagnosis of acute promyelocytic leukemia: a multi-center study in Shanghai, China.* Oncotarget, 2017. **8**(46): p. 80625-80637.
132. Weirich, E., et al., *Neutrophil CD11b expression as a diagnostic marker for early-onset neonatal infection.* J Pediatr, 1998. **132**(3 Pt 1): p. 445-51.
133. Grieshaber-Bouyer, R. and P.A. Nigrovic, *Neutrophil Heterogeneity as Therapeutic Opportunity in Immune-Mediated Disease.* Frontiers in immunology, 2019. **10**: p. 346-346.
134. Marini, O., et al., *Mature CD10(+) and immature CD10(-) neutrophils present in G-CSF-treated donors display opposite effects on T cells.* Blood, 2017. **129**(10): p. 1343-1356.

135. Wang, Y. and F. Jönsson, *Expression, Role, and Regulation of Neutrophil Fcγ Receptors.* Frontiers in immunology, 2019. **10**: p. 1958-1958.
136. Zhang, Y., et al., *Crystal Structure of the Extracellular Domain of a Human FcγRIII.* Immunity, 2000. **13**(3): p. 387-395.
137. Orr, Y., et al., *A kinetic model of bone marrow neutrophil production that characterizes late phenotypic maturation.* American Journal of Physiology-Regulatory, Integrative and Comparative Physiology, 2007. **292**(4): p. R1707-R1716.
138. Wang, Y., et al., *ADAM17 cleaves CD16b (FcγRIIIb) in human neutrophils.* Biochimica et Biophysica Acta (BBA) - Molecular Cell Research, 2013. **1833**(3): p. 680-685.
139. Guérin, E., et al., *Circulating immature granulocytes with T-cell killing functions predict sepsis deterioration*.* Crit Care Med, 2014. **42**(9): p. 2007-18.
140. Demaret, J., et al., *Marked alterations of neutrophil functions during sepsis-induced immunosuppression.* Journal of Leukocyte Biology, 2015. **98**(6): p. 1081-1090.
141. Gorczyca, W., et al., *Immunophenotypic pattern of myeloid populations by flow cytometry analysis.* Methods Cell Biol, 2011. **103**: p. 221-66.
142. Laszlo, G.S., E.H. Estey, and R.B. Walter, *The past and future of CD33 as therapeutic target in acute myeloid leukemia.* Blood Reviews, 2014. **28**(4): p. 143-153.
143. Hoyer, J.D., et al., *CD33 detection by immunohistochemistry in paraffin-embedded tissues: a new antibody shows excellent specificity and sensitivity for cells of myelomonocytic lineage.* Am J Clin Pathol, 2008. **129**(2): p. 316-23.
144. Terstappen, L.W., et al., *Quantitative comparison of myeloid antigens on five lineages of mature peripheral blood cells.* J Leukoc Biol, 1990. **48**(2): p. 138-48.
145. Bronte, V., et al., *Recommendations for myeloid-derived suppressor cell nomenclature and characterization standards.* Nature Communications, 2016. **7**: p. 12150.
146. Evrard, M., et al., *Developmental Analysis of Bone Marrow Neutrophils Reveals Populations Specialized in Expansion, Trafficking, and Effector Functions.* Immunity, 2018. **48**(2): p. 364-379.e8.
147. Mahlknecht, U. and C. Schönbein, *Histone deacetylase inhibitor treatment downregulates VLA-4 adhesion in hematopoietic stem cells and acute myeloid leukemia blast cells.* Haematologica, 2008. **93**(3): p. 443.
148. Sigua, J.A., et al., *CD49d-expressing neutrophils differentiate atopic from nonatopic individuals.* J Allergy Clin Immunol, 2014. **133**(3): p. 901-4.e5.
149. Fu, S. and J. Liesveld, *Mobilization of hematopoietic stem cells.* Blood Rev, 2000. **14**(4): p. 205-18.
150. Oostendorp, R.A. and P. Dörmer, *VLA-4-mediated interactions between normal human hematopoietic progenitors and stromal cells.* Leuk Lymphoma, 1997. **24**(5-6): p. 423-35.
151. Zhang, D., et al., *Neutrophil ageing is regulated by the microbiome.* Nature, 2015. **525**(7570): p. 528-532.
152. Stroncek, D.F., et al., *The expression of the NB1 antigen on myeloid precursors and neutrophils from children and umbilical cords.* Transfus Med, 1998. **8**(2): p. 119-23.
153. Stroncek, D.F., L. Caruccio, and M. Bettinotti, *CD177: A member of the Ly-6 gene superfamily involved with neutrophil proliferation and polycythemia vera.* Journal of translational medicine, 2004. **2**(1): p. 8-8.
154. Hu, N., et al., *Coexpression of CD177 and membrane proteinase 3 on neutrophils in antineutrophil cytoplasmic autoantibody-associated systemic vasculitis: anti-*

proteinase 3-mediated neutrophil activation is independent of the role of CD177-expressing neutrophils. Arthritis Rheum, 2009. **60**(5): p. 1548-57.
155. Domínguez-Luis, M.J., et al., *L-selectin expression is regulated by CXCL8-induced reactive oxygen species produced during human neutrophil rolling.* Eur J Immunol, 2019. **49**(3): p. 386-397.
156. Lacy, P., *Mechanisms of degranulation in neutrophils.* Allergy, asthma, and clinical immunology : official journal of the Canadian Society of Allergy and Clinical Immunology, 2006. **2**(3): p. 98-108.
157. Skubitz, K.M., K.D. Campbell, and A.P.N. Skubitz, *CD63 associates with CD11/CD18 in large detergent-resistant complexes after translocation to the cell surface in human neutrophils11Presented in part at the annual meetings of the American Society of Hematology, Miami, FL, 4–8 December 1998, and the American Society for Cell Biology, San Francisco, CA, 12–16 December 1998.* FEBS Letters, 2000. **469**(1): p. 52-56.
158. De Filippo, K. and S.M. Rankin, *CXCR4, the master regulator of neutrophil trafficking in homeostasis and disease.* European Journal of Clinical Investigation, 2018. **48**(S2): p. e12949.
159. Martin, C., et al., *Chemokines Acting via CXCR2 and CXCR4 Control the Release of Neutrophils from the Bone Marrow and Their Return following Senescence.* Immunity, 2003. **19**(4): p. 583-593.
160. Eash, K.J., et al., *CXCR2 and CXCR4 antagonistically regulate neutrophil trafficking from murine bone marrow.* J Clin Invest, 2010. **120**(7): p. 2423-31.
161. Tak, T., et al., *Human CD62Ldim neutrophils identified as a separate subset by proteome profiling and in vivo pulse-chase labeling.* Blood, 2017. **129**(26): p. 3476-3485.
162. Pillay, J., et al., *A subset of neutrophils in human systemic inflammation inhibits T cell responses through Mac-1.* J Clin Invest, 2012. **122**(1): p. 327-36.
163. Aarts, C.E.M., et al., *Neutrophils as Suppressors of T Cell Proliferation: Does Age Matter?* Frontiers in Immunology, 2019. **10**(2144).
164. Bronte, V. and P. Zanovello, *Regulation of immune responses by L-arginine metabolism.* Nature Reviews Immunology, 2005. **5**(8): p. 641-654.
165. Morris, S.M., *REGULATION OF ENZYMES OF THE UREA CYCLE AND ARGININE METABOLISM.* Annual Review of Nutrition, 2002. **22**(1): p. 87-105.
166. Jenkinson, C.P., W.W. Grody, and S.D. Cederbaum, *Comparative properties of arginases.* Comparative Biochemistry and Physiology Part B: Biochemistry and Molecular Biology, 1996. **114**(1): p. 107-132.
167. Wu, G. and S.M. Morris, Jr., *Arginine metabolism: nitric oxide and beyond.* The Biochemical journal, 1998. **336 (Pt 1)**(Pt 1): p. 1-17.
168. Munder, M., et al., *Suppression of T-cell functions by human granulocyte arginase.* Blood, 2006. **108**(5): p. 1627-34.
169. Haraguchi, Y., et al., *Molecular cloning and nucleotide sequence of cDNA for human liver arginase.* Proceedings of the National Academy of Sciences, 1987. **84**(2): p. 412-415.
170. Kung, J.T., et al., *Suppression of in vitro cytotoxic response by macrophages due to induced arginase.* J Exp Med, 1977. **146**(3): p. 665-72.
171. MacMicking, J., Q.W. Xie, and C. Nathan, *Nitric oxide and macrophage function.* Annu Rev Immunol, 1997. **15**: p. 323-50.
172. Nathan, C. and Q.W. Xie, *Regulation of biosynthesis of nitric oxide.* J Biol Chem, 1994. **269**(19): p. 13725-8.

173. Munder, M., K. Eichmann, and M. Modolell, *Alternative metabolic states in murine macrophages reflected by the nitric oxide synthase/arginase balance: competitive regulation by CD4+ T cells correlates with Th1/Th2 phenotype.* J Immunol, 1998. **160**(11): p. 5347-54.
174. Munder, M., et al., *Suppression of T-cell functions by human granulocyte arginase.* Blood, 2006. **108**(5): p. 1627-1634.
175. Rodriguez, P.C., et al., *Regulation of T Cell Receptor CD3ζ Chain Expression byl-Arginine *.* Journal of Biological Chemistry, 2002. **277**(24): p. 21123-21129.
176. Munder, M., et al., *Arginase I is constitutively expressed in human granulocytes and participates in fungicidal activity.* Blood, 2005. **105**(6): p. 2549-56.
177. Porembska, Z., et al., *Serum arginase activity in postsurgical monitoring of patients with colorectal carcinoma.* Cancer, 2002. **94**(11): p. 2930-2934.
178. Rotondo, R., et al., *Exocytosis of azurophil and arginase 1-containing granules by activated polymorphonuclear neutrophils is required to inhibit T lymphocyte proliferation.* Journal of Leukocyte Biology, 2011. **89**(5): p. 721-727.
179. Rotondo, R., et al., *IL-8 induces exocytosis of arginase 1 by neutrophil polymorphonuclears in nonsmall cell lung cancer.* International Journal of Cancer, 2009. **125**(4): p. 887-893.
180. Rotondo, R., et al., *Arginase 2 is expressed by human lung cancer, but it neither induces immune suppression, nor affects disease progression.* Int J Cancer, 2008. **123**(5): p. 1108-16.
181. Sippel, T.R., et al., *Neutrophil degranulation and immunosuppression in patients with GBM: restoration of cellular immune function by targeting arginase I.* Clinical cancer research, 2011. **17**(22): p. 6992-7002.
182. Rodriguez, P.C., et al., *Arginase I-producing myeloid-derived suppressor cells in renal cell carcinoma are a subpopulation of activated granulocytes.* Cancer research, 2009. **69**(4): p. 1553-1560.
183. Steggerda, S.M., et al., *Inhibition of arginase by CB-1158 blocks myeloid cell-mediated immune suppression in the tumor microenvironment.* J Immunother Cancer, 2017. **5**(1): p. 101.
184. Derakhshani, A., et al. *Arginase 1 (Arg1) as an Up-Regulated Gene in COVID-19 Patients: A Promising Marker in COVID-19 Immunopathy*. Journal of clinical medicine, 2021. **10**, DOI: 10.3390/jcm10051051.
185. Hemmat, N., et al., *Neutrophils, Crucial, or Harmful Immune Cells Involved in Coronavirus Infection: A Bioinformatics Study.* Frontiers in Genetics, 2020. **11**(641).
186. Cloots, R.H.E., et al., *Arginase 1 deletion in myeloid cells affects the inflammatory response in allergic asthma, but not lung mechanics, in female mice.* BMC Pulmonary Medicine, 2017. **17**(1): p. 158.
187. Burrack, K.S. and T.E. Morrison, *The Role of Myeloid Cell Activation and Arginine Metabolism in the Pathogenesis of Virus-Induced Diseases.* Frontiers in Immunology, 2014. **5**(428).
188. Wilson, E.B., et al., *Emergence of distinct multiarmed immunoregulatory antigen-presenting cells during persistent viral infection.* Cell host & microbe, 2012. **11**(5): p. 481-491.
189. Wherry, E.J., et al., *Viral persistence alters CD8 T-cell immunodominance and tissue distribution and results in distinct stages of functional impairment.* J Virol, 2003. **77**(8): p. 4911-27.

190. Cai, W., et al., *Clinical Significance and Functional Studies of Myeloid-Derived Suppressor Cells in Chronic Hepatitis C Patients.* Journal of Clinical Immunology, 2013. **33**(4): p. 798-808.
191. Cloke, T.E., et al., *Increased level of arginase activity correlates with disease severity in HIV-seropositive patients.* The Journal of infectious diseases, 2010. **202**(3): p. 374-385.
192. Takele, Y., et al., *Arginase Activity in the Blood of Patients with Visceral Leishmaniasis and HIV Infection.* PLoS Neglected Tropical Diseases, 2013. **7**(1): p. 1-7.
193. Mora, A.L., et al., *Activation of alveolar macrophages via the alternative pathway in herpesvirus-induced lung fibrosis.* Am J Respir Cell Mol Biol, 2006. **35**(4): p. 466-73.
194. Ui Mhaonaigh, A., et al., *054. LOW DENSITY GRANULOCYTES IN ANCA VASCULITIS: PHENOTYPE AND FUNCTION.* Rheumatology, 2019. **58**(Supplement_2).
195. Cao, W., et al., *Hepatitis C virus targets ove' expression of arginase I in hepatocarcinogenesis.* International Journal of Cancer, 2009. **124**.
196. Sandalova, E., et al., *Increased levels of arginase in patients with acute hepatitis B suppress antiviral T cells.* Gastroenterology, 2012. **143**(1): p. 78-87.e3.
197. Wang, J., et al., *Bacterial colonization dampens influenza-mediated acute lung injury via induction of M2 alveolar macrophages.* Nature Communications, 2013. **4**(1): p. 2106.
198. Shirey, K.A., et al., *Agents that increase AAM differentiation blunt RSV-mediated lung pathology.* J Leukoc Biol, 2014. **96**(6): p. 951-5.
199. Liu, W., et al., *Cross-regulation of T regulatory-cell response after coxsackievirus B3 infection by NKT and γδ T cells in the mouse.* The American journal of pathology, 2013. **183**(2): p. 441-9.
200. Marini, O., et al., *Mature CD10⁺ and immature CD10⁻ neutrophils present in G-CSF-treated donors display opposite effects on T cells.* Blood, 2017.
201. Adrover, J.M., et al., *A Neutrophil Timer Coordinates Immune Defense and Vascular Protection.* Immunity, 2019. **50**(2): p. 390-402.e10.
202. Farzeen, T., *Role of low density neutrophils in human health and disease*. Vol. 11. 2016. 1-17.
203. Cossarizza, A., et al., *Guidelines for the use of flow cytometry and cell sorting in immunological studies.* European Journal of Immunology, 2017. **47**(10): p. 1584-1797.
204. Jones, B.E., et al., *ANCA autoantigen gene expression highlights neutrophil heterogeneity where expression in normal-density neutrophils correlates with ANCA-induced activation.* Kidney International, 2020. **98**(3): p. 744-757.
205. Manz, M.G. and S. Boettcher, *Emergency granulopoiesis.* Nat Rev Immunol, 2014. **14**(5): p. 302-14.
206. Chevrier, S., et al., *A distinct innate immune signature marks progression from mild to severe COVID-19*. 2020, bioRxiv.
207. Falk, R.J. and J.C. Jennette, *Anti-neutrophil cytoplasmic autoantibodies with specificity for myeloperoxidase in patients with systemic vasculitis and idiopathic necrotizing and crescentic glomerulonephritis.* N Engl J Med, 1988. **318**(25): p. 1651-7.

208. Martin, C., et al., *Chemokines acting via CXCR2 and CXCR4 control the release of neutrophils from the bone marrow and their return following senescence.* Immunity, 2003. **19**(4): p. 583-93.
209. Brusselle, G.G., *Pulmonary-renal syndromes.* Acta Clin Belg, 2007. **62**(2): p. 88-96.
210. Song, R., et al., *Anca-associated vasculitis under a COVID-19 mask.* Journal of the American Society of Nephrology, 2020. **31**: p. 291.
211. Coughlan, A.M., et al., *Myeloid Engraftment in Humanized Mice: Impact of Granulocyte-Colony Stimulating Factor Treatment and Transgenic Mouse Strain.* Stem Cells and Development, 2016. **25**(7): p. 530-541.
212. Elghetany, M.T., *Surface Antigen Changes during Normal Neutrophilic Development: A Critical Review.* Blood Cells, Molecules, and Diseases, 2002. **28**(2): p. 260-274.
213. McKenna, E., et al., *Neutrophils: Need for Standardized Nomenclature.* Frontiers in Immunology, 2021. **12**(1081).
214. Hart, S.P., et al., *Molecular characterization of the surface of apoptotic neutrophils: implications for functional downregulation and recognition by phagocytes.* Cell Death Differ, 2000. **7**(5): p. 493-503.
215. Marini, O., et al., *Mature CD10⁺ and immature CD10⁻ neutrophils present in G-CSF-treated donors display opposite effects on T cells.* Blood, 2017.
216. Pedersen, C.C., et al., *Changes in Gene Expression during G-CSF–Induced Emergency Granulopoiesis in Humans.* The Journal of Immunology, 2016. **197**(5): p. 1989.
217. Ndlovu, L.N., et al., *Increased Neutrophil Count and Decreased Neutrophil CD15 Expression Correlate With TB Disease Severity and Treatment Response Irrespective of HIV Co-infection.* Frontiers in Immunology, 2020. **11**(1872).
218. Cassetta, L., et al., *Differential expansion of circulating human MDSC subsets in patients with cancer, infection and inflammation.* Journal for ImmunoTherapy of Cancer, 2020. **8**(2): p. e001223.
219. Uppal, N.N., et al., *De Novo ANCA-Associated Vasculitis With Glomerulonephritis in COVID-19.* Kidney International Reports, 2020. **5**(11): p. 2079-2083.
220. Moeinzadeh, F., et al., *Newly Diagnosed Glomerulonephritis During COVID-19 Infection Undergoing Immunosuppression Therapy, a Case Report.* Iran J Kidney Dis, 2020. **14**(3): p. 239-242.
221. Fousert, E., R. Toes, and J. Desai, *Neutrophil Extracellular Traps (NETs) Take the Central Stage in Driving Autoimmune Responses.* Cells, 2020. **9**(4).
222. Sanyaolu, A., et al., *Comorbidity and its Impact on Patients with COVID-19.* SN comprehensive clinical medicine, 2020: p. 1-8.
223. Morrissey, S.M., et al., *A specific low-density neutrophil population correlates with hypercoagulation and disease severity in hospitalized COVID-19 patients.* JCI Insight, 2021. **6**(9).
224. Schulte-Schrepping, J., et al., *Severe COVID-19 Is Marked by a Dysregulated Myeloid Cell Compartment.* Cell, 2020. **182**(6): p. 1419-1440.e23.
225. Hoffmann, K., et al., *Mutations in the gene encoding the lamin B receptor produce an altered nuclear morphology in granulocytes (Pelger-Huët anomaly).* Nat Genet, 2002. **31**(4): p. 410-4.
226. Nakayama, F., et al., *CD15 Expression in Mature Granulocytes Is Determined by α1,3-Fucosyltransferase IX, but in Promyelocytes and Monocytes by*

*α1,3-Fucosyltransferase IV **.* Journal of Biological Chemistry, 2001. **276**(19): p. 16100-16106.
227. Alberca, R.W., et al., *Frequencies of CD33+CD11b+HLA-DR-CD14-CD66b+ and CD33+CD11b+HLA-DR-CD14+CD66b- Cells in Peripheral Blood as Severity Immune Biomarkers in COVID-19.* Frontiers in medicine, 2020. **7**: p. 580677-580677.
228. Cicchese, J.M., et al., *Dynamic balance of pro- and anti-inflammatory signals controls disease and limits pathology.* Immunol Rev, 2018. **285**(1): p. 147-167.
229. Minns, D., K.J. Smith, and E.G. Findlay, *Orchestration of Adaptive T Cell Responses by Neutrophil Granule Contents.* Mediators of Inflammation, 2019. **2019**: p. 8968943.
230. Mukhtyar, C., et al., *Modification and validation of the Birmingham Vasculitis Activity Score (version 3).* Ann Rheum Dis, 2009. **68**(12): p. 1827-32.
231. Aschenbrenner, A.C., et al., *Disease severity-specific neutrophil signatures in blood transcriptomes stratify COVID-19 patients.* Genome Med, 2021. **13**(1): p. 7.
232. Sinha, S., et al., *Dexamethasone modulates immature neutrophils and interferon programming in severe COVID-19.* Nature medicine, 2022. **28**(1): p. 201-211.
233. Okun, J.G., et al., *Molecular regulation of urea cycle function by the liver glucocorticoid receptor.* Mol Metab, 2015. **4**(10): p. 732-40.
234. Kelly-Scumpia, K.M., et al., *ER Stress Regulates Immunosuppressive Function of Myeloid Derived Suppressor Cells in Leprosy that Can Be Overcome in the Presence of IFN-γ.* iScience, 2020. **23**(5): p. 101050.
235. Falk, R.J., et al., *Anti-neutrophil cytoplasmic autoantibodies induce neutrophils to degranulate and produce oxygen radicals in vitro.* Proc Natl Acad Sci U S A, 1990. **87**(11): p. 4115-9.
236. Ingersoll, S.A., et al., *Mature Cystic Fibrosis Airway Neutrophils Suppress T Cell Function: Evidence for a Role of Arginase 1 but Not Programmed Death-Ligand 1.* The Journal of Immunology, 2015. **194**(11): p. 5520.
237. Abebe, T., et al., *Arginase activity - a marker of disease status in patients with visceral leishmaniasis in ethiopia.* PLoS neglected tropical diseases, 2013. **7**(3): p. e2134-e2134.
238. Hsu, B.E., et al., *Immature Low-Density Neutrophils Exhibit Metabolic Flexibility that Facilitates Breast Cancer Liver Metastasis.* Cell Reports, 2019. **27**(13): p. 3902-3915.e6.
239. Quach, A. and A. Ferrante, *The Application of Dextran Sedimentation as an Initial Step in Neutrophil Purification Promotes Their Stimulation, due to the Presence of Monocytes.* Journal of Immunology Research, 2017. **2017**: p. 10.
240. Quintelier, K., et al., *Analyzing high-dimensional cytometry data using FlowSOM.* Nature Protocols, 2021. **16**(8): p. 3775-3801.
241. Monteseirín, J., et al., *L-selectin expression on neutrophils from allergic patients.* Clin Exp Allergy, 2005. **35**(9): p. 1204-13.
242. McKenna, K.C., et al., *Delayed processing of blood increases the frequency of activated CD11b+ CD15+ granulocytes which inhibit T cell function.* J Immunol Methods, 2009. **341**(1-2): p. 68-75.
243. Vlad, G., *Chapter 27 - Sources of errors in flow cytometry*, in *Accurate Results in the Clinical Laboratory (Second Edition)*, A. Dasgupta and J.L. Sepulveda, Editors. 2019, Elsevier. p. 401-422.
244. Fridlender, Z.G., et al., *Polarization of tumor-associated neutrophil phenotype by TGF-beta: "N1" versus "N2" TAN.* Cancer cell, 2009. **16**(3): p. 183-194.

245. Mócsai, A., *Diverse novel functions of neutrophils in immunity, inflammation, and beyond.* The Journal of Experimental Medicine, 2013. **210**(7): p. 1283.
246. Jiménez-Cortegana, C., et al., *Low Levels of Granulocytic Myeloid-Derived Suppressor Cells May Be a Good Marker of Survival in the Follow-Up of Patients With Severe COVID-19.* Frontiers in Immunology, 2022. **12**.
247. Wang, J.F., et al., *Upregulated PD-L1 delays human neutrophil apoptosis and promotes lung injury in an experimental mouse model of sepsis.* Blood, 2021. **138**(9): p. 806-810.
248. Rajarathnam, K., et al., *How do chemokines navigate neutrophils to the target site: Dissecting the structural mechanisms and signaling pathways.* Cell Signal, 2019. **54**: p. 69-80.
249. Deniset, J.F. and P. Kubes, *Neutrophil heterogeneity: Bona fide subsets or polarization states?* Journal of Leukocyte Biology, 2018. **103**(5): p. 829-838.